Theses and Dissertations   Theses and Dissertations

12-13-2002

Two and Three-Dimensional Finite Element Analysis of Plasticity-Induced Fatigue Crack Closure: A Comprehensive Parametric Study

Kiran N. Solanki

Follow this and additional works at: https://scholarsjunction.msstate.edu/td

TWO AND THREE-DIMENSIONAL FINITE ELEMENT ANALYSIS OF

PLASTICITY-INDUCED FATIGUE CRACK CLOSURE

–A COMPREHENSIVE PARAMETRIC STUDY

By

Kiran Nainmal Solanki

A Thesis
Submitted to the Faculty of
Mississippi State University
in Partial Fulfillment of the Requirements
for the Degree of Master of Science
in Mechanical Engineering
in the Department of Mechanical Engineering

Mississippi State, Mississippi

December 2002

TWO AND THREE-DIMENSIONAL FINITE ELEMENT ANALYSIS OF

PLASTICITY-INDUCED FATIGUE CRACK CLOSURE

– A COMPREHENSIVE PARAMETRIC STUDY

By

Kiran Nainmal Solanki

Approved:

_____
Steven R. Daniewicz
Associate Professor of Mechanical
Engineering (Director of Thesis)

_____
James C. Newman, Jr.
Professor of Aerospace Engineering
(Committee Member)

_____
E. William Jones
Professor of Mechanical Engineering
(Committee Member)

_____
James C. Newman, III
Associate Professor of Aerospace
Engineering and Engineering Mechanics
(Committee Member)

_____
Rogelio Luck
Graduate Coordinator of the Department
of Mechanical Engineering

_____
A. Wayne Bennett
Dean of the College of Engineering

Name: Kiran Nanimal Solanki

Date of Degree: December 13, 2002

Institution: Mississippi State University

Major Field: Mechanical Engineering

Major Professor: Dr. Steven R. Daniewicz

Title of Study: TWO AND THREE-DIMENSIONAL FINITE ELEMENT ANALYSIS OF PLASTICITY-INDUCED FATIGUE CRACK CLOSURE – A COMPREHENSIVE PARAMETRIC STUDY

Pages in Study: 195

Candidate for Degree of Master of Science

Finite element analyses are frequently used to model growing fatigue cracks and the associated plasticity-induced crack closure. Two-dimensional, elastic-perfectly plastic finite element analyses of middle-crack tension (M(T)), bend (SEB), and compact tension (C(T)) geometries were conducted to study fatigue crack closure and to calculate the crack opening values under plane-strain and plane-stress conditions. The loading was selected to give the same maximum stress intensity factor in both geometries, and thus similar initial forward plastic zone sizes. Mesh refinement studies were performed on all geometries with various element types. For the C(T) geometry, negligible crack opening loads under plane-strain conditions were observed. In contrast, for the M(T) specimen, the plane-strain crack opening stresses were found to be significantly larger. This difference was shown to be a consequence of in-plane constraint. Under plane-stress conditions, it was found that the in-plane constraint has negligible effect, such that the

opening values are approximately the same for the C(T), SEB, and M(T) specimens. Next, the crack opening values of the C(T), SEB and M(T) specimens were compared under various stress levels and load ratios. The effect of a highly refined mesh on crack opening values was noted and significantly lower crack opening values than those reported in literature were found. A new methodology is presented to calculate crack opening values in planar geometries using the crack surface nodal force distribution under minimum loading as determined from finite element analyses. The calculated crack opening values are compared with values obtained using finite element analysis and more conventional crack opening assessment methodologies. It is shown that the new method is independent of loading increment, integration method (normal and reduced integration), and crack opening assessment location. The compared opening values were in good agreement with strip-yield models.

ACKNOWLEDGEMENTS

TABLE OF CONTENTS

LIST OF FIGURES

CHAPTER I

INTRODUCTION

1-1 Background

Fatigue has been defined as "the progressive localized permanent structural change that occurs in a material subjected to repeated or fluctuating strains at stresses having a maximum value less that the tensile strength of the material" [1].

Many different mechanical failure modes exist. These failures can occur in simple, complex, inexpensive, or expensive components or structures. It has been estimated that between 50 and 90 % of these failures are due to fatigue [2]. Failures due to fatigue culminate in cracks (or) fracture after a sufficient number of fluctuations of load.

Fracture of a structural member due to repeated cycles of load is commonly referred to as a *fatigue failure* or *fatigue fracture*. The corresponding number of load cycles or the time during which the member is subjected to these loads before fracture occurs is referred to as the *fatigue life* of the member. The fatigue life of a member is affected by many factors [1]. For example, it is affected by (1) the type of load (uniaxial, bending, torsion), (2) the nature of the load-displacement curve (linear, nonlinear), (3) the frequency of load repetitions or cycling, (4) the load history (cyclic loading with constant or variable amplitude), (5) the size of the member, (6) the material flaws, (7) the manufacturing method (surface roughness, notches), (8) the operating temperature (high temperature that results in creep, low temperature that results in brittleness), (9) the

1

environmental operating conditions (corrosion) [1]. In practice, accurate estimates of fatigue life are difficult to obtain, because for many materials, small changes in these conditions may strongly affect fatigue life. The designer may therefore be forced to rely on testing of full-scale members under in-service conditions. However, testing of full-scale members is time-consuming and costly. Therefore data from laboratory tests are often used to establish fatigue failure criteria.

1-2 Fatigue Crack Propagation

The total period of fatigue life may be considered to consist of three phases: (1) initial fatigue damage that produces crack initiation, (2) propagation of a crack or cracks that results in partial separation of a cross section of a member, until the remaining uncracked cross section unable to support the applied load, and (3) final fracture of the member. The typical log-log plot of *da/dN* versus *ΔK* is shown schematically in Figure 1-1. The sigmoidel shape can be divided into three major regions. Region I is the near threshold region and exhibits a threshold value, ΔK_{th}, below which there is no observable crack growth. Below ΔK_{th}, fatigue cracks are characterized as nonpropagating cracks. Microstructure, mean stress, frequency, and environment primarily control region I crack growth. Region II shows essentially a linear relationship between *log da/dN* and *log ΔK*, which corresponds to the formula

$$\frac{da}{dN} = C\left(\Delta K\right)^{m} \tag{1}$$

first suggested by Paris et al.[3]. Here m and C are material constants. Region II (Paris

region) fatigue crack growth corresponds to stable macroscopic crack growth that is

typically controlled by environment. Microstructure and mean stress have less influence

on fatigue crack growth behavior in region II than region I. In the region III the fatigue

crack growth rates are very high as they approach instability, and little fatigue crack

growth life is involved. This region is controlled primarily by fracture toughness K_c,

which in turn depends on the microstructure and environment.
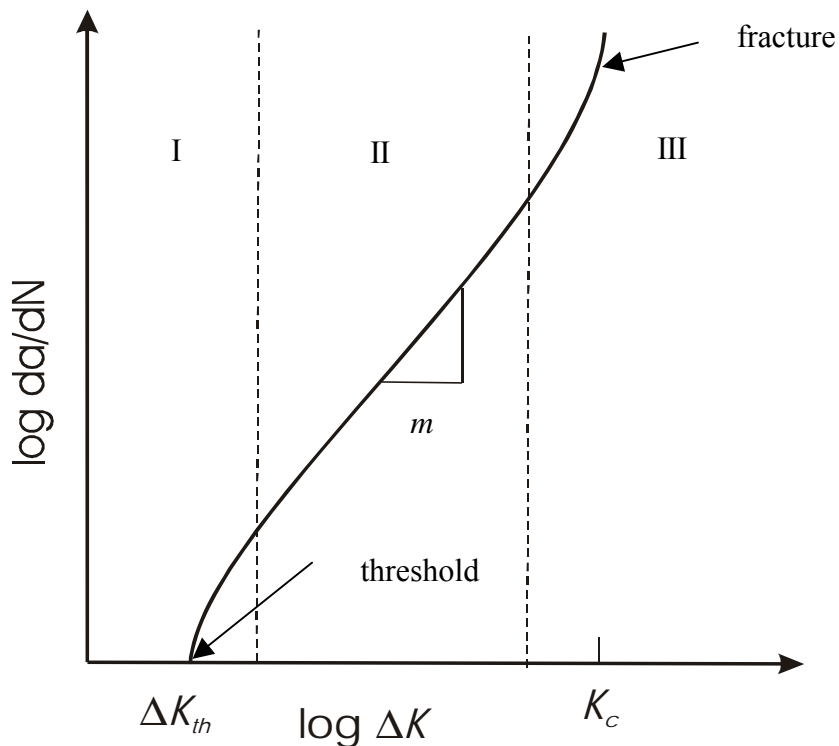
Figure 1-1 Typical Fatigue Crack Growth Behavior in Metals

1-3 Fatigue Crack Closure

The phenomenon of plasticity-induced crack closure was first proposed and investigated by Elber [4], and led to new concepts in fatigue crack growth. Since then, several additional closure mechanisms have been identified [2-6], but the primary mechanism under many conditions is plasticity. During loading, large tensile plastic strains are developed near the crack tip, which are not fully reversed upon unloading as the crack extends. This leads to the formation of a plastic wake with plastic deformation in a direction normal to the advancing crack.

Roughness and oxide induced fatigue crack closure are predominate in the near threshold crack growth regime. These two mechanisms are similar to plasticity-induced fatigue crack closure in that the material in the wake region contacts while under tensile loading. Roughness-induced fatigue crack closure occurs when the crack growth is not planer and the mixed-mode loading at the kinked crack tip causes a mismatch of the wake region material. For oxide-induced fatigue crack closure, an oxide film forms on the surface in the wake region and makes contact while under tensile loads.

(a) Plasticity-induced closure   (b) Roughness-induced closure   (c) Oxide/corrosion product-induced closure
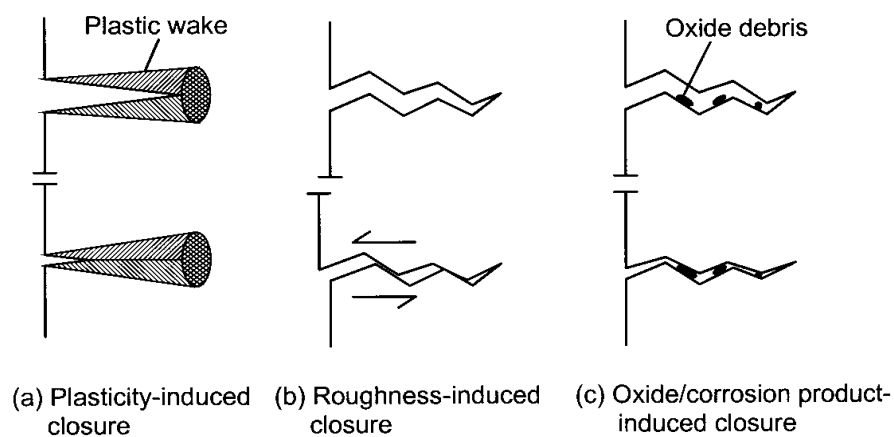
Figure 1-2 Typical Fatigue Crack Closure in Metals [5]

Elber postulated that crack closure decreases the fatigue crack growth rate by reducing the effective stress intensity range. Figure 1-3 illustrates the closure concept. When a specimen is cyclically loaded between K_{max} and K_{min}, the crack faces are in contact below K_{open}, the stress intensity at which the crack fully opens. Elber assumed that the portion of the cycle that is below K_{open} does not contribute to fatigue crack growth. He defined an effective stress intensity range as follows:

$$\Delta K_{eff} = K_{max} - K_{open} \tag{2}$$

Elber then proposed a modified Paris equation:

$$da/dN = C\left(\Delta K_{eff}\right)^{m} \tag{3}$$
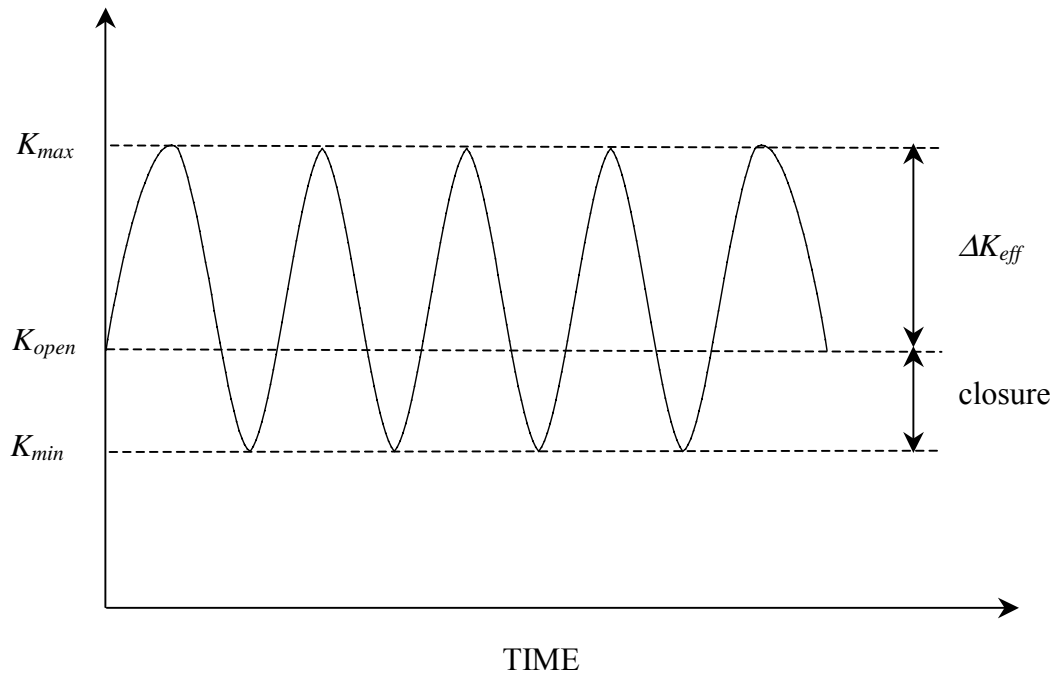
Figure 1-3 Definition of Effective Stress Intensity Range

1-4 Crack Tip Nomenclature

As a fatigue crack propagates, two different types of crack tip plastic zones are generated as shown in Figure 1-4. The forward plastic zone is defined as the material near the crack tip undergoing plastic deformation at the maximum load. The second zone of interest is the reversed plastic zone, which is defined as the material near the crack tip undergoing compressive yielding at the minimum load [6]. These crack tip plastic zones will be used to characterize the degree of finite element mesh refinement later.
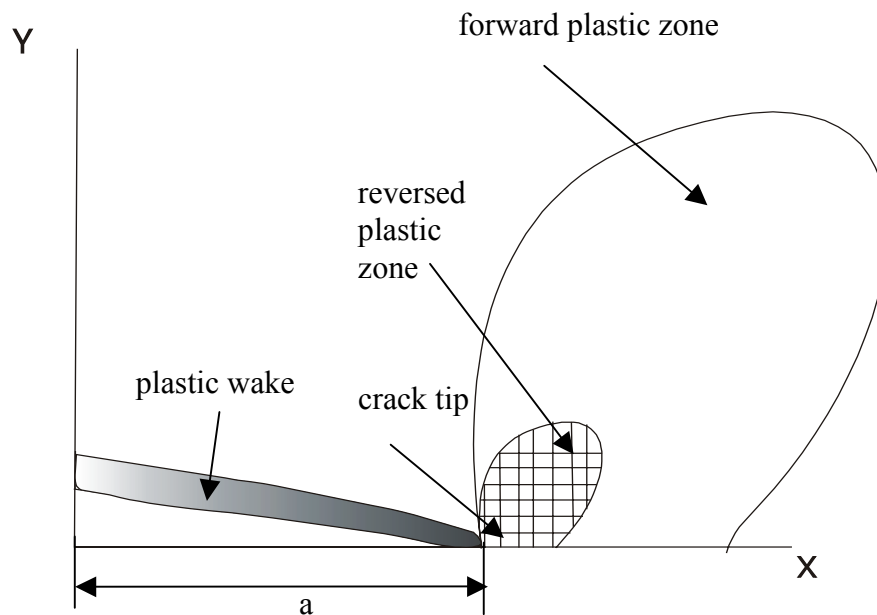
Figure 1-4 Plastic Deformation Around a Growing Crack

The nature of plastic deformation near the crack tip is strongly influenced by the 2-D idealization assumed. The permanent elongation of material in the direction normal

to the crack requires the transfer of material from somewhere in the cracked body due to incompressibility requirements during plastic deformation [7]. Under plane-stress, a potential mechanism of material transfer is obvious. Since out-of-plane deformation is not constrained, material can be transferred from the thickness direction to the axial direction [7]. However, the mechanism of material transfer postulated for plane-stress is not admissible for plane-strain. By definition, no net out-of-plane contraction can occur, and therefore it has been suggested that there can be no net axial stretch of material in the plastic wake behind the crack tip as discussed by Fleck [8], which implies no plasticity-induced crack closure. The existence of plasticity-induced crack closure under plane-strain conditions has been a topic of intense debate [9-27].

Many researchers have performed finite element analyses simulating plasticity-induced fatigue crack closure, considering different two-dimensional configurations under plane-strain or plane-stress conditions [7-52]. Far fewer efforts have been directed toward the three-dimensional problem [53-63]. Newman [5] and McClung [64] have presented general reviews in their respective papers.

In this research work, a detailed and comprehensive finite element analysis of plasticity-induced fatigue crack closure for both planer geometries and three-dimensional geometries is performed. Emphasis is focused on the difficulties in modeling with respect to mesh refinement level, crack advancement schemes, crack opening assessment location, crack shape evolution, overload effects, and opening value assessment techniques.

CHAPTER II

LITERATURE REVIEW

Finite element analysis of plasticity-induced fatigue crack growth is conceptually simple. A mesh is created with an initial crack, and the mesh is loaded by remotely applied tractions. For constant amplitude loading, the loading is cycled between a maximum applied stress S_{max} and the minimum applied stress S_{min}. During the cyclic loading the crack is advanced in some fashion, leading to the formation of a plastic wake behind the crack tip. This modeling concept is simple; however, there are several issues which must be addressed during the fatigue crack growth simulation. These issues have been summarized and categorized into different sections in this chapter.

2-1 Two-dimensional Finite Element Modeling Issues

2-1-1 Crack Surface Contact

A changing boundary condition characterizes a crack under cyclic loading. In order to prevent the crack surfaces from penetrating as the minimum load is approached, some mechanism must be implemented into the finite element simulation. This can be achieved by changing the stiffness of spring elements attached to the crack surface, by removing or imposing crack surface nodal constraints, by using truss elements on the crack surface, or by using contact elements. The implementation of contact

elements along the crack surface, however, can lead to convergence problems and long execution times [60].

Newman [48] was the first to implement spring (truss) elements to simulate the changing boundary condition. The element was connected to each boundary node on the crack surface. For open nodes, the spring stiffness was set equal to zero, and for closed nodes, the stiffness was assigned a large value. McClung et al. [7,14,30,31,42-44,49,50] followed Newman's approach in their earlier studies. However, the large imposed stiffness values for constrained crack surface nodes were found to be a source of numerical difficulties, and they investigated an alternate approach to simulate the cyclic crack surface contact. During loading and unloading, stresses and displacements were monitored along the crack surface. A negative nodal displacement indicated that the crack was closed at this point, and the displacement was set to zero. A tensile nodal stress indicated that the crack was open at this point, and the nodal restraint was removed. This more direct approach has also been used by Blom et al. [11].

Wu et al. [46] have used a truss element with a varying stiffness together with pairs of contact elements and the element death option. The element death option was incorporated to deactivate truss elements or cut the truss elements. They have shown that with this approach a node can be released any time during a load cycle irrespective of the magnitude of the deformation caused by the release of the node. Consequently, fewer problems with convergence were encountered and also several nodes can be released simultaneously.

2-1-2 Mesh Refinement

As a fatigue crack propagates, two different types of crack tip plastic zones are generated. The forward plastic zone is defined as the material near the crack tip undergoing plastic deformation at the maximum load. The second zone of interest is the reversed plastic zone, which is defined as the material near the crack tip undergoing compressive yielding at the minimum load [6]. These crack tip plastic zones have been used to characterize the degree of finite element mesh refinement required when modeling plasticity-induced closure [13,14,28,29].

Newman [48] was the first to study the effects of finite element mesh refinement on opening load computations under plane-stress conditions. He modeled a middle-crack tension (M(T)) specimen of width 2W with constant-strain triangle (CST) elements and found that the crack opening loads converged with increasing levels of mesh refinement at high applied stress levels as shown in Figure 2-1.
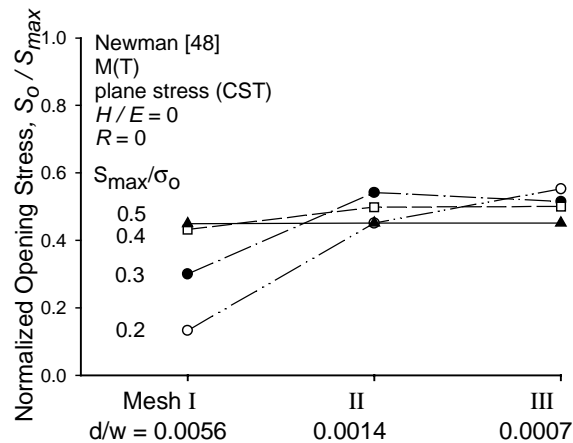
Figure 2-1   Mesh Refinement Studies

In the figure, d is the element size ahead of the crack tip. For small applied stresses, convergence was not observed. Convergence may be a consequence of the number of

elements present in the reversed crack tip plastic zone. Newman considered the discretization of the forward plastic zone only, and did not consider the reversed plastic zone. Thus, the reversed zone may have been discretized with an insufficient number of elements.

McClung et al. [14,30,31] performed mesh refinement studies on a crack emanating from a circular hole, the M(T) specimen, and an edge-crack specimen. They found that mesh refinement should be based on the number of elements present in the forward plastic zone in the crack plane. They also suggested that adequate refinement to capture the reversed plastic zone may be important. Dougherty et al. [13] performed mesh refinement and element shape studies on C(T) and M(T) geometries under plane-strain, and found that an aspect ratio less than or equal to 2 should be used for elements ahead of the crack. They also found that the mesh density ahead of the crack should satisfy $\Delta a / r_f \leq 0.1$, where $2r_f$ is an approximation of the forward plastic zone given by:

$$r_f = \frac{1}{2\alpha\pi} \left(\frac{K_{max}}{\sigma_0} \right)^2$$

(2-1)

where α is equal to 1 and 3 for plane-stress and plane-strain respectively, σ_o is the flow stress, and K_{max} is the maximum stress intensity factor. Park et al. [41] suggested that mesh refinement levels for the M(T) specimen should be chosen to produce opening stress values that compare well with experimental results. In the opinion of the authors, this approach is flawed given the difficulties associated with measuring opening load values [54,65-68].

Most of the work reported in the literature has incorporated large applied stresses, which allows for the use of coarse meshes while still satisfying mesh refinement requirements.

2-1-3 Stabilization of Crack Opening Load

Under constant amplitude loading, the crack opening load will typically increase monotonically with increasing crack growth until a stabilized value is reached as illustrated in Figures 2-2a and 2-2b
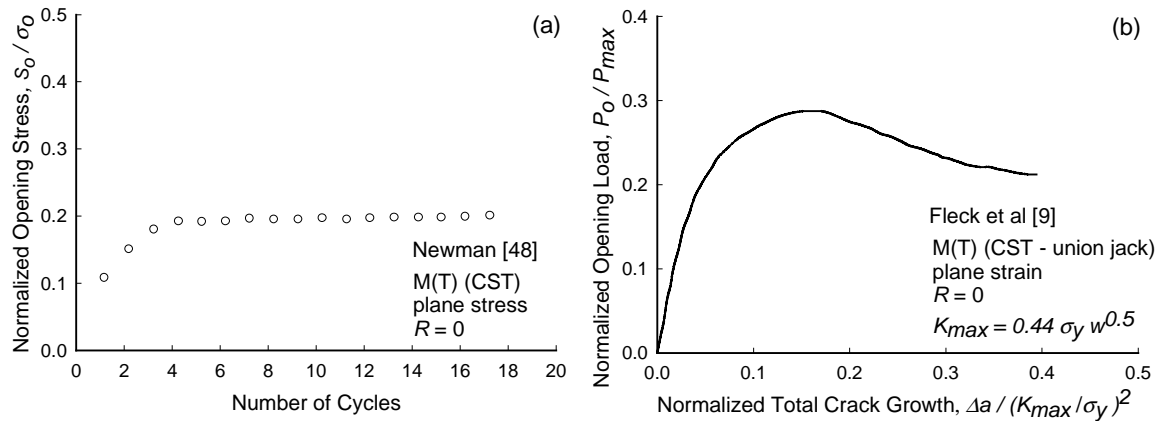
Figure 2-2   Stabilization of Crack Opening Values under Plane-stress and Plane-strain

McClung [14] has shown that under constant amplitude loading conditions, the crack must be advanced completely through the initial forward plastic zone to form a stabilized plastic wake. This is necessary to obtain non-varying crack opening values. However, Fleck et al. [9] and Wu et al. [46] have shown a variation in crack opening values even after the crack has progressed through initial forward plastic zone. Fleck's results are shown in Figure 2-2b. Using a strip-yield model, Daniewicz et al. [69] have

shown that a large amount of crack growth will produce a decreasing opening value if the remaining ligament becomes small enough. Achieving the large amounts of crack growth required to observe an initial stabilization followed by a subsequent decay in the crack opening value is difficult when using finite element analysis, because of the computationally intensive nature of the simulation. However, such an effort has been reported by McClung [49].

2-1-4 Crack Advance Scheme

To produce a plastic wake behind the crack tip, the crack must be incrementally advanced is some fashion under the applied cyclic loading. The most common means of crack advance is to release the crack tip node, thus advancing the crack by an amount equal to the crack tip element size. It is important to realize that modeling an incremental crack advance with a node release involves no consideration of the physics of fatigue crack growth, since the crack extension is independent of stress level and the strain in the vicinity of the crack tip. Consequently, the finite element analysis is used to predict the crack opening value, but not the fatigue crack propagation life. Recently, some researchers have suggested the use of a cohesive element to advance the crack in a physics-based manner [70]. Newman used a critical strain to advance the crack [46]. Nakagaki and Atulri [26] proposed a stress criterion for advancing the crack tip.

When performing analyses using the conventional node release technique, the preferred node release scheme for simulating an incremental crack advance is unclear. The crack tip node may be advanced at the minimum load level [7,10,14,28,33-35,37-40,46], at the maximum load level [8,10,11,15,16,42,47-49], after the maximum load

[14,30,31,23,24], during the loading/unloading cycle [26,37,32,51] or during the second cycle [7]. Ogura et al. [10] have implemented a simple criteria for crack advance. The crack was advanced by one element when the crack tip reaction force became zero during the loading cycle. Alternately, Palazotto et al. [32] in their study proposed a criterion of growing the crack at 98% of the maximum load.

Advancing the crack at the maximum load level may create convergence problems; conversely, there is no such problem with advancing the crack using the minimum load level scheme. The convergence problem related to the maximum load released can be eased by incrementally releasing the crack front nodes [11,28].

Some research [7,28] has concluded that in terms of the resulting crack opening value, there is no difference when using the either maximum or minimum load node release schemes. However, other research has shown significant differences [14,30,31,46].
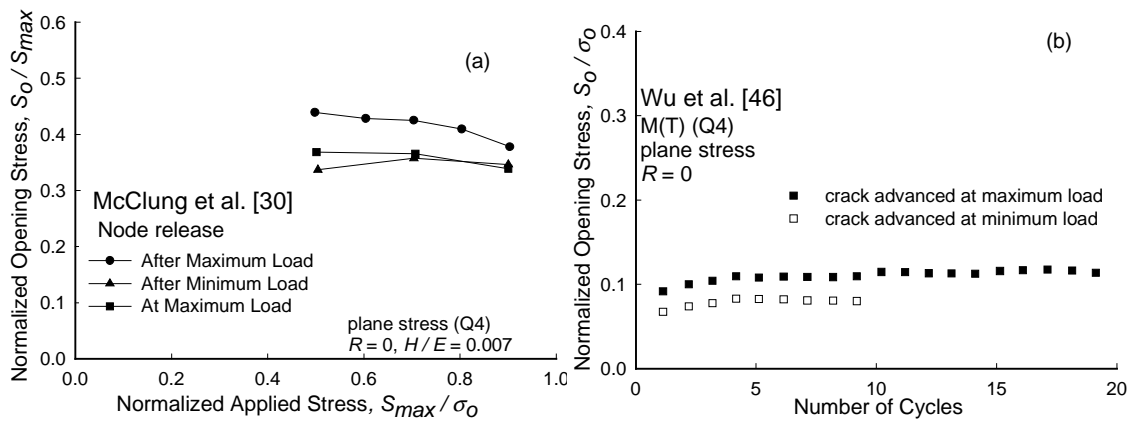
Figure 2-3 Comparison of Crack Opening Values Based on Crack Advance Scheme

Figure 2-3a shows results from a crack advance scheme comparison performed by McClung et al. [30,31]. From the figure, there is a significant difference in opening value when using a different crack advance scheme. Later, McClung et al. [7] showed that this difference was a consequence of using truss elements for crack surface node fixity, and that changing the boundary conditions on the crack surface nodes directly yields approximately the same results for the different crack advance schemes. Wu et al. [46] in their independent study found a variation in crack opening values when using the minimum and maximum loading node release schemes, and their results are shown in Figure 2-3b. This difference may be a consequence of computing the crack opening values based upon zero crack tip nodal reaction force, which is likely influenced by the size of the elements near the crack tip. This variation may also be due to a insufficient discretization of the reversed plastic zone.

2-1-5 Crack Opening Assessment Location

Under constant amplitude loading, the crack tip is the last point to open along the crack surface under an increasing load. Most researchers have used the first node behind the crack tip to assess the crack opening values [7-12,15-51]. Wu et al. [46] have used the crack tip itself to assess the crack opening values. They have proposed that when the compressive stress borne by the crack tip node changes to a tensile one, the crack is fully open. Others have used the second node behind the crack tip [29,55]. McClung et al. [7] and Fleck et al. [9] have shown that the results obtained when using first node behind the crack tip can be mesh dependent.

2-1-6 Variable Amplitude Loading

It may be argued that crack closure analyses are primarily of interest when considering variable amplitude loading. However, the majority of research has considered only constant amplitude loading. Some effort has been directed toward simple load histories such as low-high, or high-low, or a single overload [10,13,16,22,26,27, 36,39,41,43,48]. This research has been used to explain crack growth acceleration and retardation. Due to the computationally intensive nature of closure modeling with finite element analysis, complex load histories are generally not suitable for study, since a large amount of crack growth and a subsequently large number of load cycles are required.

2-1-7 Plane-stress and Plane-strain Condition

The nature of plastic deformation near the crack tip is strongly influenced by the two-dimensional idealization assumed. The permanent elongation of material in the direction normal to the crack requires the transfer of material from somewhere in the cracked body due to incompressibility requirements during plastic deformation. Under plane-stress, a potential mechanism of material transfer is obvious. Since out-of-plane deformation is not constrained, material can be transferred from the thickness direction to the axial direction. However, the mechanism of material transfer postulated for plane-stress is not admissible for plane-strain. By definition, no net out-of-plane contraction can occur, and therefore it has been suggested that there can be no net axial stretch of material in the plastic wake behind the crack tip, which implies no plasticity-induced crack closure [7-9,13,28]. The existence of plasticity-induced crack closure under plane-strain conditions has been a topic of intense debate [9-27].

A study of crack tip plastic zone sizes and crack opening behavior for the M(T)
specimen under plane-strain and plane-stress conditions has been performed by McClung
et al. [30,31]. Crack closure was found to occur in plane-strain, with lower opening
values than those observed under plane-stress. Ogura et al. [10] have also simulated
fatigue crack growth under plane-strain conditions using the finite element method. They
also found that closure does exist under plane-strain conditions, and that the opening
values reached a constant steady-state value after a sufficient amount of crack growth.
Their results, however, are suspect as the ratio of the element length Δa to the forward
plastic zone size r_f was a relatively coarse $\Delta a / r_f = 0.66$. A combined numerical and
experimental study of crack closure in AA2024-T3 was conducted by Blom and Holm
[11]. A plane-stress and plane-strain model of the C(T) specimen was constructed with
constant strain triangular (CST) elements. Under plane-strain conditions closure was
observed, and the plane-strain closure levels were smaller than those for plane-stress.
Their results are also questionable due to a relatively coarse mesh and the use of element
type which is susceptible to plane-strain locking [71]. Under a stress ratio $R = -1$, Lalor
and Sehitoglu found that the plane-strain closure levels were lower than those for plane-
stress. However, when the applied stress was increased to $S_{max} / \sigma_o = 0.8$, the opening
values were larger [24].

Dougherty et al. [13] performed two-dimensional analyses of C(T) and M(T)
geometries under plane-strain, and demonstrated a good comparison between predicted
closure levels and experimental results. Their finite element meshes were composed of
four-noded and eight-noded quadrilateral elements. Ashbaugh et al. [12] performed a
study similar to that conducted by Blom and Holm [11], focusing on finite element

analysis of plasticity-induced crack closure in the C(T) specimen under plane-strain

conditions. In their analyses four-noded quadrilateral elements were used, and their

results indicated that closure does occur in plane-strain. Again, their results are also

suspect due to a lack of mesh refinement and potential plane-strain locking. Conversely,

Fleck and Newman [9] have shown that closure does not occur for a bend specimen

under plane-strain conditions, while closure does occur for the M(T) geometry under

plae-strain. This may be due to the fact that the M(T) geometry has a compressive T-

stress, while the bend specimen has a tensile T-stress. They found crack closure occurring

for a single element on the crack surface of the bend specimen, and suggested that this

closure was an artifact of the finite element analysis.

2-1-8 Geometry Effects

Fleck [18], Fleck and Newman [9], Larsson and Carlsson [72], and Rice [73] have

shown that an influence of specimen geometry upon crack tip plastic deformation,

beyond that associated with the stress intensity factor, may be accounted for in terms of

the T-stress. This stress is the nonsingular constant second term in the near crack tip

series expansion, and represents a normal stress parallel to the crack. The T-stress is

directly proportional to the applied load and also depends on geometry. A two-

dimensional asymptotic expansion for the stresses σ_{ij} near the crack tip for mode I

loading is given by [74]:

$$\sigma_{ij} = \frac{K_I}{\sqrt{2\pi r}} f_{ij}(\theta) + T\delta_{1i}\delta_{1j} + O(\sqrt{r}) + \dots \qquad (2\text{-}2)$$

where r and θ are polar coordinates located at the crack tip, δ_{ij} is the kronecker delta,

K_I is the stress intensity factor, and the f_{ij} are dimensionless functions.

The C(T) and M(T) geometries differ in that each exhibits a distinctly different in-plane constraint, as quantified using the elastic T-stress, where the T-stress is defined as [74]:

$$T = \frac{K_I \beta}{\sqrt{\pi a}} \qquad (2\text{-}3)$$

where a is the crack length, K_I is the stress intensity factor, and β is the biaxiality ratio. This ratio is equal to -1 and 0.425 for the M(T) and C(T) geometries respectively [75].

Fleck [8] has shown a decrease in the closure level as the T-stress was varied from compressive to tensile using bend and M(T) specimens. The effect of T-stress on the crack opening value stabilization and crack opening process for different geometries is shown in Figure 2-4.
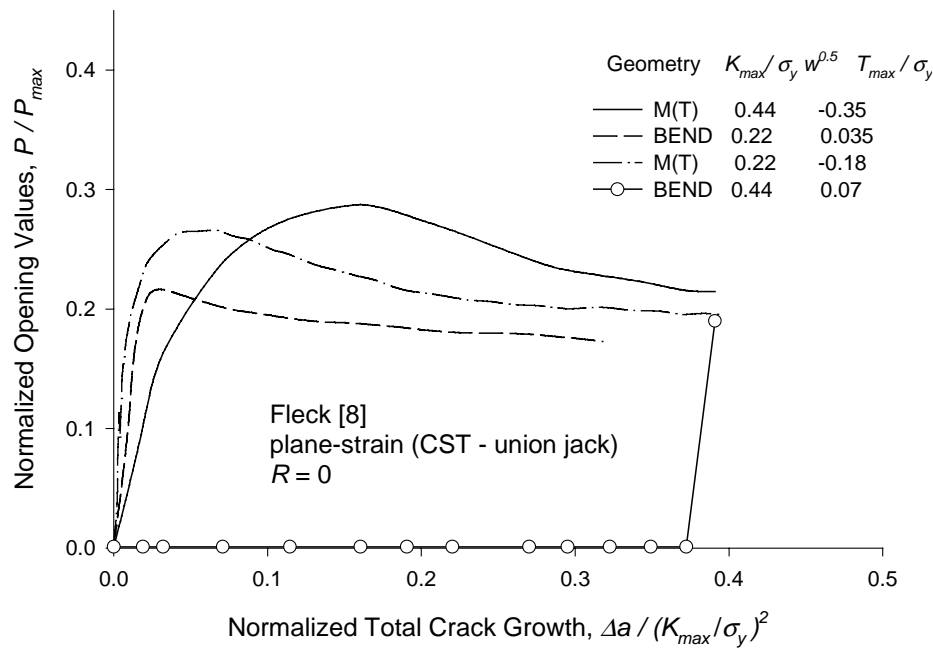
Figure 2-4 Effect of *T*-stress on the Crack Opening Value Stabilization

Fleck [8] studied the effect of *T*-stress variation on the crack opening value stabilization for different geometries by changing the applied maximum stress intensity factor, and results are shown in Figure 2-4. It should be noted from Figure 2-4 that as the *T*-stress becomes more tensile in nature, the opening values are approximately zero except for the single element immediately behind the crack tip.

Under a plane-stress condition, the effect of *T*-stress on closure is negligible. Fleck [8] performed finite element analysis under plane-stress on two-different geometries with the same applied maximum stress intensity factor and found no difference in the crack opening process as shown in Figure 2-5a.
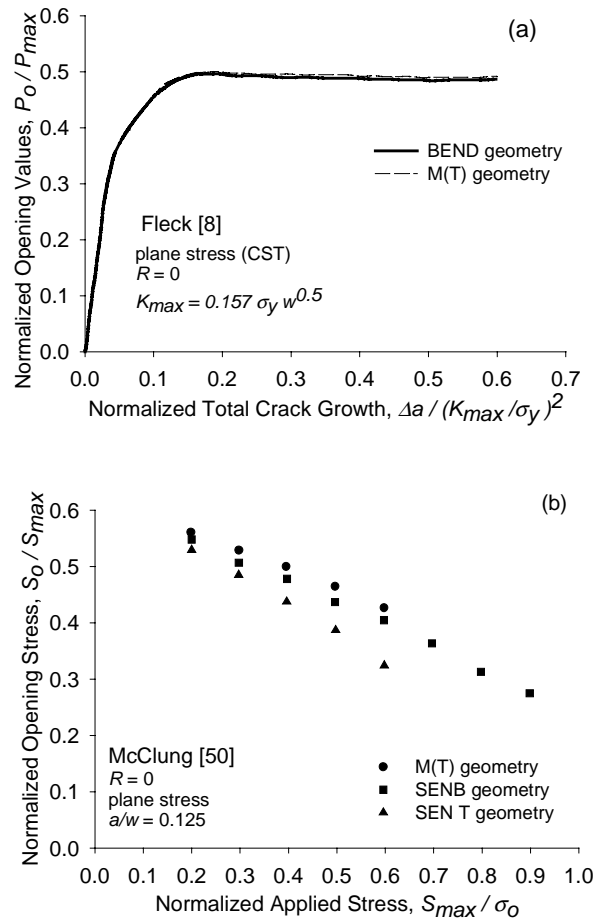
Figure 2-5   Effect of *T*-stress under Plane-stress

However, McClung [50] has shown a significant difference in the crack opening stress at

higher applied stresses, and negligible difference at lower applied stresses as shown in

Figure 2-5b.

2-1-9 *R* Ratio Effects

Of the many finite element analyses of plasticity-induced crack closure, the

majority have considered a small positive stress ratio *R*. A larger positive *R* results in a

smaller reversed plastic zone, and hence increases the mesh refinement requirements.

The effect of R on the crack opening stress for an M(T) specimen has been investigated by McClung et al. [31] and Newman [48] under plane-stress, and their results are shown in Figure 2-6.
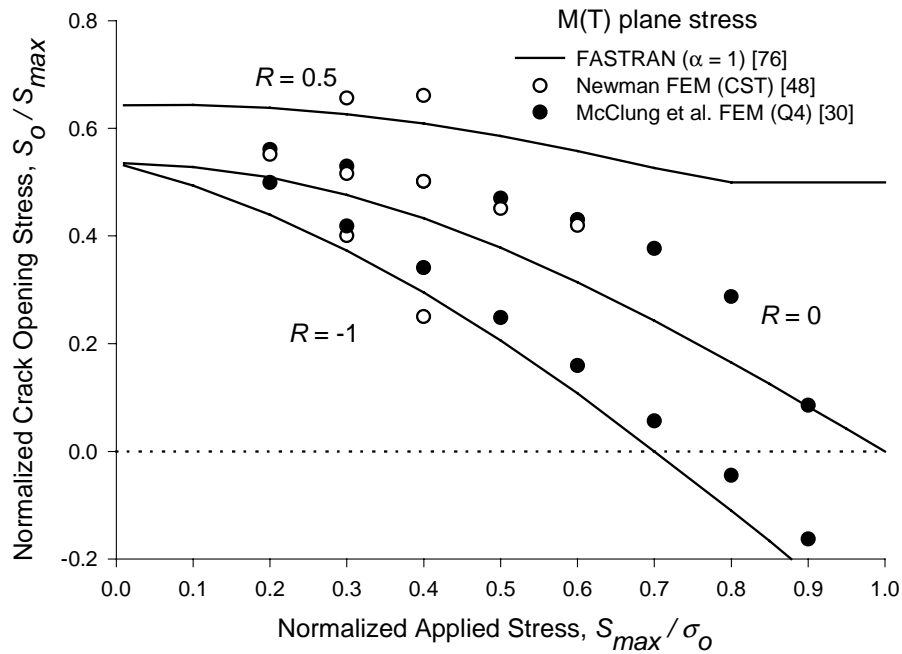
Figure 2-6   Effect of Stress Ratio on Crack Opening Values under Plane-stress

Both of these researchers had approximately 10 elements in the forward plastic zone, which may have resulted in an insufficient number of elements in the reversed plastic zone. This suggests that mesh refinement study is essential to predict crack closure levels and further study is required with higher and lower R ratio, both for positive and negative values.

2-2 Three-dimensional Modeling Aspects

A three-dimensional description of fatigue crack closure would increase the ability to predict crack growth behavior, which is inherently a three-dimensional problem. Even the simplest geometries and loading conditions, such as constant amplitude loading of middle-crack tension (M(T)) specimens, exhibit three-dimensional crack shapes in the form of crack tunneling. More complex geometries, such as surface cracks, or loading conditions, such as spectrum loading, will exhibit or result in even more dramatic shape changes. These shape changes are due to the three-dimensional variation of both the opening stress and the stress intensity factor along the crack front, and cannot be predicted by two-dimensional models.

A relatively small number of investigators have modeled plasticity-induced crack closure in three-dimensional geometries using finite element methods [53-63]. In a three-dimensional geometry, the crack opening value will vary along the crack front. This variation will result in different portions of the crack front growing with different rates under the cyclic loading. Consequently, the crack front shape will naturally evolve. This shape evolution makes modeling of three-dimensional geometries much more complex. For simplicity this shape evolution is generally neglected and the crack front is extended uniformly during the finite element analysis. The three-dimensional component is also more difficult to model because the required finite element meshes are large, inducing a severe computational burden.

The majority of the three-dimensional modeling efforts have considered the M(T) geometry [54,56,57,61-63]. In addition, limited modeling of the plasticity-induced crack

closure in the part-through surface flawed geometry [53,58-60,63] has also been performed.

Chermahini et al. [56-58] were the first to simulate crack growth and closure in three-dimensional geometries, and they considered both the M(T) specimen and the semi-elliptical surface crack. They found an initial rise in the crack opening stresses followed by a subsequent decay. Their results are suspect due to a lack of mesh refinement and an inadequate amount of crack growth, such that the crack opening stresses were not stabilized. However, Riddell et al. [62], using a more refined mesh for the M(T) specimen, have shown similar results.

Recently, Roychowdhury et al. [55] performed finite element analysis of plasticity-induced crack closure under small scale yielding conditions with a zero T-stress and a stress ratio $R = 0$. They computed the opening stresses for a through-crack with thickness B using the second node behind the crack tip. Their results indicated that for a give R value, the normalized opening stress S_o / S_{max} scales with $\lambda = K_{max}/\left(\sigma_o \sqrt{B}\right)$ such that a constant value of λ will always result in the same crack opening stress. They have also shown that for $\lambda = 1$, in the mid-thickness region (plane-strain zone) of the model, little or no closure was noted. On the other hand, at the free surfaces (plane-stress zone), a significant amount of closure was observed. As $\lambda \rightarrow 2$, a sharp change in closure was observed at the mid-thickness region and little change was noted at the free surface.

Seshadri [63] compared predicted opening and closing stresses with experimental (fractograpic) results for the compact-tension, single edge notch, and part-through crack geometries. Significant differences were observed between the experimental and

numerical results. Recently, Skinner et al. [60] compared results from a three-dimensional finite element analysis of the part-through crack with experimental results reported by Putra et al. [77], and showed significant differences between measured and computed crack opening stresses. Blandford et al. [54] and other researchers [65-68] have discussed the difficulties associated with measuring opening load values using experimental methods [54,67-70]. Dawicke et al. [67] have shown that displacement and strain gage crack closure measurements techniques may fail to give a complete description of plasticity-induced crack closure behavior in a thick specimen. They have also shown that while these techniques may be suitable for simple loading conditions, when the loading conditions become more complicated the three-dimensional effects become more pronounced. To accurately model these effects, a better understanding of the three-dimensional aspects of fatigue crack closure is needed.

2-2-1 Mesh Refinement

Mesh refinement issues are more complicated for three-dimensional models. Along the crack front near the free surface a near plane-stress condition exists while a plane-strain condition exists in the interior. Since a plane-stress forward plastic zone is approximately three times larger than a plane-strain forward plastic zone, the numbers of elements in the forward plastic zone in the interior must be used to determine an appropriate mesh size, and regions near the free surface may be over meshed. Zhang et al. [59] was the first to perform a mesh refinement study on a semicircular surface crack, and suggested that the crack opening and closing stresses are influenced by the degree of mesh refinement. Skinner et al. [60] have attempted to determine the required level of

mesh refinement for surface flaws. They proposed that mesh refinement can be quantified in terms of the number of elements present in the forward plastic zone. Their research efforts suggested that five elements in the forward plastic zone are sufficient to obtain stabilized crack opening values as shown in Figure 2-7.
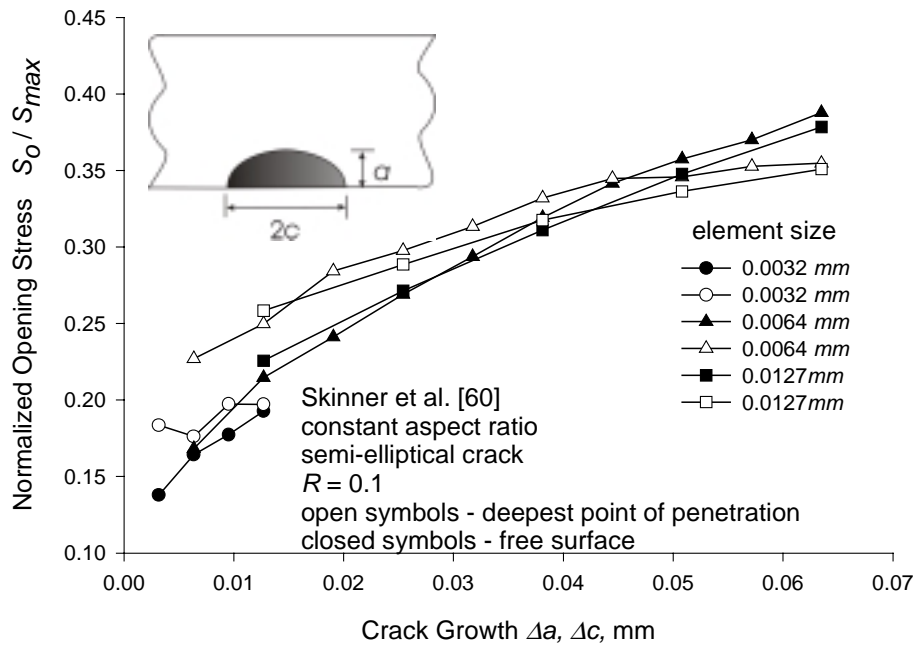
Figure 2-7   Surface Crack Mesh Refinement Studies

2-2-2 Crack Advance Scheme

When modeling crack advance using a node-release scheme, two-dimensional finite element analyses of plasticity-induced crack closure have shown a negligible influence of the specific crack release scheme used. Zhang et al. [59] have performed node releases at three different values of load, 10% of S_{max}, 50% of S_{max}, and at S_{max}, and

found no difference in the crack opening displacement for these crack release schemes, while small differences were noted for the crack opening and closing stresses.

2-2-3 Aspect Ratio Evolution

There is ample experimental evidence to show that the shape of a three-dimensional fatigue crack front changes as the crack grows under cyclic loading [65,77-79]. The aspect ratio (a / c) of a part-through crack changes under cyclic loading [79]. While the crack shape for a through-crack evolves from a straight line to a curved line, with faster growth in the interior. Many researchers have modeled the through-crack and part-through surface crack with a uniform crack extension such that the initial crack shape remains unchanged. However, this is inconsistent with the concept of crack closure where crack growth rate is governed by:

$$ d\eta/dN = C\left(\Delta K_{\mathit{eff}}\right)^{m} \tag{2-4} $$

where $d\eta/dN$ is the growth rate normal to the crack front at a point on the crack front, C and m are material constants and ΔK_{eff} is the effective stress intensity factor.

2-2-4 Influence of Loading History

A number of researchers have modeled plasticity-induced crack closure using two-dimensional finite element analysis with simplified load histories and shown crack retardation and acceleration. Daniewicz et al. [61] was first to attempt a three-dimensional elastic-plastic finite element analysis of a M(T) specimen under variable

amplitude loading. A continual load reduction to simulate the load history associated with fatigue crack growth threshold measurement was employed. Their results indicated the crack opening process is three-dimensional in nature, with regions in the interior opening prior to regions near the free surface.

2-3 Element Types and Configuration

The selection of element types for finite element analysis of plasticity-induced closure has become well established, however there are some important issues that need to be considered when implementing plane-strain conditions for two-dimensional finite element analysis. Most researchers have utilized constant strain triangle or 4-noded quadrilateral elements [8-52], while some of have used higher order quadrilateral elements [13,21] as shown in Figure 2-8.
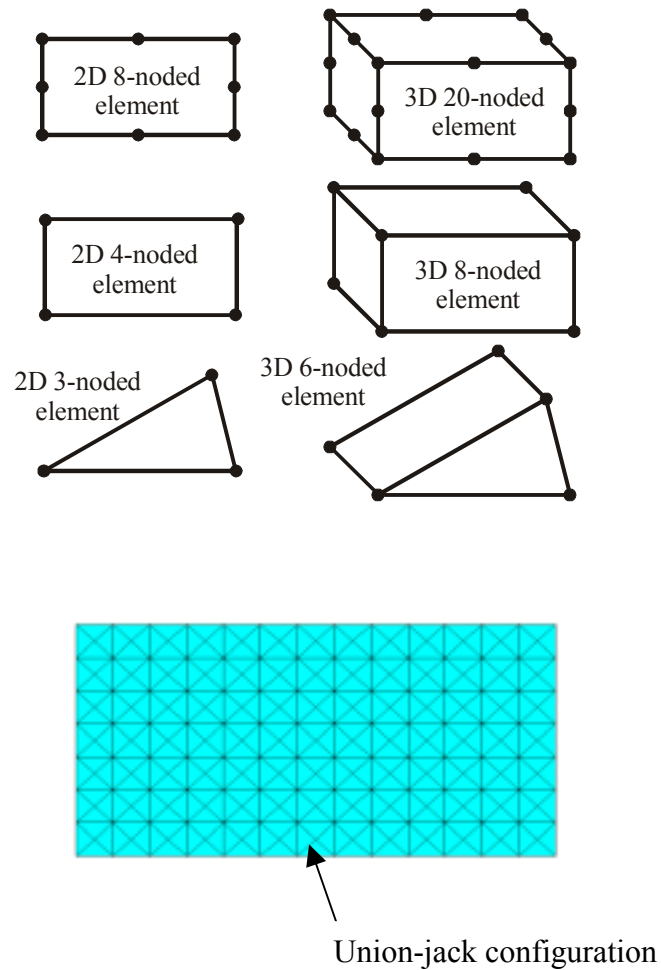
Figure 2-8   Typical Elements and Configuration

During plane-strain analysis these elements generally do not meet the

incompressibility requirement associated with plastic strains as shown by Nagtegaal et al.

[71], and are thus susceptible to plane-strain locking. It has been shown that an

arrangement of constant strain triangular elements in a "union-jack" configuration will

enable the incompressibility requirement to be nearly satisfied [71]. Using a reduced

integration scheme for quadrilateral or constant strain elements is also helpful for

avoiding plane-strain locking. When locking occurs, the stresses oscillate from one element to the next.

For three-dimensional analysis, generally 8-noded elements have been used [53-63], although some researchers have used a 6-noded element [59] as shown in Figure 2-8. In regions along the crack front under plane-strain, these elements are susceptible to plane-strain locking [71]. Again, using a reduced integration scheme for 8-noded and 6-noded elements is helpful for avoiding plane-strain locking [71]. Another similar method to avoid plane-strain locking is the $\bar{B}$ element formulation developed by Hughes [80]. This method replaces the volumetric strain at the Gauss integration points with the average volumetric strain of the element.

2-4 Material Model Effects

The elastic-perfectly plastic material model has been used extensively for two-dimensional and three-dimensional finite element analysis of plasticity-induced crack closure. However, the effects of material hardening have been considered as well, assuming both kinematic hardening and isotropic hardening. Using kinematic hardening will approximate the Bauschinger effect, and the use of isotropic hardening neglects this effect. Hardening will also affect plastic zone sizes, and hence mesh refinement requirements. To date, no finite element modeling effort have employed constitutive equations invoking concepts from cyclic plasticity theory. This, cyclic hardening and softening effects have not been considered, the crack opening values are assumed unaffected by potential shakedown and ratcheting.

Ashbaugh et al. [12] and McClung et al. [31] have shown that power law relationships between effective stress and effective strain generally give higher opening values than linear relationships. McClung et al. [31] have also show that variations in the linear hardening slope also impact the crack opening values. Seshadri [63] was the first to investigate linear and power law material model effects on three-dimensional closure analyses of the compact-tension specimen, the single edge notch specimen, and the part-through crack, and he showed significant differences in the crack opening and closing stress. This may be consequence of inadequate refinement. Similarly, Skinner et al. [60] have used a bi-linear material with kinematic hardening when modeling the surface flaw. A significant change in the opening values was observed as the hardening slope was changed as shown in Figure 2-9.
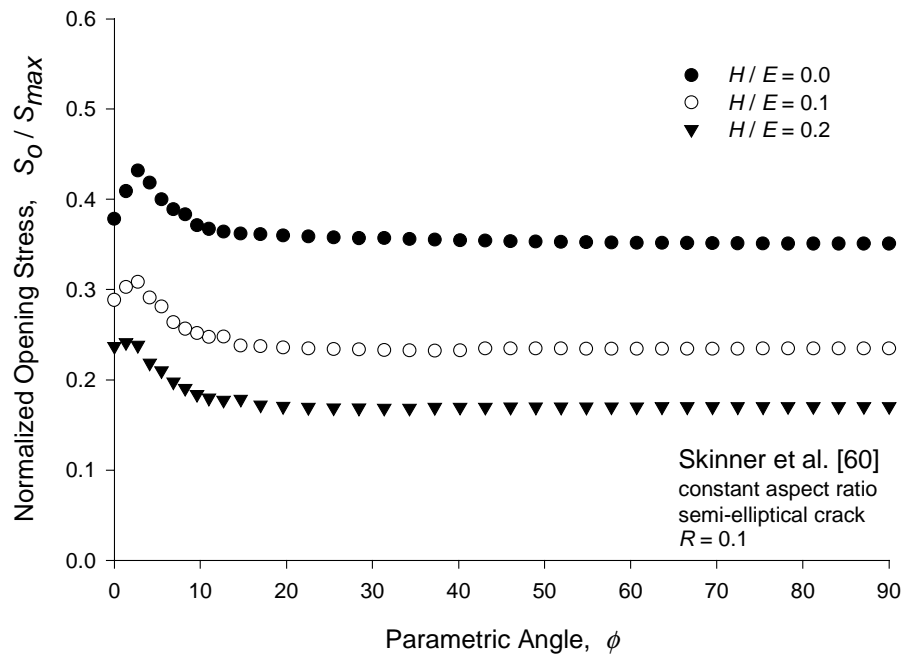
Figure 2-9 Effect of Strain Hardening

Recently, Roychowdhury et al. [55] performed small scale yielding analyses of the three-dimensional through-crack with pure kinematic hardening and they have shown that normalized opening load values remain unchanged for materials with a varying σ_o / E ratio, provided the strain-hardening modulus E_T retains a fixed ratio with E, where E is the Young's modulus and σ_o is the material flow stress.

When the crack of interest is small with respect to the grain size, then the plastic deformation is no longer isotropic and constitutive relationships from crystal plasticity theory are needed. A study of plasticity-induced fatigue crack closure using crystal plasticity theory was first conducted by Gall et al. [81,82]. They studied the growth of a fatigue crack in a single crystal, and showed the effect of crystallographic parameters on the crack opening value. Recently, Potirniche et al. [83] have implemented crystal plasticity theory to study fatigue crack closure for growing fatigue cracks propagating through a grain boundary. As the crack approaches the grain boundary, acceleration and retardation of the crack were noted based upon the crystallographic orientation of the adjacent grain.

2-5 Overview of Thesis

Finite element analysis is a promising tool for simulating and predicting plasticity-induced fatigue crack closure based parameters. In this thesis several modeling issues were considered. First, a two-dimensional mesh refinement study was performed considering different geometries with different element types and configurations under both plane-stress and plane-strain. Different means of mesh refinement were also

considered, in order to reduce the number of elements and nodes, thereby reducing computational time. Secondly, in-plane constraint was varied to predict the effect on computed crack closure level under plane-strain. The effect of the crack node release schemes on the crack opening values were also studied. Under plane-stress, the effect of varying the load ratio R with different stress levels on different geometries was studied. Next, the different crack opening value assessment locations were compared and a unique new methodology was developed to compute crack opening values.

For three-dimensional analyses, mesh refinement criteria were set for the part-through crack. The effect of crack node release schemes and a spike overload on the crack opening values were studied. A new methodology was developed to model crack shape evolution.

CHAPTER III

FINITE ELEMENT ANALYSIS

The plasticity-induced fatigue crack closure model concepts were incorporated into the finite element package ANSYS using ANSYS Parametric Design Language (APDL) by Skinner [53], and were modified to accommodate many other aspects of modeling plasticity-induced crack closure in this research. A command line listing for all the routines involved for two-dimensional finite element analysis is included in Appendix A. Sample input files for different planer geometries are included in Appendix B. For three-dimensional analysis, command line routines involved are included in Appendix C.

The basic finite element algorithm of modeling plasticity-induced fatigue crack closure is conceptually simple. A mesh is created with an initial crack, and the mesh is loaded by remotely applied tractions. For constant amplitude loading, the loading is cycled between a maximum applied stress S_{max} and a minimum applied stress S_{min}. During the cyclic loading the crack is advanced in some fashion, leading to the formation of a plastic wake behind the crack tip. This modeling concept is simple; however, there are several issues which must be addressed during the fatigue crack growth simulation.

34

3-1 Two-dimensional Finite Element Analysis

Fatigue crack closure analyses were performed using ANSYS 6.1 [84]. Two-dimensional finite element analyses of compact-tension (C(T)), middle-crack tension (M(T)) and bend (SEB) geometries were conducted using 4-noded quadrilateral elements and 3-noded triangular elements under plane-stress and plane-strain conditions. The material was assumed to be elastic-perfectly plastic with modulus of elasticity $E =$ 200 GPa and flow stress $\sigma_o = 230$ MPa. A load ratio $R = 0$ and -1.0 was selected. The von-Mises yield criterion and associated flow rule were used. Small deformation theory was employed, except where noted.

Most of the previous finite element analyses reported in the literature for plane-strain analysis utilized CST and 4-noded quadrilateral elements. These elements generally do not meet the incompressibility requirement associated with plastic strains as shown by Nagtegaal et al. [71], and are thus susceptible to plane-strain locking. They have shown that an arrangement of constant strain triangular elements in a "union-jack" configuration will enable the incompressibility requirement to be nearly satisfied. They also found that a reduced integration method for quadrilateral or CST elements is helpful for avoiding plane-strain locking. When locking occurs, the stresses oscillate from one element to the next. Another similar method to avoid plane-strain locking is the $\overline{B}$ element formulation developed by Hughes [80]. This method replaces the volumetric strain at the Gauss integration points with the average volumetric strain of the element. The present study includes an evaluation of all the above element types and configurations, as well as the reduced integration method.

Fatigue crack growth was modeled by repeatedly loading the geometry, advancing the crack, then unloading. A large amount of crack growth may be required before stabilized crack opening values are generated. The model was incrementally loaded to the maximum load (loading increments of 0.0125 S_{max}), at which time the crack tip node was released, allowing the crack front to advance one elemental length Δa per load cycle. The applied load was then incrementally lowered until the minimum load was attained (unloading increments of 0.0125 S_{max}). Crack surface closure was modeled by changing the boundary conditions on the crack surface nodes. During unloading the crack surface nodal displacements were monitored and if the nodal displacement became negative the node was closed and node fixity was applied to prevent crack surface penetration. Similarly, during loading the reaction forces on the closed nodes were monitored and when the reaction force became positive the nodal fixity was removed. Herein, the remote load at which the last fixity is removed is defined as the crack opening load and corresponds to the closest node to the crack tip. The opening loads can be found only to the resolution of the loading increment. To obtain a better estimate of the load when the crack surface actually opens, linear interpolation was used. For the load step before the crack surface node opens, the nodal reaction force is negative. Upon opening, the reaction force becomes positive. Linear interpolation is used to determine the remote load at which the reaction force became zero. The cyclic loadings were repeated as necessary to produce a prescribed amount of crack growth. Meshes with a higher degree of refinement and smaller element size Δa required more load cycles to produce a prescribed amount of crack growth. Each load cycle consisted of two complete elastic-plastic monotonic analyses.

In order to determine the initial finite element mesh, an iterative technique was employed. An initial mesh was designed to give perhaps 2 to 3 elements ahead of crack tip in the initial forward plastic zone using the following approximate equation [74]

$$2r_f = \frac{1}{\alpha\pi}\left(\frac{K_{max}}{\sigma_0}\right)^2 \tag{3-1}$$

where α is equal to 1 and 3 for plane-stress and plane-strain respectively. Following a monotonic analysis, if the actual initial forward plastic zone extended out of the refined region and into the transition region (as shown in Figure 3-3) then the refined region was enlarged so that the entire plastic zone was captured. This procedure was used to obtain the initial mesh and subsequent initial Δa value to perform crack growth analyses for both geometries. To study the effects of mesh refinement, crack growth analyses were next performed after reducing the element size consecutively by a factor of 1/2 or 1/3. Each time a more refined mesh was used, the same amount of total crack growth was modeled. This naturally led to an extremely refined mesh and the use of many load cycles. For perspective, the element sizes reported in the literature normalized with equation 3-1 are shown in Figures 3-1a and 3-2. In Figure 3-1b the element sizes are normalized with the specimen width W. Clearly, the meshes used in the current study are significantly more refined than many of those discussed in the literature.

plane strain (a)

● present study
□ Fleck et al. (1988) [9]
△ McClung et al. (1991) [7]
○ Kfouri (1983) [15]
▽ Ashburgh et al. (1997) [12]
⬡ Blom et al. (1985) [11]
⊙ Ogura et al. (1977) [10]
⌂ Fleck (1986) [8]

Normalized Element Size, $\Delta a/r_f$

plane strain (b)

● present study
□ Fleck et al. (1988) [9]
△ McClung et al. (1991) [7]
○ Kfouri (1983) [15]
▽ Ashburgh et al. (1997) [12]
⬡ Blom et al. (1985) [11]
⊙ Ogura et al. (1977) [10]
⌂ Fleck (1986) [8]

Normalized Element Size, $\Delta a/W$ (log scale)
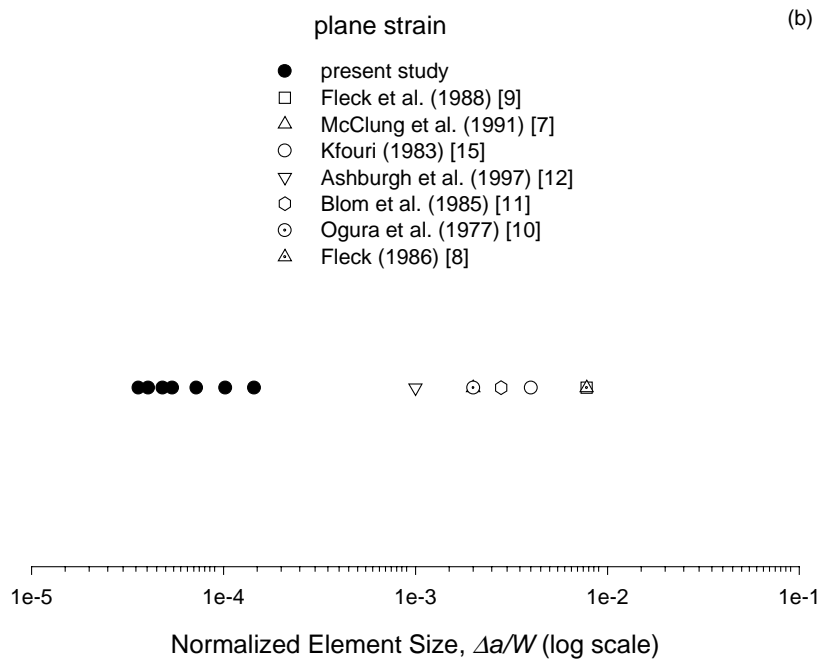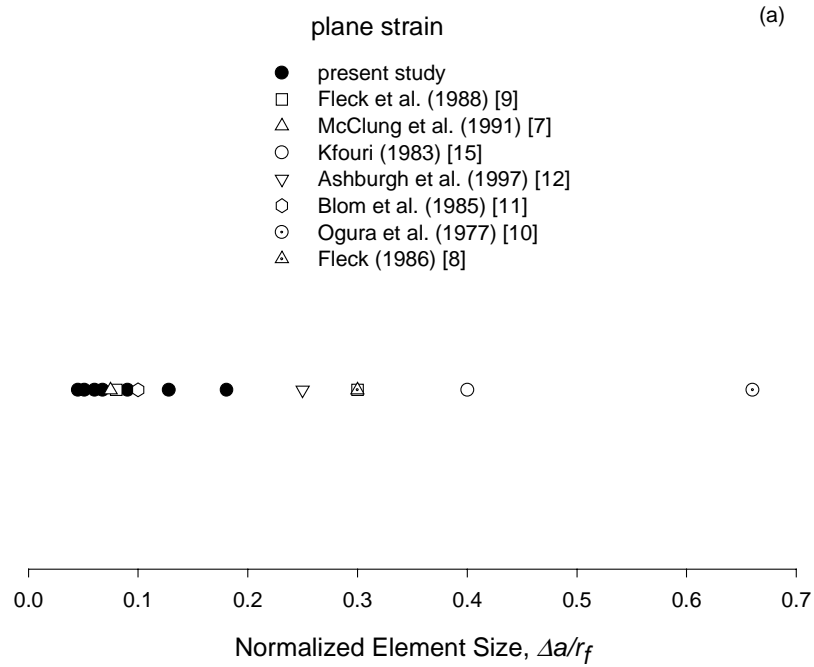
Figure 3-1   Distribution of Mesh Refinement Levels under Plane-strain

The C(T), SEB and M(T) geometries are shown in Figure 3-3. The C(T) geometry had an initial crack length of 25 mm with $a/W = 0.33$, SEB geometry has initial crack length of 2 mm with $a/W = 0.1$, and the M(T) geometry had an initial crack length of 4 mm with $a/W = 0.1$. The maximum loading was selected to give the same initial maximum normalized stress intensity factor $K_{max}/\sigma_o = 1.07 \sqrt{mm}$ in all the geometries, and thus approximately similar initial forward plastic zone sizes. The effect of different applied stress levels and load ratios under plane-stress condition were also study with the M(T) and the SEB specimens.
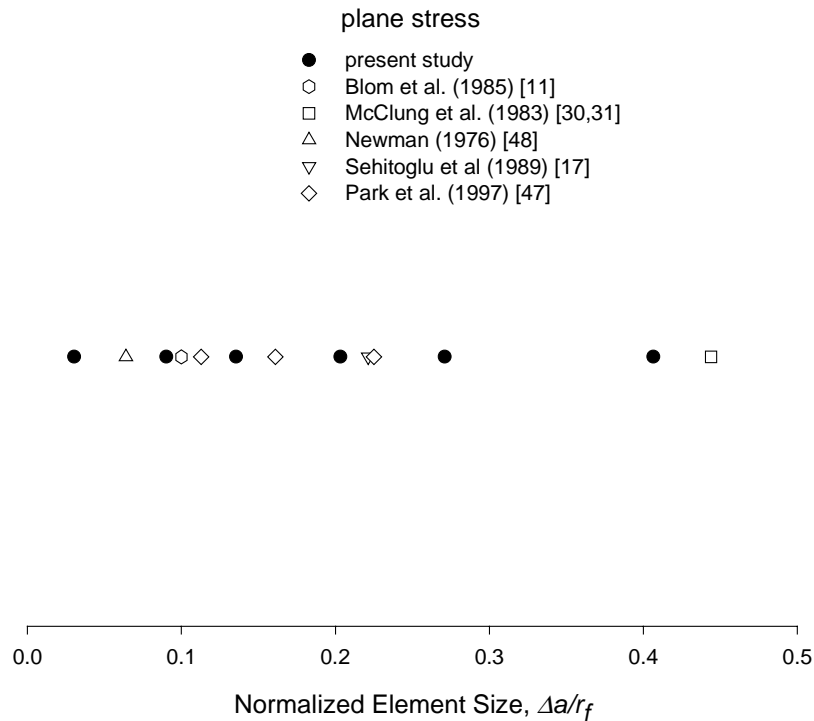
Figure 3-2   Distribution of Mesh Refinement Levels under Plane-stress

$a = 4 \; mm$

$H = 40 \; mm$

$W = 40 \; mm$

$S = 69 \; N/mm^2$

Number of elements = 7759
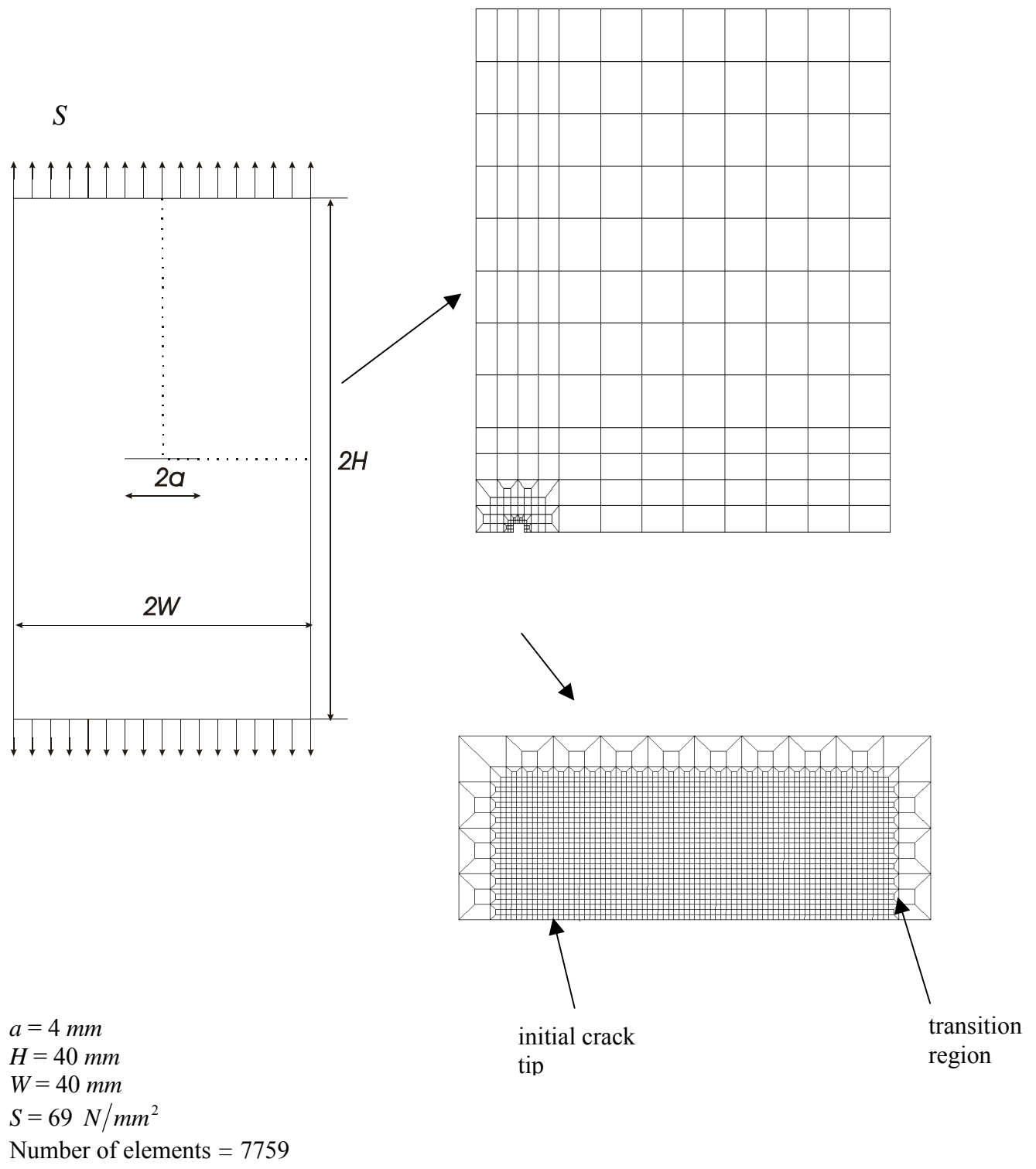
Figure 3-3a   Typical Middle-crack Tension Model

a = 25 *mm*
W = 76 *mm*
P = 355 *N*
Number of elements = 11759
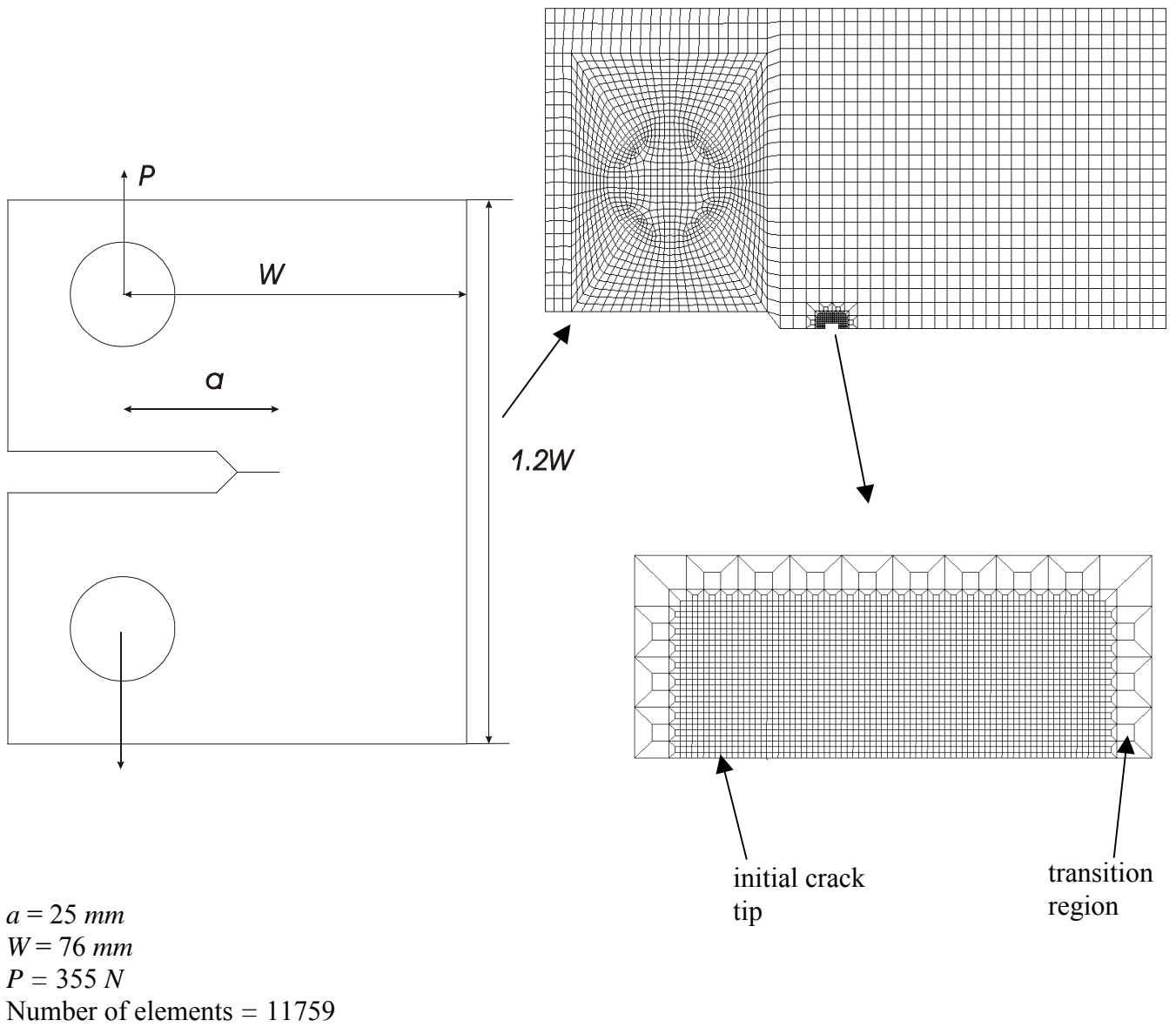
Figure 3-3b   Typical Compact Tension Model

$a = 2\ mm$
$W = 20\ mm$
$H = 40$ mm
$M = 314.385\ N\ mm$
Number of elements = 30444

transition region

initial crack tip
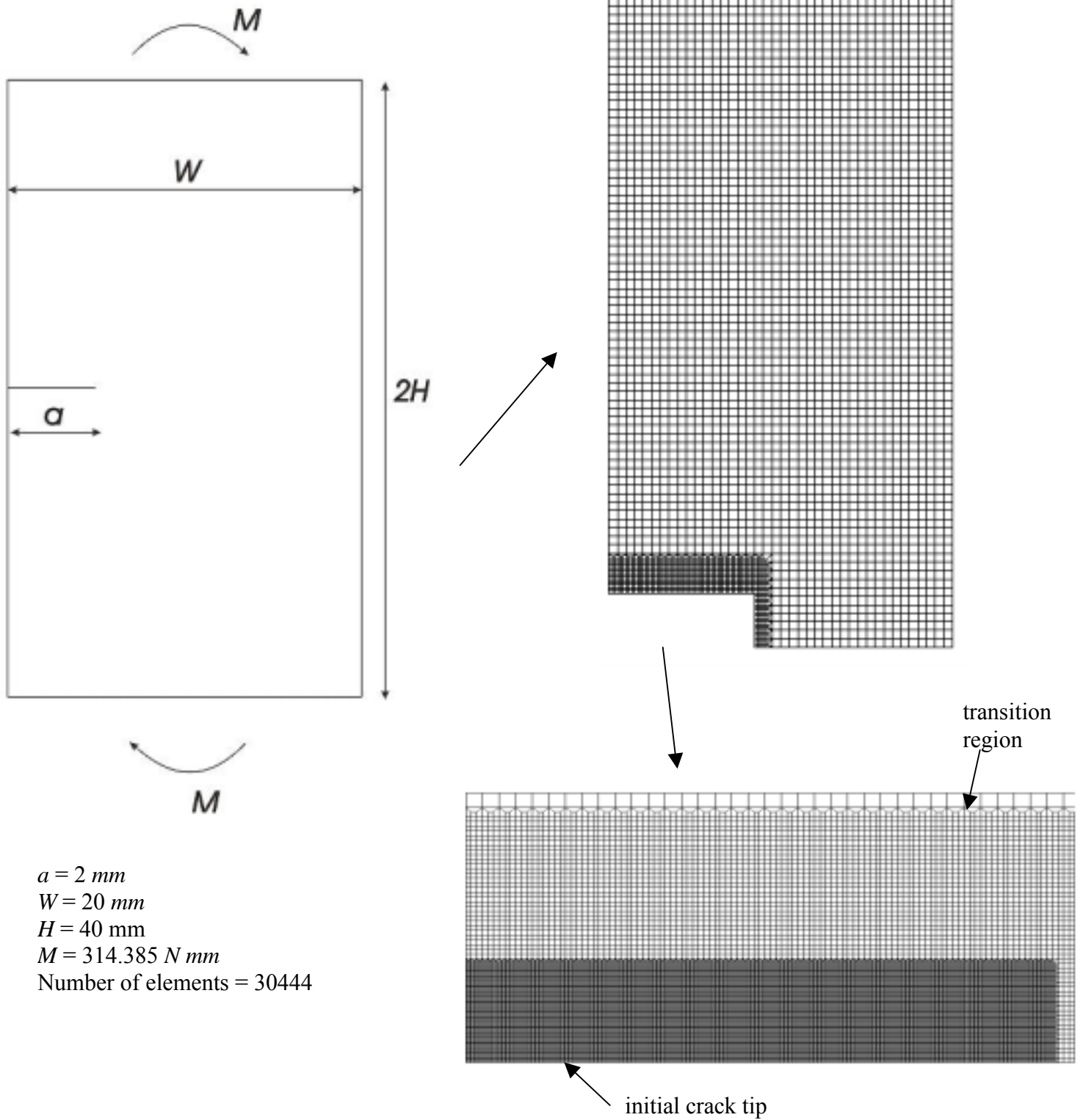
Figure 3-3c   Typical Side Edge Bend Model

3-2 Three-dimensional Finite Element Analysis

A three-dimensional description of fatigue crack closure would increase the ability to predict crack growth behavior, which is inherently a three-dimensional problem. Even the simplest geometries and loading conditions, such as constant amplitude loading of middle crack tension (M(T)) specimens, exhibit three-dimensional crack shapes in the form of crack tunneling. More complex geometries, such as surface cracks, or loading conditions, such as spectrum loading, will exhibit or result in even more dramatic crack shape changes. These shape changes are due to the three-dimensional variation of both the opening stress and the stress intensity factor along the crack front, and cannot be predicted by two-dimensional models.

Fatigue crack closure analyses were performed using ANSYS 6.1 [84]. Three-dimensional finite element analyses of part-through surface crack were conducted using 8-noded brick elements. The material was assumed to be elastic-perfectly plastic with modulus of elasticity $E = 1060$ ksi and flow stress $\sigma_o = 75$ ksi. A load ratio $R = 0.1$ was selected. The von-Mises yield criterion and associated flow rule were used. Small deformation theory was employed, except where noted. The part-through surface flaw geometry is shown in Figure 3-4. The surface crack geometry had an initial aspect ratio $a/c = 1.0$ with $a/w = 0.1$ and $t/w = 1.0$.
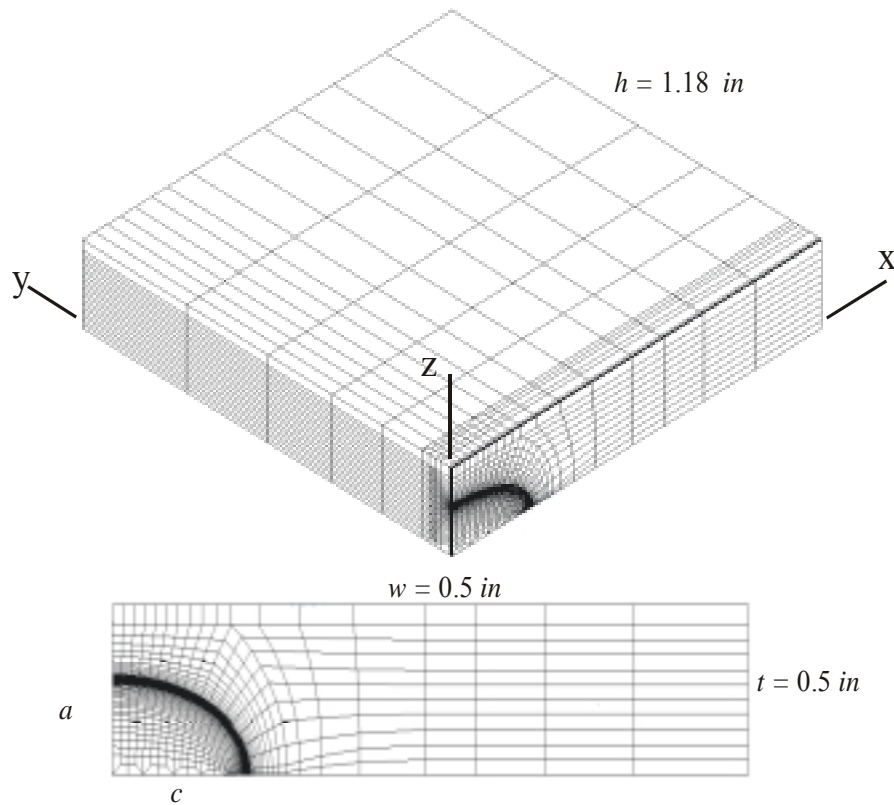
Figure 3-4   Typical Surface Crack Mesh

Mesh refinement issues become complicated for three-dimensional models. For a semi-circular flaw, at the free surface a plane-stress condition exists while a plane-strain condition is present at the deepest point of penetration. Since a plane stress plastic zone is approximately three times larger than a plane strain plastic zone, the number of elements in the plastic zone at the deepest point of penetration should be used to determine an appropriate mesh size. Unfortunately, this forces the mesh to have more than adequate refinement at the free surface, and necessitates nearly three times as many load cycles for crack opening level stabilization in this region. Similar approach was employed to determine initial mesh size as used for two-dimensional.

There is ample experimental evidence to show that the shape of a three-dimensional fatigue crack front changes as the crack grows under cyclic loading [65,77-79]. The aspect ratio (a / c) of a part-through crack changes under cyclic loading [79], while the crack shape for a through-crack evolves from a straight line to a curved line, with faster growth in the interior. To date, most researchers have modeled the through-crack and the part-through surface crack with a uniform crack extension such that the initial crack shape remains unchanged. However, this is inconsistent with the concept of crack closure where crack growth rate is governed by:

$$\frac{d\eta}{dN} = C\left(\Delta K_{eff}\right)^{m} \tag{3-2}$$

where $\frac{d\eta}{dN}$ is the growth rate normal to the crack front at a point on the crack front, C and m are the material constants, and ΔK_{eff} is the effective stress intensity factor at the point of interest.

The above methodology will be employed and equation 3-2 will be used at each point along a semi-circular crack front to model both plasticity-induced crack closure and the subsequent aspect ratio evolution. Since the fatigue crack growth behavior of materials can be anisotropic, unique material constants C and m were determined for the deepest point of penetration and the free surface using experimental data [78,79]. A linear interpolation was used to find the material constants for each node along the crack front. The Newman-Raju stress intensity factor equation [85] was employed to compute ΔK_{eff}, using the opening stress values from the finite element analysis. Lastly closure behavior will be studied under single spike overload factor of 1.5.

CHAPTER IV

FINITE ELEMENT RESULT

4-1 Two-dimensional Finite Element Analysis

4-1-1 Geometry Effect on Closure under Plane-strain Condition

To determine the sizes of the forward and reversed plastic zones in all the geometries, normalized values of the von-Mises stress σ_e/σ_o were plotted ahead of crack tip. A typical result is shown in Figure 4-1 for the M(T) geometry under plane-strain. Similar results were also found for the C(T) geometry. A crack growing under cyclic loading with $R = 0$ showed a reversed plastic zone of about 1/10 the forward plastic zone. This is in contrast to the stationary crack, which theoretically exhibits a reversed plastic zone of 1/4 the forward plastic zone [86]. This difference is a consequence of the plastic wake which forms behind the growing crack. A criterion of $0.95 \leq \sigma_e/\sigma_o \leq 1$ was assumed to define the number of elements in the reversed and forward plastic zones.
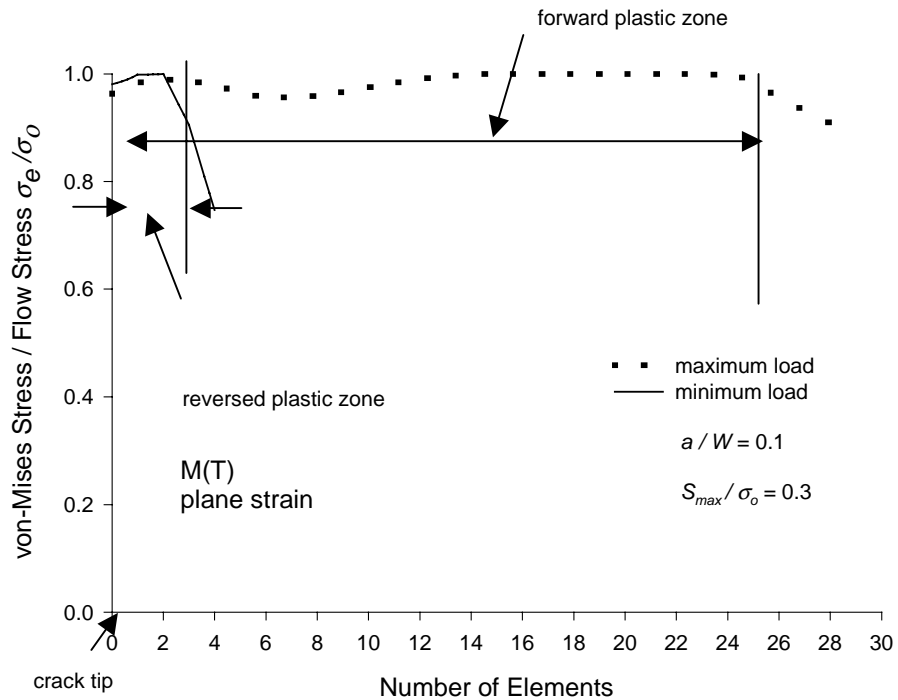
Figure 4-1 Crack Tip Plastic Deformation for Growing Crack

The mesh refinement studies were next performed. Each mesh was refined until a converged opening load was determined. Figure 4-2 illustrates the variation in the number of elements in the plastic zones for the C(T) and the M(T) specimens as the mesh refinement was carried out. It is clear from the figure that the number of elements along the crack plane in the reversed plastic zone are significantly lower than in the forward plastic zone. Thus, a large refinement level is required to accurately capture the reversed plastic zone.
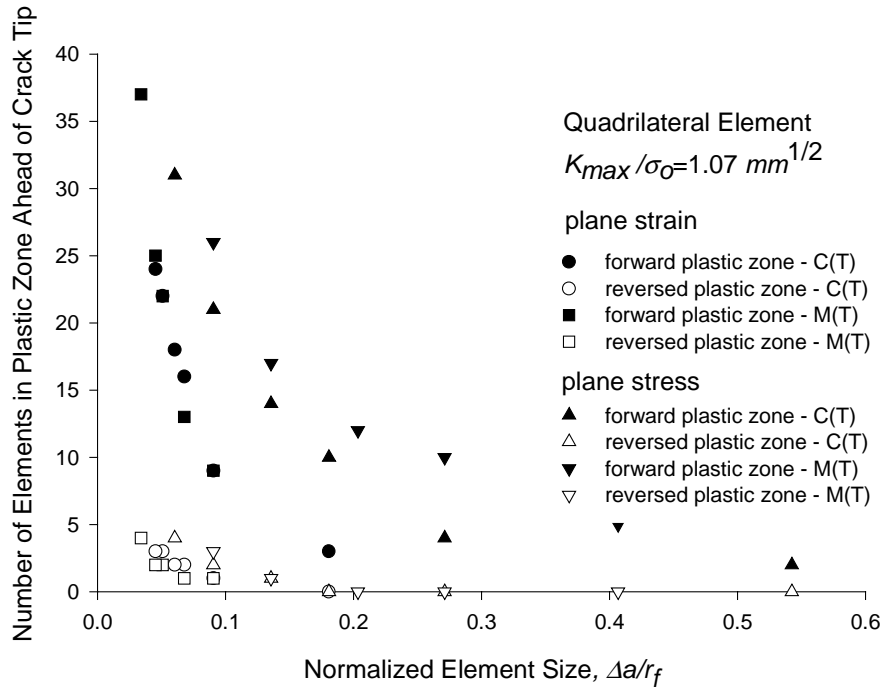
Figure 4-2 Variation in the Plastic Zone Sizes with Mesh Discretization

Several mesh refinement issues were studied in an effort to reduce the number of nodes and elements. If the total size of the highly refined region is reduced such that the initial plastic zone extends outside this region, then a significant reduction in the total number of elements can be achieved. However, when the initial forward plastic zone was allowed to extend into the transition region, the opening value found gave poor agreement with the value found when the initial forward plastic zone was fully captured by the finely meshed region. The influence of the proximity of the crack tip to the transition elements was studied. It was found that if the crack tip was too close to the transition region, significant variation in the opening values resulted. Thus, a refined mesh was required behind, ahead, and above the crack tip. Lastly, the size of adjacent

elements within the transition region was studied and it was found that a gradual

transition with a size ratio less than or about 3 is needed.
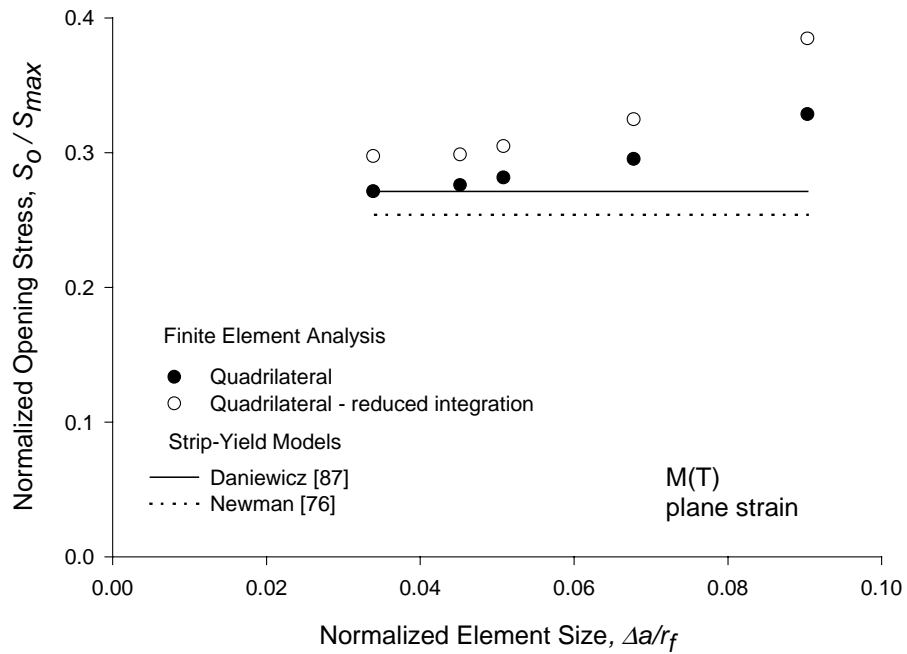
Figure 4-3a Comparison of Calculated Crack Opening Values under Plane-strain (M(T) Specimen)
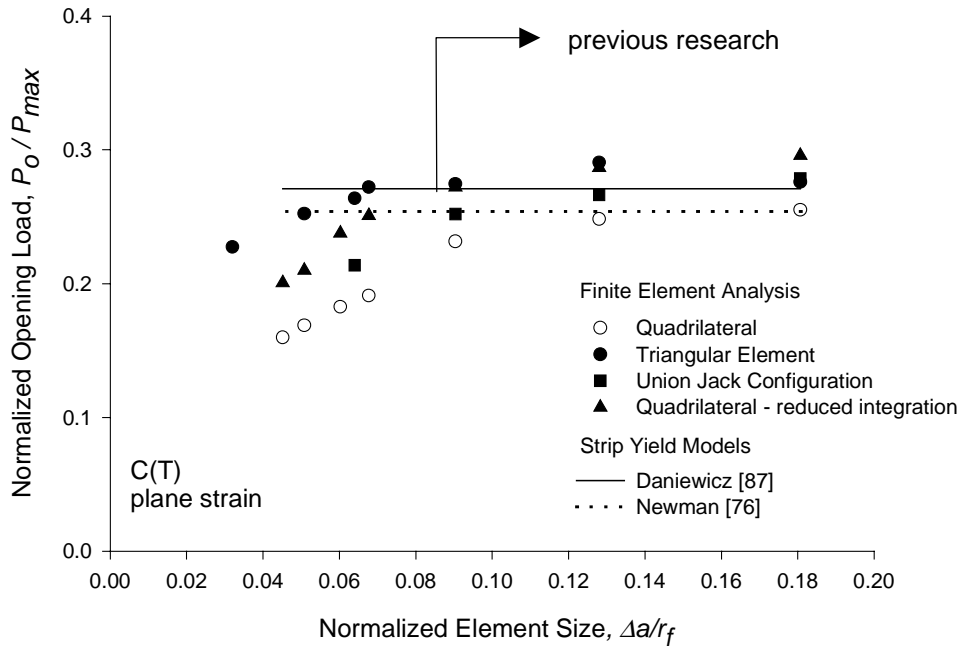
Figure 4-3b Comparison of Calculated Crack Opening Values under Plane-strain (C(T) Specimen)

The degree of mesh refinement was continued until convergence of the opening

values was observed as shown in Figure 4-3. The opening loads were also compared with

results from two strip-yield models [76,87] assuming plane-strain conditions. It is clear

from Figure 4-3a that for the M(T) geometry the opening stresses converged as the mesh

refinement was carried out. For the C(T) geometry, the opening loads did not converge as

seen in Figure 4-3b. The opening values reported were steady state after growing

approximately twice the initial forward plastic zone, and typical results are illustrated in

Figure 4-4. It should be noted from Figures 4-2 and 4-3a that for the M(T) specimen,

approximately 3 to 4 elements are required in the reversed plastic zone to obtain an

accurate opening stress. Considering only the coarse meshes in Figure 4-3b, some

semblance of convergence is apparent, which explains why previous studies found in the

literature have reported the existence of crack closure under plane-strain. Further

refinement results in a continuing decrease in the opening values, which suggests that

little or no closure exists under plane-strain for the C(T) specimen. The author would

discourage the notion of extrapolating the results in Figure 4-3b to smaller Δa values

since a converged crack opening value would approach a horizontal asymptote. Other

potential reasons for this lack of convergence include plane-strain locking and excessive

plastic deformation.
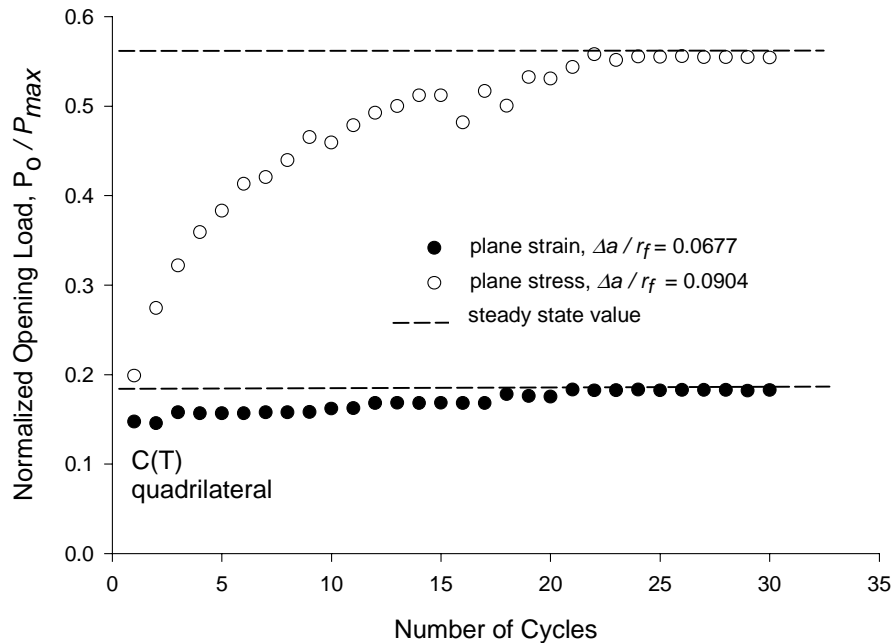
Figure 4-4 Typical Crack Opening Load Transient Behavior

Analyses were also performed using CST elements. A similar variation in opening

values was noted as the mesh refinement was carried out. The results are also shown in

Figure 4-3b. The opening values found utilizing the CST elements were higher than those

obtained using the quadrilateral elements. Plane-strain locking behavior can potentially

influence the predicted opening values and the arrangement of CST elements in a "union-jack" configuration can help to minimize this effect [71]. Additional analyses were performed utilizing CST elements arranged in a "union-jack" configuration and the results are again shown in Figure 4-3b. As seen in the figure, no improvement was observed with regard to convergence. Another technique to minimize the effects of plane-strain locking is to employ a reduced integration method [71]. Analyses were performed on the C(T) and the M(T) specimens using quadrilateral elements with reduced integration. It can be seen from Figure 4-3b that using reduced integration also resulted in a lack of convergence for the C(T) specimen.

Additional analyses were performed to determine if excessive plasticity was the reason for the lack of C(T) convergence, with the applied maximum load reduced by a factor of 2. The total amount of crack growth simulated was the same. The results are shown in Figure 4-5a. It is seen that the C(T) geometry with the lower load also did not converge. Lastly, the large-scale deformation option within ANSYS was used. From Figure 4-5a, enabling large-scale deformations also did not improve convergence.
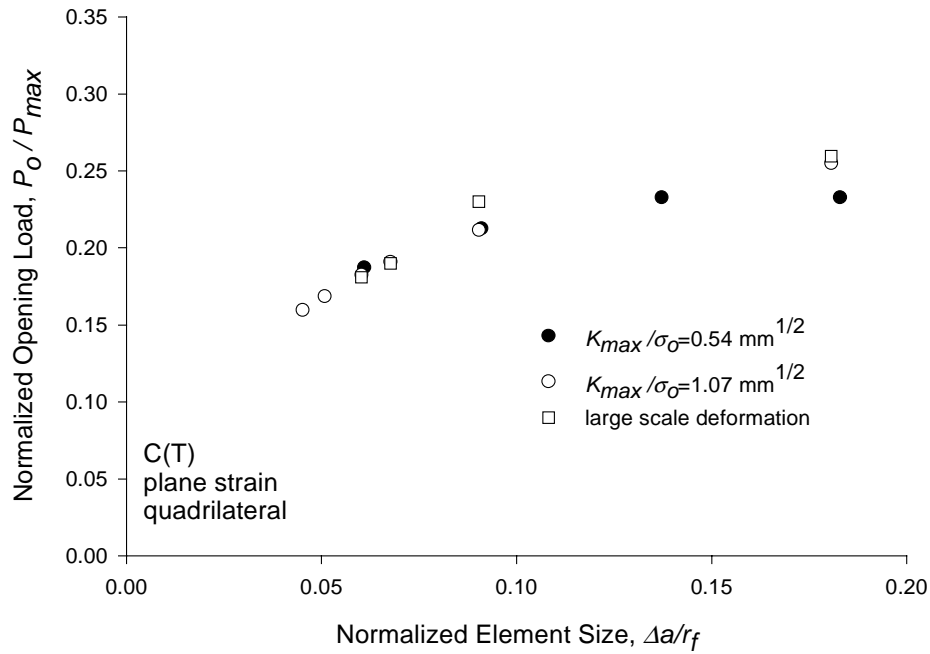
Figure 4-5a Effect of Load and Large-scale Deformation

It is also possible that the observed lack of C(T) convergence is an artifact of the crack growth algorithm. McClung et al. [7,30,31] have shown little or no difference in opening behavior when the crack is advanced at maximum or minimum load. To verify this, analyses were performed to observe the effects of the node-released scheme. The C(T) specimen was modeled to allow the node to release and the crack to advance at minimum load. A similar opening behavior trend was observed and is shown in Figure 4-5b. The results presented in this figure indicate that the node-released schemes are not responsible for the lack of opening value convergence.
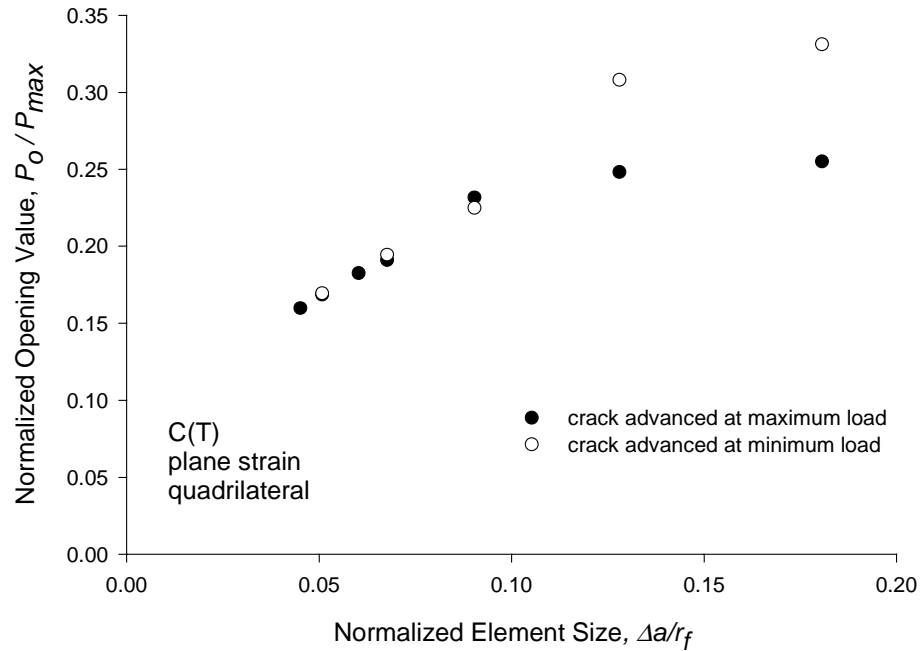
Figure 4-5b Effect of Node-Release Schemes

The consequence of assuming plane-strain for the C(T) geometry was next

investigated. Plane-stress analyses were performed for the M(T) and the C(T) specimens

with the same original crack length and maximum stress intensity factor. The results are

shown in Figures 4-4 and 4-6, and it appears that under plane-stress conditions

convergence is readily achieved and in-plane constraint has negligible effects on closure.

It should be noted from the Figures 4-2 and 4-6 that approximately 3 to 4 elements are

required in the reversed plastic zone to obtain an accurate opening value.
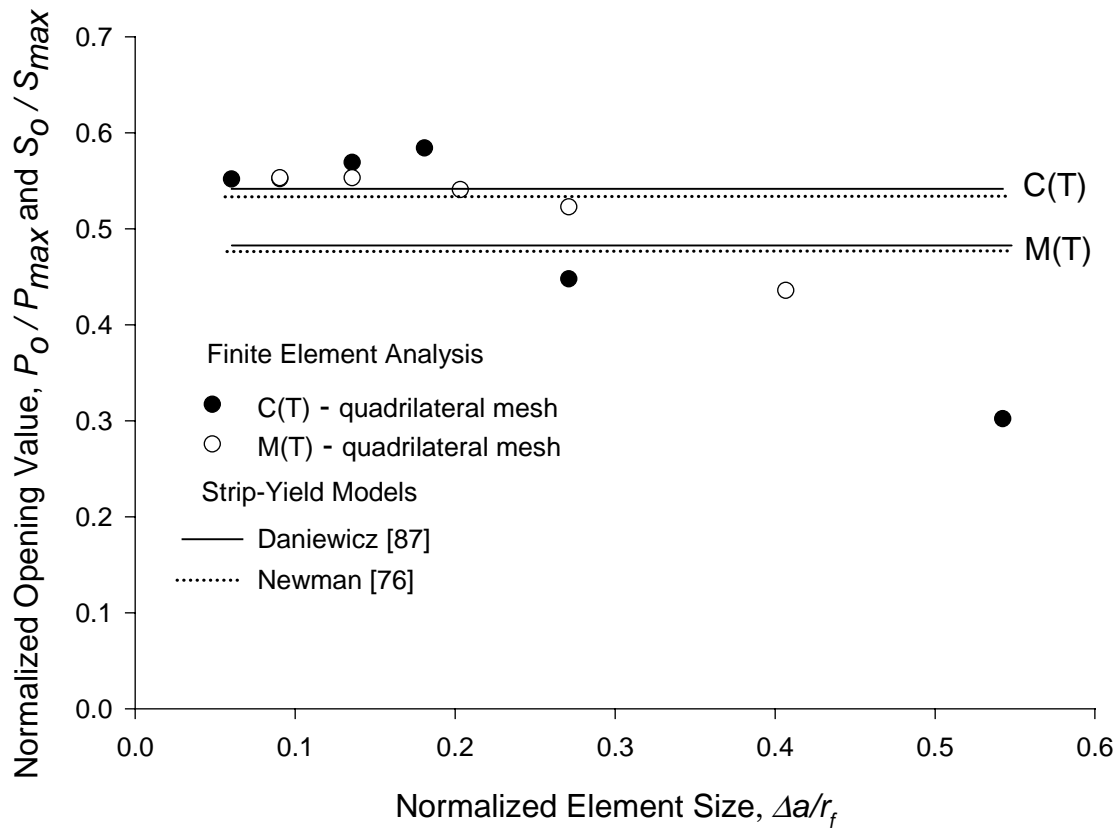
Figure 4-6 Comparison of Calculated Crack Opening Values under Plane-stress

To further address the existence of closure for the C(T) specimen under plane-strain, the crack opening profile for the final cycle of loading was evaluated and is shown in Figure 4-7. If closure does occur, then the opening process should be smooth with the load required to open the crack monotonically increasing as the distance from the original crack tip increases. From Figure 4-7a, a coarse mesh under plane-strain exhibits some semblance of a smooth opening process, but as the refinement is carried out the entire crack is predicted to open instantaneously with the exception of the node just behind the crack tip. This would suggest that there is negligible closure in plane-strain for the C(T)

specimen. To justify this statement further, the opening behavior of the M(T) and C(T)

specimens were compared. An approximately monotonically increasing opening of the

crack was noted for the M(T) specimen during loading as shown in Figure 4-7b, which

implies that closure does occur for the M(T) specimen under plane-strain conditions. For

further evaluation, the crack opening behavior was compared under plane-strain and

plane-stress conditions for the C(T) specimen. Monotonically increasing opening

behavior under plane-stress was observed, similar to the M(T) specimen under plane-

strain, as shown in Figure 4-7c.
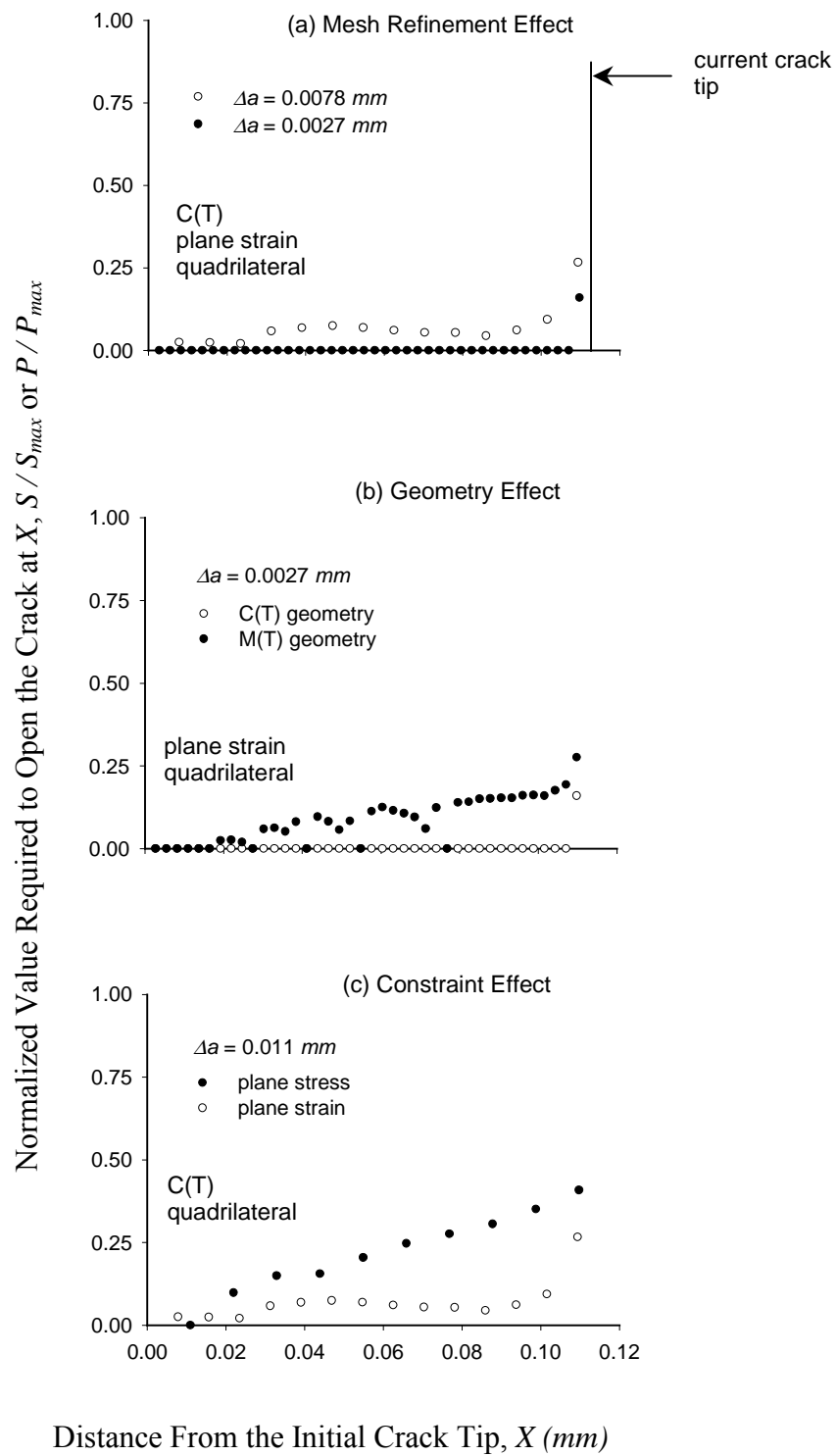
Figure 4-7 Crack Opening Process

Crack closure was observed immediately behind the crack tip for the C(T)

specimen under plane-strain as seen for the refined mesh in Figure 4-7a. This behavior is

believed to be an artifact of the finite element approximation. Computing opening values

at the second node behind the crack tip may help to reduce the approximation error.

Figure 4-8 shows the opening behavior convergence for the C(T) specimen under plane-

strain when using the second node behind the crack tip to obtain the opening load. Trends

similar to those observed when using the node immediately behind the crack tip were

seen for constant strain triangle, but in case of quadrilateral, quadrilateral with reduced

integration, and union-jack, as the mesh refinement is carried out a zero opening value

was observed which again suggests that closure is negligible for the C(T) specimen under
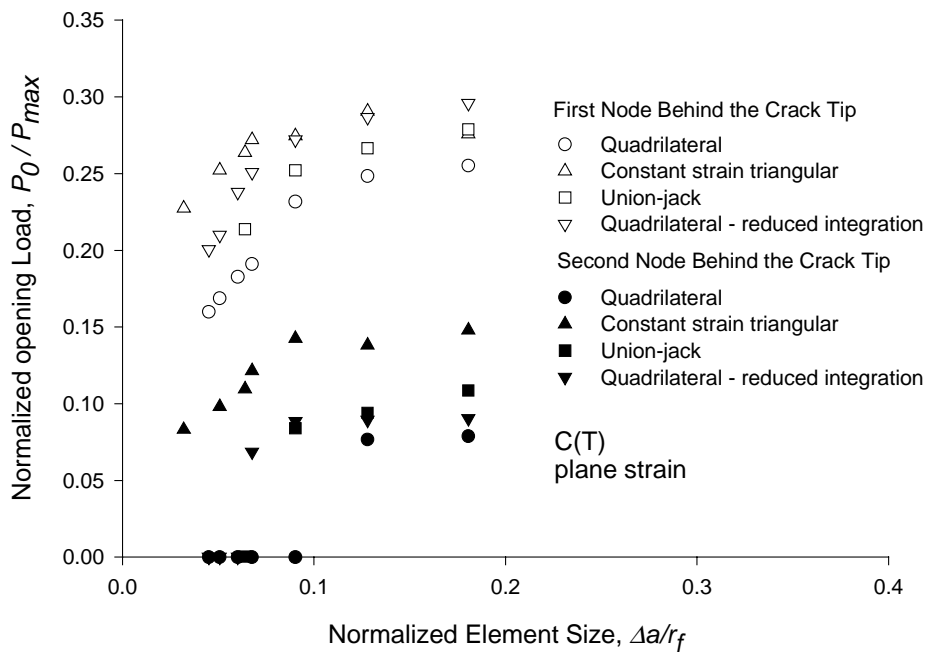
plane-strain.

Figure 4-8 Effect of Assessment Location

Significant closure levels were observed under plane-strain conditions for the

M(T) specimen, but not for the C(T) specimen. Consequently, a geometry effect is clearly

evidenced. One way these two geometries differ is that each exhibits a distinctly different

in-plane constraint, as quantified using the elastic T-stress. To evaluate the influence of

the T-stress, the M(T) specimen was modeled with an externally induced T-stress to

observe the subsequent change in closure levels. A T-stress was induced by applying

tractions parallel to the crack in addition to the conventional tractions perpendicular to

the crack. When no tractions parallel to the crack are applied, the M(T) specimen exhibits

an inherent compressive T-stress, where the T-stress is defined as [74]:

$$T = \frac{K_I \beta}{\sqrt{\pi a}} \tag{6}$$

where a is the crack length, K_I is the stress intensity factor, and β is the biaxiality ratio.

This ratio is equal to -1 and 0.425 for the M(T) and C(T) geometries respectively [75].

The M(T) specimen has $T = 0$ when it is loaded biaxially [75].
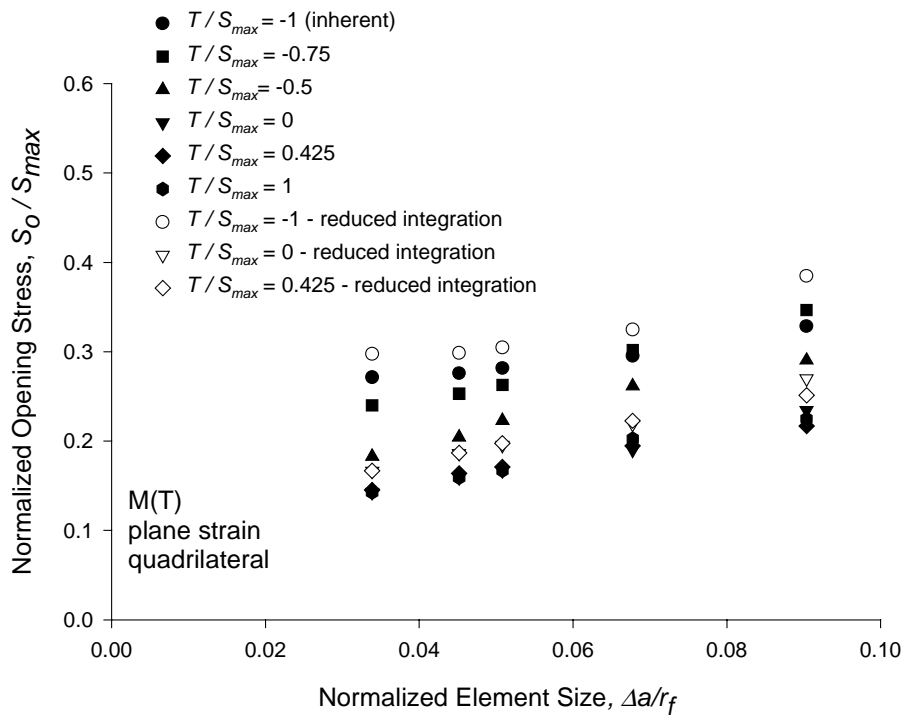
Figure 4-9 Effect of *T*-stress

To explore the influence of the *T*-stress, the M(T) specimen was modeled with an externally induced *T*-stress $-0.75 \leq T/S_{max} \leq 1$. The subsequent opening behavior is shown in Figure 4-9. This figure shows the opening behavior convergence of the M(T) specimen under different in-plane constraint values. As the mesh refinement was carried out non-convergence was noted for $-0.75 \leq T/S_{max} \leq 1$, including the value β = 0.425 associated with the C(T) specimen. The crack opening process is shown in Figure 4-10. Both of these figures indicate that crack closure is negligible or is not occurring for $-0.75 < T/S_{max} \leq 1$. As the *T*-stress become more tensile in value (including the *T*-

stress related to C(T) specimen), the crack front was fully open except for the element

just behind the crack tip, which would indicate negligible closure.
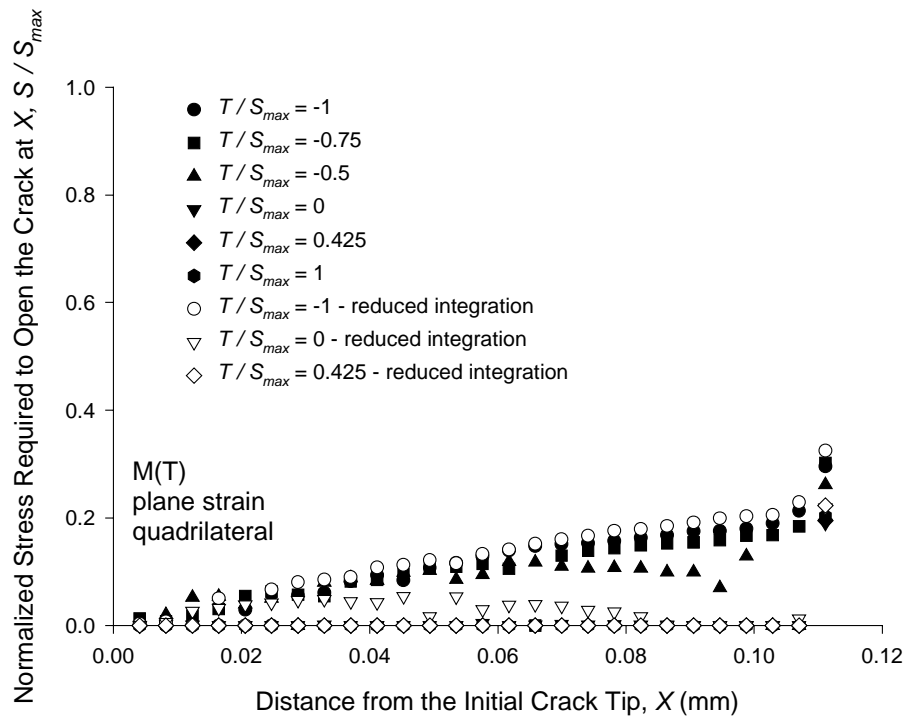
Figure 4-10 Effect of *T*-stress on the Crack Opening Process

4-1-2 Effect of Load Ratios and Stress Levels under Plane-stress

The effect of R on the crack opening stress for an M(T) specimen has been

investigated by McClung et al. [31] and Newman [48] under plane-stress. Similar finite

element analyses were performed with M(T), C(T) and SEB geometries to study the

effect of highly refined mesh.

To determine the sizes of the forward and reversed plastic zones in all the geometries, normalized values of the von-Mises stress σ_e/σ_o were plotted ahead of crack tip as discussed previously. The mesh refinement studies were next performed with a stress level of 0.3 and a load ratio of 0.0. Each mesh was refined until a converged opening load was determined. Figure 4-11 illustrates the variation in the number of elements in the plastic zones for the C(T), the SEB and the M(T) specimens as the mesh refinement was carried out. It is clear from the figure that the number of elements along the crack plane in the reversed plastic zone are significantly lower than in the forward plastic zone. Thus, a large refinement level is required to accurately capture the reversed plastic zone.
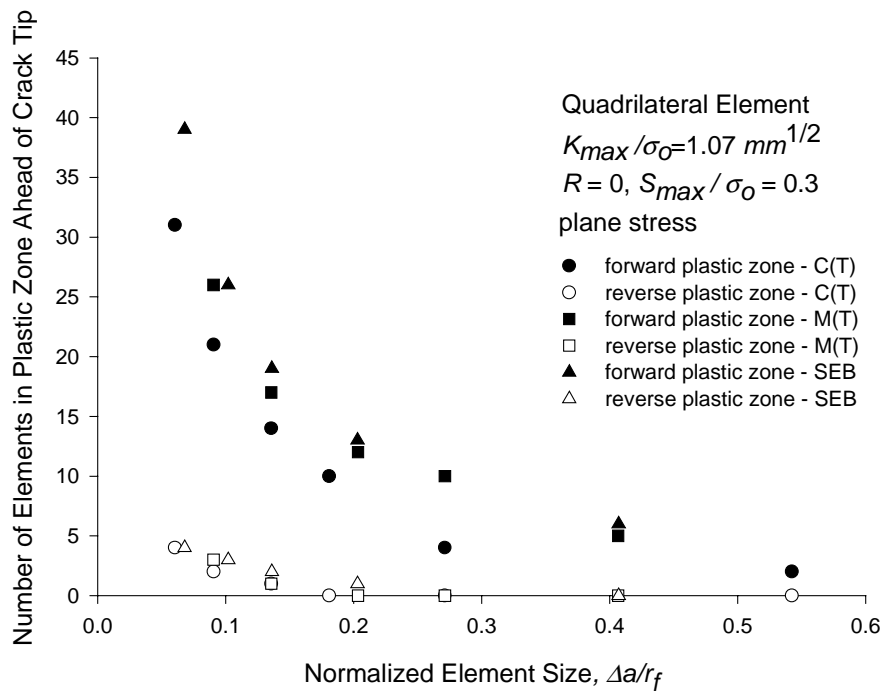
Figure 4-11 Variation in the Plastic Zone Sizes with Mesh Discretization under Plane-stress

For perspective forward plastic zone sizes were compared with stationary FEA, cyclic FEA, and Irwin's approximation of the forward plastic zone and as shown in Figure 4-12. Significant changes in the forward plastic zone sizes were noted between the cyclic and the stationary analysis. These differences were a consequence of the plastic wake formation. However, negligible difference was noted between Irwin's approximation and stationary FEA.
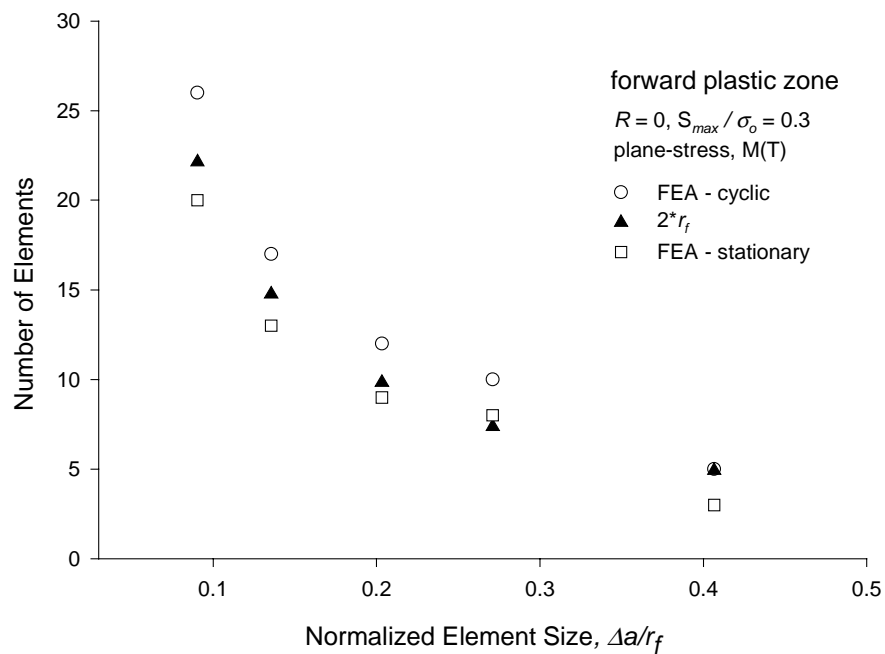
Figure 4-12a   Comparison of the Forward Plastic Zone Size – M(T) Specimen
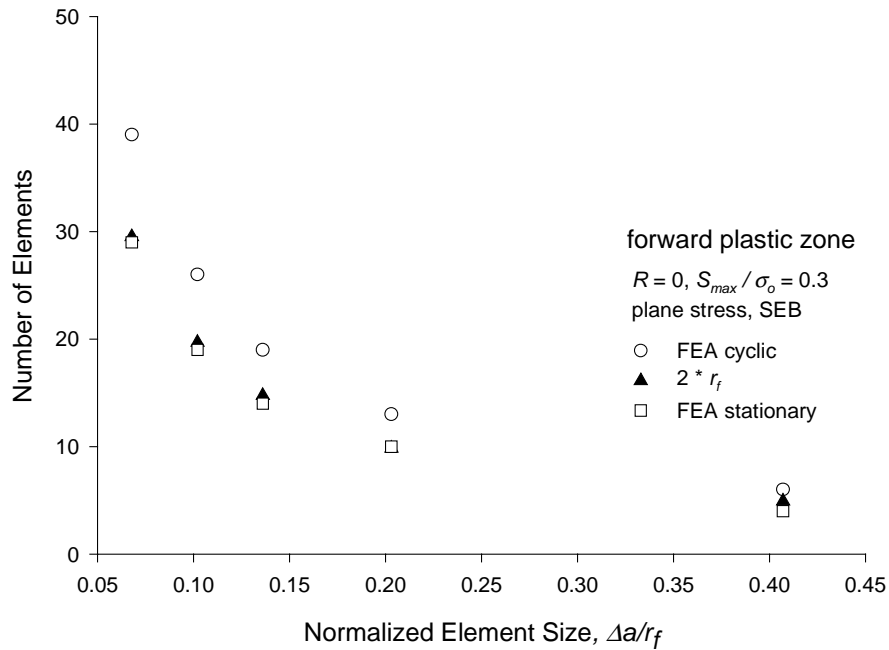
Figure 4-12b   Comparison of the Forward Plastic Zone Size – SEB Specimen

The degree of mesh refinement was increased until convergence of the opening values was observed as shown in Figure 4-13. It is clear from Figure 4-13 that the convergence of opening values was noted for the geometries as the mesh refinement was carried out. The opening values reported were steady state after growing approximately twice the initial forward plastic zone, and typical results are illustrated in Figure 4-14. Negligible difference in the crack opening values was noted with mesh refinement as shown in Figure 4-13, which suggests that under plane-stress condition, the effect of T-stress on closure is not significant.
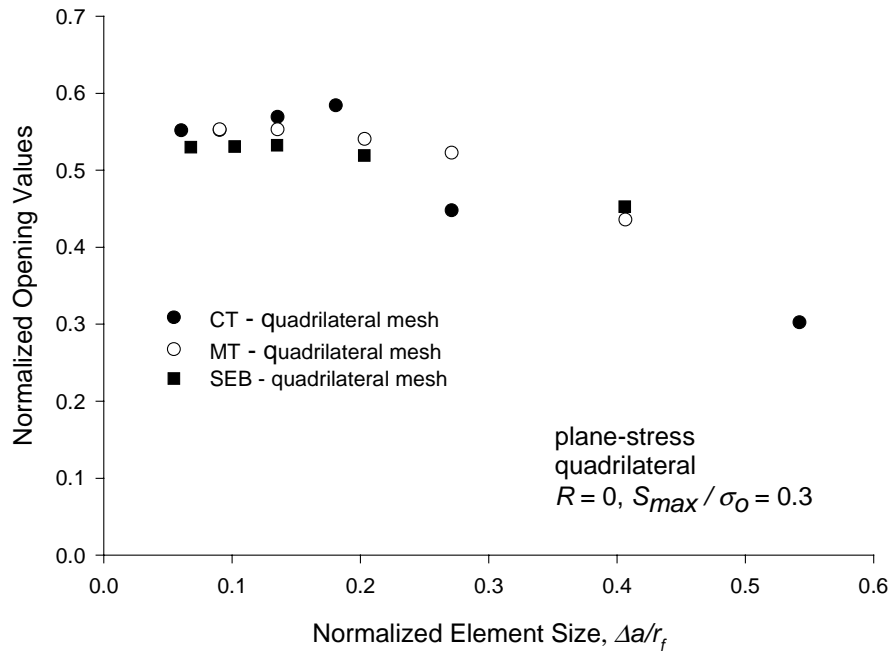
Figure 4-13 Comparison of Calculated Crack Opening Values under Plane-stress
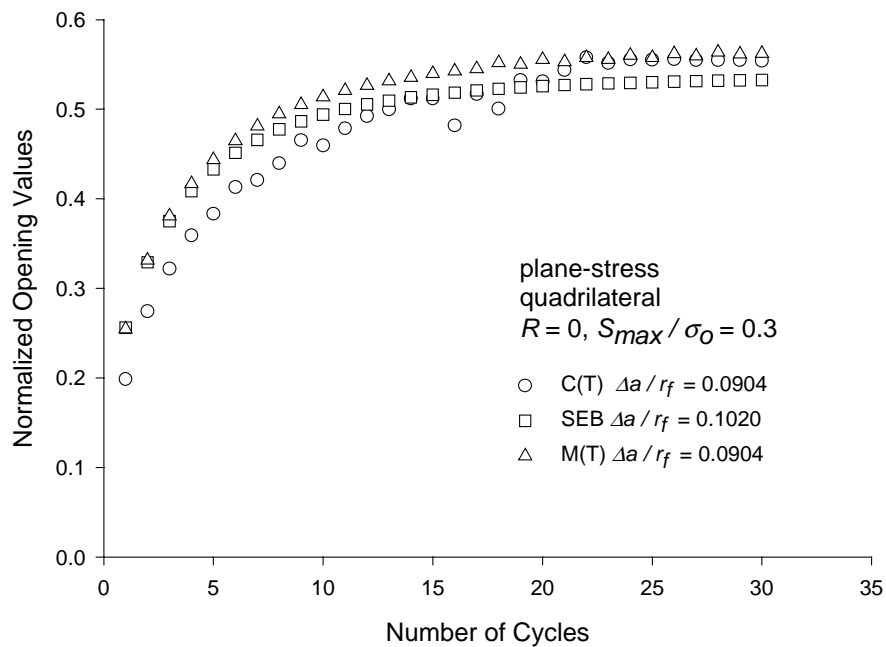
Figure 4-14 Typical Crack Opening Value Transient Behavior under Plane-stress

The mesh refinement studies were performed for M(T), C(T) and SEB geometries with a load ratio of 0.0 and a stress level of 0.3. For further analysis with different stress levels, the cyclic forward plastic size and total crack growth were fixed as those for the converged opening value for a stress level of 0.3. Approximately 35 elements were present in the cyclic forward plastic zone, which results in 3 to 4 elements in the reversed plastic zone. Next, the effect of stress levels on the crack opening value were studied under $R = 0.0$ and -1.0 with the M(T) and the SEB geometries and results are shown in Figure 4-15.
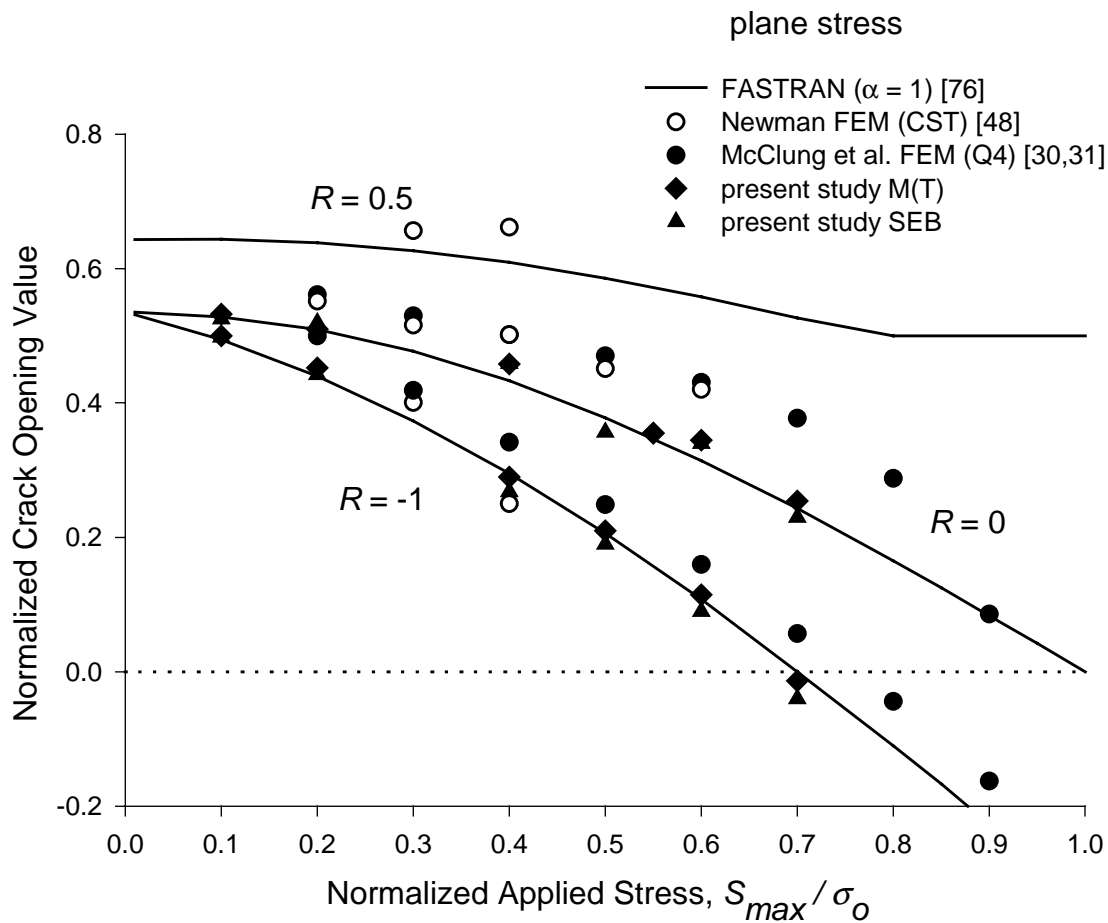
Figure 4-15 Effect of Stress Ratio on Crack Opening Values under Plane-stress

From the above figure it should be noted that the crack opening values from highly refined converged mesh were lower than those reported in literature, and were in better agreement with strip-yield model results generated using FASTRAN [76]. The meshes employed in the present study were more refined than those used by McClung et al. [30,31] and Newman [48]. Mesh refinement is the likely reason for the discrepancy, since to accurately capture the reversed plastic zone as shown in Figure 4-11, a high degree of refinement is required.

4-2 Three-dimensional Finite Element Analysis

Fatigue crack closure analyses were performed using ANSYS 6.1 [84]. Three-dimensional finite element analyses of part-through surface crack with initial aspect ratio of 1.0 were conducted using 8-noded brick elements. The methodology described in chapter 3 was used to model crack shape evolution.

To determine the sizes of the forward and reversed plastic zones at the deep point of penetration and at the free surface in the three-dimensional geometry, normalized values of the von-Mises stress σ_e/σ_o were plotted ahead of crack tip as discussed previously for two-dimensional analysis. Mesh refinement issues become complicated for three-dimensional models. For a semi-circular flaw, at the free surface a plane-stress condition exists while a plane-strain condition is present at the deepest point of penetration. Since a plane stress plastic zone is approximately three times larger than a plane strain plastic zone, the number of elements in the plastic zone at the deepest point of penetration should be used to determine an appropriate mesh size. Unfortunately, this forces the mesh to have more than adequate refinement at the free surface, and

necessitates nearly three times as many load cycles for crack opening level stabilization in this region. Due to hardware limitations, the mesh refinement studies were performed with respect to the deep point of penetration. To determine the initial mesh size, similar approached is used as described earlier for two-dimensional. The degree of mesh refinement was continued until convergence of the opening values was observed as shown in Figure 4-16. A maximum of 20 elements were present in the forward plastic zone, but it is found that five elements in the forward plastic zone is sufficient to obtain converged crack opening values.
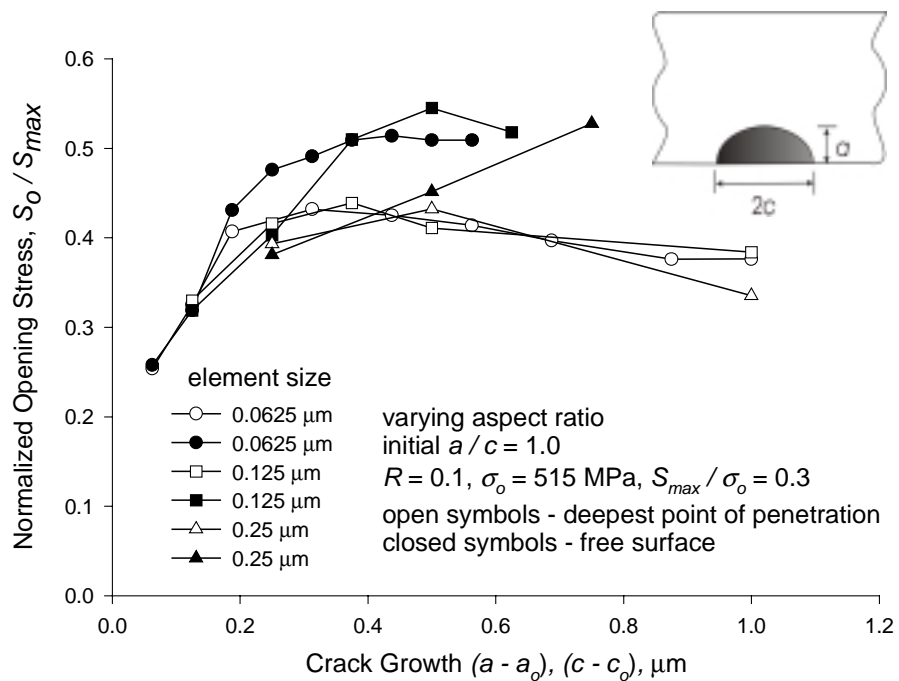
Figure 4-16 Surface Crack Mesh Refinement Studies

Next, the fatigue crack growth analysis was performed using different node release schemes. Negligible differences in the crack opening stresses when the crack front nodes are released at the minimum and maximum load are noted and shown in Figure 4-17. For these results, at the deepest point of penetration, approximately 2 elements yielded in compression under the minimum loading.
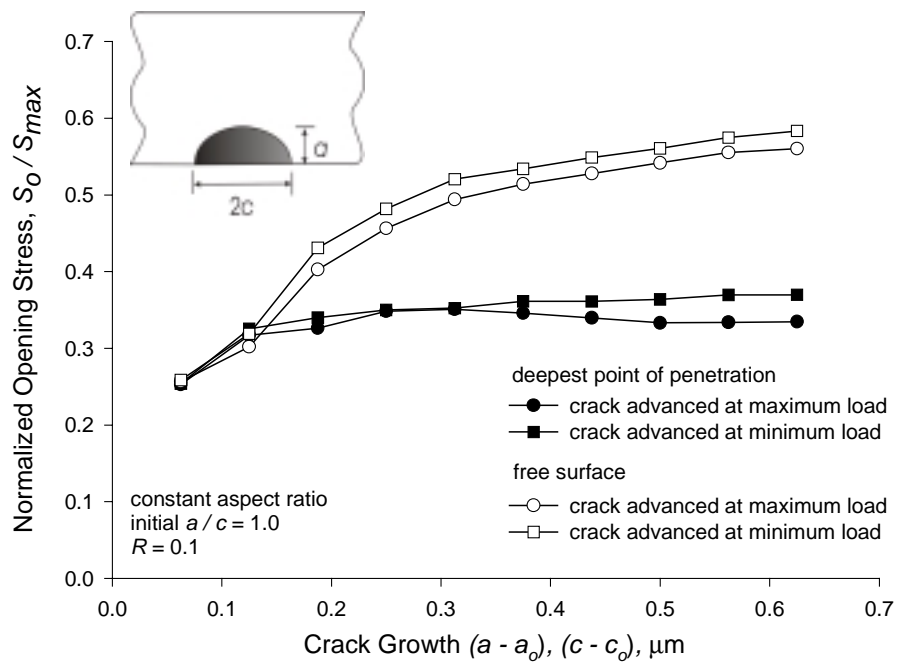
Figure 4-17 Effect of Crack Advance Scheme

The effects of crack shape evolution and spike overload on crack opening stress and consequently the fatigue crack closure behavior was next studied. A spike overload factor of 1.5 was used. Differences in the predicted opening values were noted when the aspect ratio was allowed to vary and also when spike overload is applied as shown in Figure 4-18. Crack retardation was also noted at the free surface as shown in Figure 4-19.

These results suggest that crack shape evolution can be successfully model and predicted using finite element analysis. Further study is required with significant crack growth at the free surface.
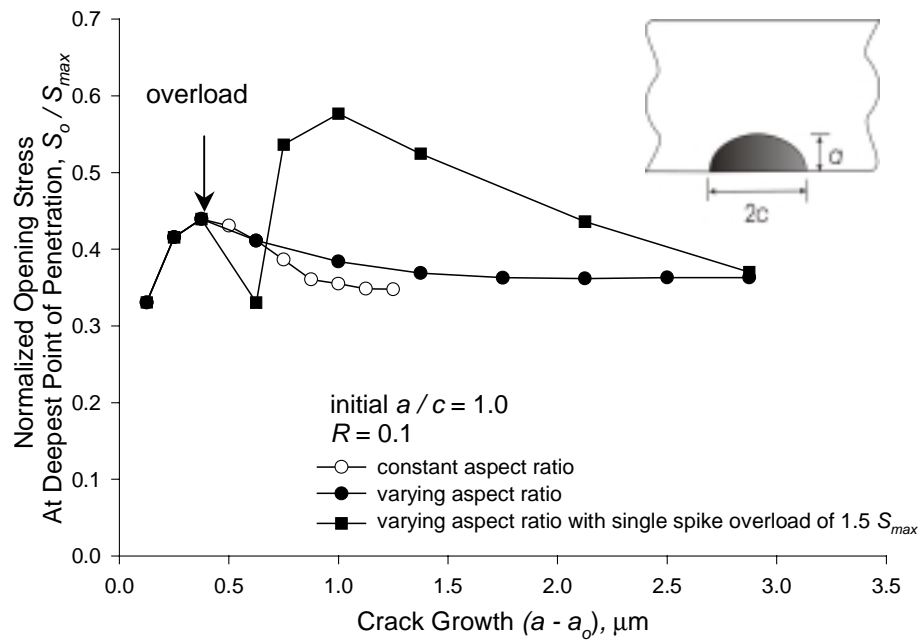
Figure 4-18 Surface Flaw Crack Opening Stress Transient
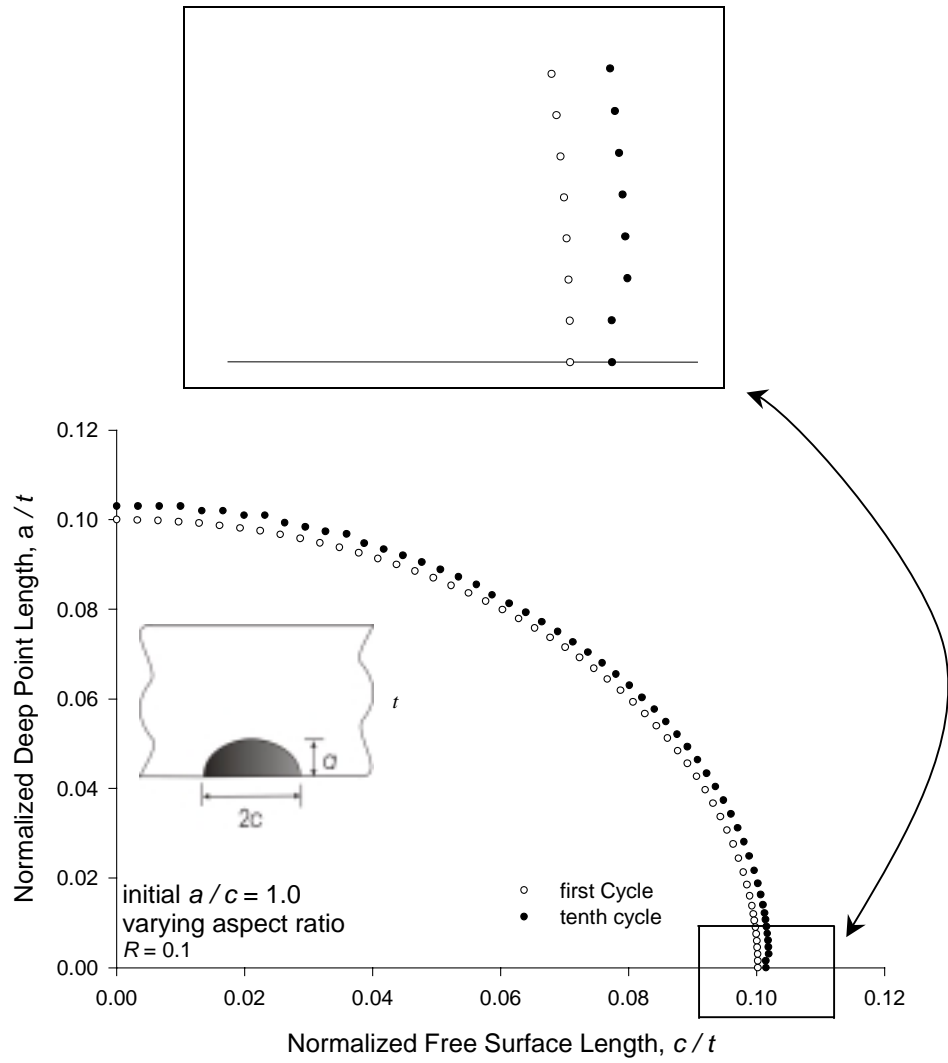
Figure 4-19 Predicted Crack Shape Evolution under Constant Amplitude Loading

CHAPTER V

CONTACT STRESS METHOD FORMULATION

The discussion from the earlier chapters suggests some discrepancy in the calculation of crack opening values from finite element analysis. Significant closure level was observed for the M(T) specimen under plane-strain, however, elemental or negligible closure was observed for the C(T) specimen under plane-strain. Results reported in the literature by some researchers suggest that the computed crack opening values from the node immediately behind the crack tip node should not be used because this node is too close to the poorly modeled crack tip, and suggest that second node behind the crack tip should be used to overcome this artifact of the FEA. On the other hand, results discussed in the earlier chapter indicate that the use of the second node behind the crack tip yields a zero opening value for the C(T) specimen under plane-strain, which implies no closure. It may be wise to compute the opening load considering whole crack front, not just one node. In the following chapter a new methodology will be discussed and developed to compute the crack opening value.

5-1 Formulation

Dill and Saff [88] were the first to introduce a contact stress method to compute crack opening loads, and employed the methodology in a strip-yield model. In this method, the stress intensity factor required to open the crack K_o is computed using the contact stresses along the closed crack surface under the minimum loading. The stress intensity factor K_c associated with this loading must be overcome to open the crack giving $K_c = K_o$. In the research described herein, this methodology was revisited and applied to compute crack opening values from finite element analysis results.

To compute K_o for the C(T) specimen from the crack surface nodal stress distribution under the minimum loading, first consider the stress intensity factor for an infinite plane with a semi-infinite crack subjected to point load p on the crack surface [89]

$$K = \sqrt{\frac{2}{\pi \varepsilon}} \, p \qquad (5\text{-}1)$$

where K is the stress intensity factor and ε is the distance from the origin.
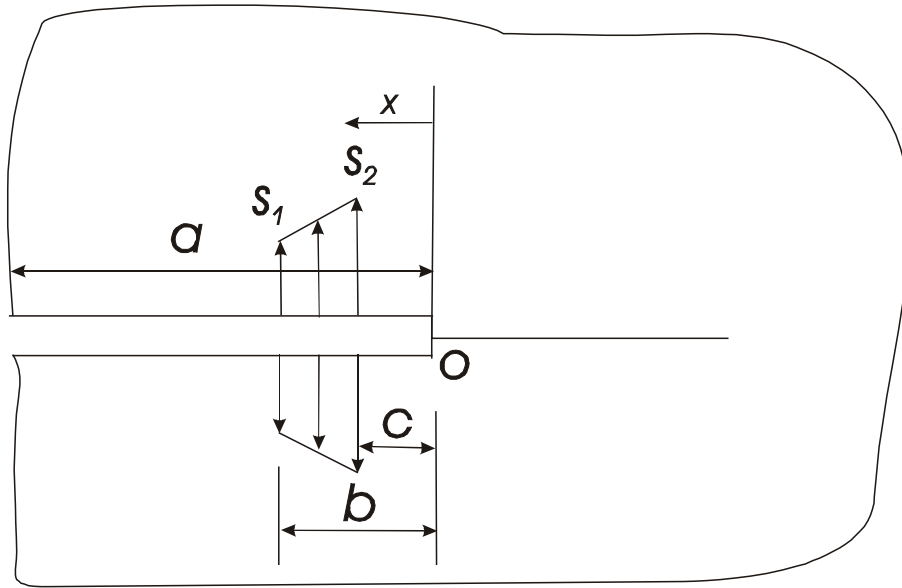
Figure 5-1 Infinite Plane with a Semi-infinite Crack Subjected to a Segment of Linearly Varying Stress.

If the crack surface is subjected to a segment of linearly distributed stress as shown in Figure 5-1, then equation 5-1 may be used to write the incremental stress intensity factor

$$dK = \sqrt{\frac{2}{\pi x}} s\, dx \qquad (5\text{-}2)$$

where s is the linear stress distribution at any distance x from the origin

$$s = (c_1 + x c_2) \qquad (5\text{-}3)$$

and c_1 and c_2 are constants. As shown in Figure 5-1, when $x = b$, $s = s_1$ and when $x = c$, $s = s_2$. Consequently

$$c_1 = \frac{b s_2 - c s_1}{b - c} \quad \text{and} \quad c_2 = \frac{s_1 - s_2}{b - c} \qquad (5\text{-}4)$$

The nodal stresses s_1 and s_2 are computed from the nodal forces p_1 and p_2 as follows

$$s_1 = \frac{p_1}{\Delta a} \text{ and } s_2 = \frac{p_2}{\Delta a}$$

(5-5)

where Δa is the element size. Substituting equation 5-3 into 5-2 and integrating over

$c \leq x \leq b$ yields

$$K = \frac{2}{3}\sqrt{\frac{2}{\pi}}\left[\sqrt{c}\left(3\frac{bs_2 - cs_1}{b-c} + c\frac{s_1 - s_2}{b-c}\right) - \sqrt{b}\left(3\frac{bs_2 - cs_1}{b-c} + b\frac{s_1 - s_2}{b-c}\right)\right]$$

(5-6)

The K_o value associated with the contact stress for each finite element on the

crack surface can be calculated using equation 5-6. Superposition may then be applied to

find the K_o value for the entire crack surface loading.

$$\frac{K_o}{K_{\max}} = \frac{2}{3}\sqrt{\frac{2}{\pi}}\sum_{i=1}^{n}\frac{\left[\sqrt{c_i}\left(3\frac{b_i(s_2)_i - c_i(s_1)_i}{b_i - c_i} + c_i\frac{(s_1)_i - (s_2)_i}{b_i - c_i}\right) - \sqrt{b_i}\left(3\frac{b_i(s_2)_i - c_i(s_1)_i}{b_i - c_i} + b_i\frac{(s_1)_i - (s_2)_i}{b_i - c_i}\right)\right]}{K_{\max}}$$

(5-7)

where $K_{\max}$ is the maximum stress intensity factor, $(s_1)_i$ and $(s_2)_i$ are the ith nodal stress

values at distances b_i and c_i from the crack tip respectively, and n is the total number of

nodal stress values.

To compute K_o for the M(T) specimen, next consider the stress intensity factor for

an infinite plane with a finite crack subjected to point load p on the crack surface [89]

$$K = \sqrt{\frac{2}{\pi a}}\frac{p}{\sqrt{a^2 - \varepsilon^2}}$$

(5-8)

where K is the stress intensity factor, $2a$ is the crack length and ε is the distance from

the origin.
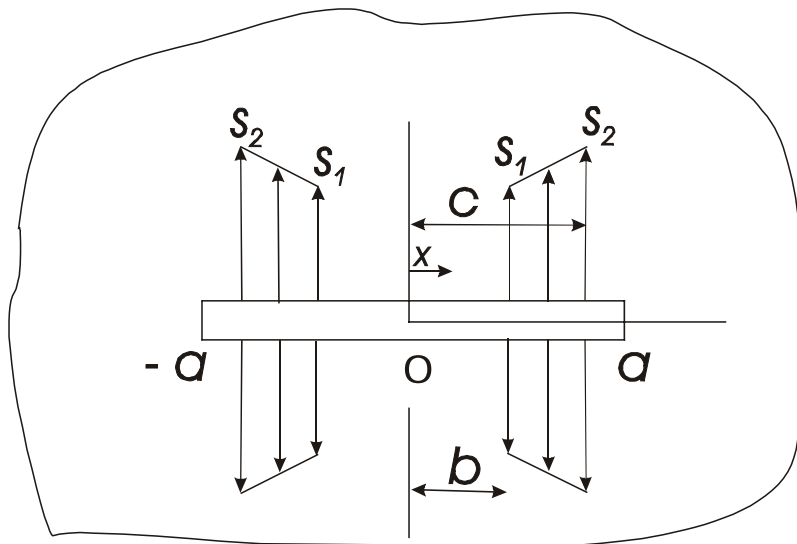
Figure 5-2 Infinite Plane with a Finite Crack Subjected to a Segment of Linearly Varying Stress

If the crack surface is subjected to a segment of linearly distributed stress as shown in

Figure 5-2, then equation 5-8 may be used to write the incremental stress intensity factor

$$dK = \sqrt{\frac{2}{\pi a}} \frac{s}{\sqrt{a^2 - x^2}} dx \qquad (5\text{-}9)$$

where s is the linear stress distribution at any distance x from the origin

$$s = (c_1 + xc_2) \qquad (5\text{-}10)$$

and c_1 and c_2 are constants. As shown in Figure 5-2, when $x = b$, $s = s_1$ and when $x = c$,

$s = s_2$. Consequently

$$c_1 = \frac{bs_2 - cs_1}{b - c} \text{ and } c_2 = \frac{s_1 - s_2}{b - c} \tag{5-11}$$

Substituting equation 5-10 into 5-9 and integrating over $b \leq x \leq c$ yields

$$K = \frac{2}{\sqrt{a\pi}} \left[\left(\sqrt{a^2 - b^2} - \sqrt{a^2 - c^2} \right) \frac{s_1 - s_2}{b - c} + \left(\sin^{-1}\left(\frac{c}{a}\right) - \sin^{-1}\left(\frac{b}{a}\right) \right) \frac{bs_2 - cs_1}{b - c} \right] \tag{5-12}$$

For the entire crack surface

$$\frac{K_o}{K_{max}} = \frac{2}{\sqrt{a\pi}} \sum_{i=1}^{n} \frac{\left[\left(\sqrt{a^2 - b_i^2} - \sqrt{a^2 - c_i^2} \right) \frac{(s_1)_i - (s_2)_i}{b_i - c_i} + \sin^{-1}\left(\frac{c_i}{a}\right) \frac{b_i(s_2)_i - c_i(s_1)_i}{b_i - c_i} - \sin^{-1}\left(\frac{b_i}{a}\right) \frac{b_i(s_2)_i - c_i(s_1)_i}{b_i - c_i} \right]}{K_{max}} \tag{5-13}$$

To compute K_o for the SEB specimen, next consider the stress intensity factor for

an semi-infinite plane with an edge crack subjected to point load p on the crack surface

[89]

$$K = \frac{2.6}{\sqrt{\pi a}} \frac{p}{\sqrt{1 - (\varepsilon/a)^2}} \tag{5-14}$$

where K is the stress intensity factor, a is the crack length and ε is the distance from the

origin.
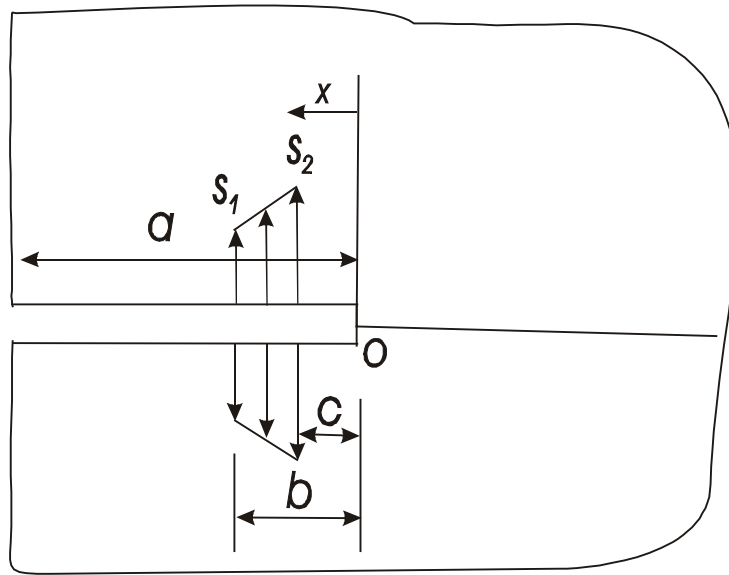
Figure 5-3 Semi-infinite Plane with a Edge Crack Subjected to a Segment of Linearly Varying Stress

If the crack surface is subjected to a segment of linearly distributed stress as shown in Figure 5-3, then equation 5-14 may be used to write the incremental stress intensity factor

$$dK = \frac{2.6}{\sqrt{\pi a}} \frac{s}{\sqrt{1 - (x/a)^2}} \tag{5-15}$$

where s is the linear stress distribution at any distance x from the origin

$$s = (c_1 + xc_2) \tag{5-16}$$

and c_1 and c_2 are constants. As shown in Figure 5-3, when $x = b$, $s = s_1$ and when $x = c$, $s = s_2$. Consequently

$$c_1 = \frac{bs_2 - cs_1}{b - c} \quad \text{and} \quad c_2 = \frac{s_1 - s_2}{b - c} \tag{5-17}$$

Substituting equation 5-16 into 5-15 and integrating over $b \leq x \leq c$ yields

$$K = \frac{2.6}{\sqrt{\pi a}}\left[a\left(\sqrt{a^2-b^2} - \sqrt{a^2-c^2}\right)\frac{s_1-s_2}{b-c} + \left(\sin^{-1}\left(\frac{c}{a}\right) - \sin^{-1}\left(\frac{b}{a}\right)\right)a\frac{bs_2-cs_1}{b-c}\right] \quad (5\text{-}18)$$

For the entire crack surface

$$\frac{K_o}{K_{max}} = 2.6\sqrt{\frac{a}{\pi}\sum_{i=1}^{n}} \frac{\left[\left(\sqrt{a^2-b_i^2} - \sqrt{a^2-c_i^2}\right)\frac{(s_1)_i-(s_2)_i}{b_i-c_i} + \sin^{-1}\left(\frac{c_i}{a}\right)\frac{b_i(s_2)_i-c_i(s_1)_i}{b_i-c_i} - \sin^{-1}\left(\frac{b_i}{a}\right)\frac{b_i(s_2)_i-c_i(s_1)_i}{b_i-c_i}\right]}{K_{max}} \quad (5\text{-}19)$$

When modeling fatigue crack growth under constant amplitude loading, most researchers have conventionally monitored the first node behind the crack tip to assess the crack opening value from the finite element analysis results. However, the accuracy of finite element results are suspect in the neighborhood of the crack tip due to the severe stress gradients which result [7,28,9,90]. While using the second node behind the crack tip when computing the opening load may help reduce this problem, as the mesh refinement is carried out any benefit will be eliminated due to the decreasing distance between the crack tip and the second node. The contact stress method described above overcomes the limitation of focusing attention on a single node considering instead the global behavior of the entire crack surface. In addition, when using the contact stress method, the opening values are computed at the minimum load after the unloading cycle is complete. This eliminates any consideration of loading increments as required in the more conventional method. Thus the contact stress method is also independent of the unloading increment size.

When using the conventional methodology, the crack opening value is defined based on the last node to open. Consequently, the element immediately behind the crack

tip is not considered. This limitation is eliminated when using the contact stress

method. The nodal forces were used to compute the required contact stress under the

minimum loading, because forces are more accurate than stresses in any finite element

analysis.

5-2 Result

The opening values computed for the C(T), the SEB and the M(T) specimens

under plane-strain and plane-stress are shown in Figures 5-4 and 5-5.
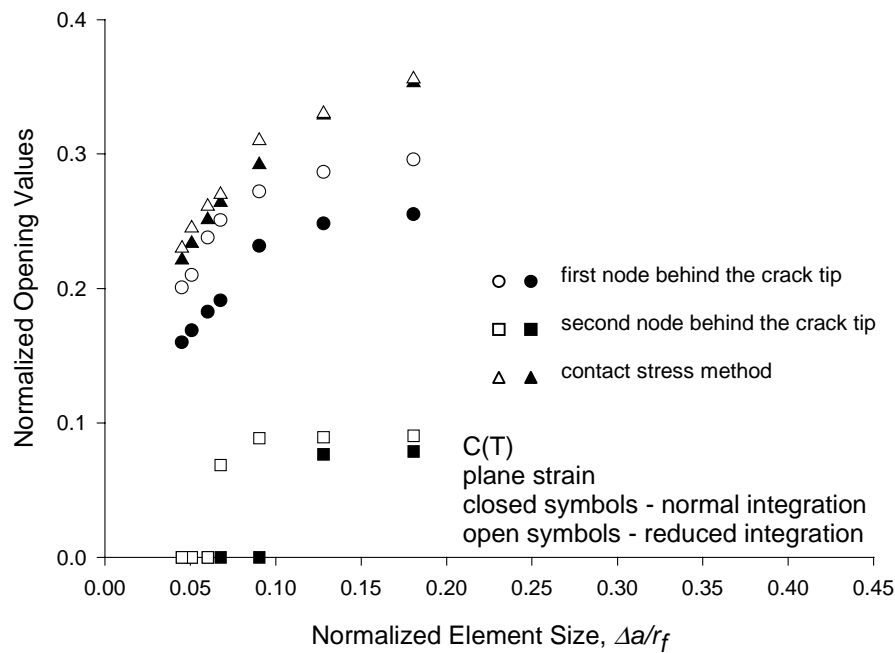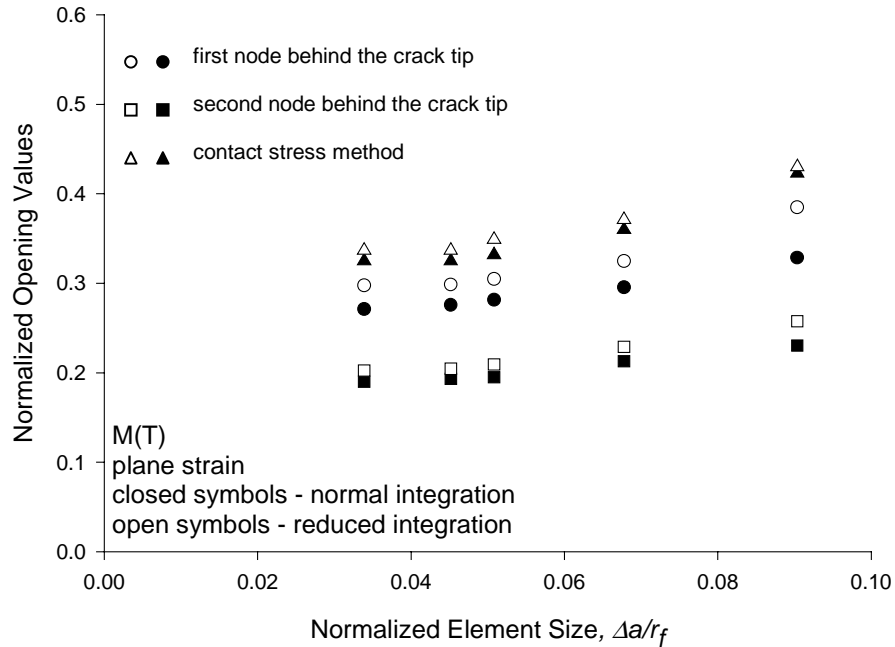
Figure 5-4 Comparison of Predicted Crack Opening Values under Plane-strain Conditions

It may be noted from Figure 5-4 that assessment of crack opening loads at the second node behind the crack tip yields significantly lower plane-strain crack opening values. For all these geometries under plane-strain, the opening values from the contact stress method were higher than those found using the first node behind the crack tip, however small difference was noted under plane-stress. This was expected, since the element immediately behind the crack tip is also considered when calculating the opening load using the contact stress method. The opening values were approximately the same when using the contact stress method with reduced and full integration, which suggests that the contact stress method is resistant to the effects of plane-strain locking [71]. It may also be noted that under plane-strain conditions, the C(T) specimen opening values

did not converge as the mesh refinement was carried out. This would suggest that

plasticity-induced closure does not exist or is negligibly small.
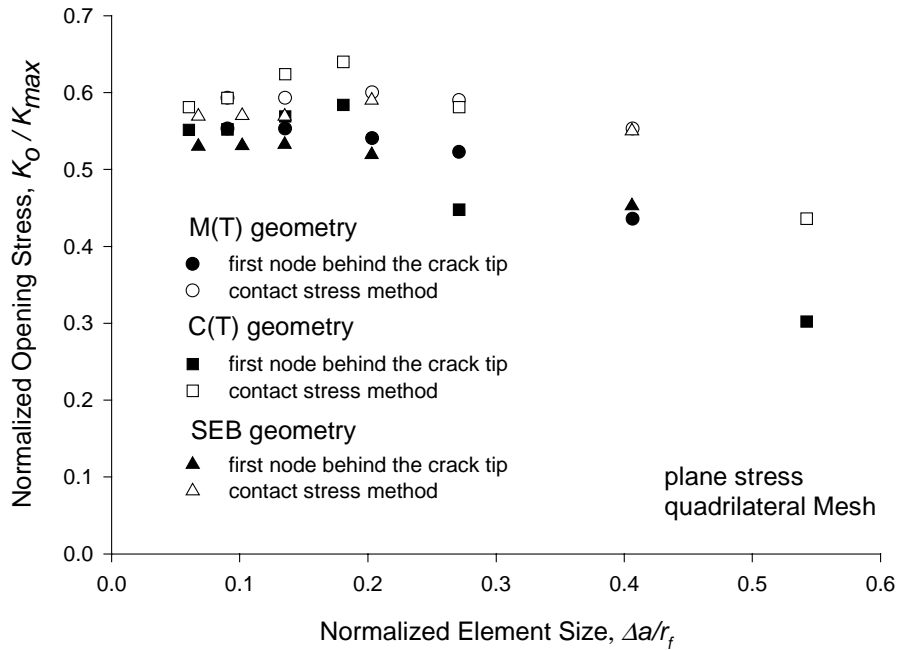
Figure 5-5 Comparison of Predicted Crack Opening Values Using Contact Stress Method and Conventional Method under Plane-stress Conditions

Next, the nodal force distribution used to compute K_o was plotted and is shown in

Figures 5-6 and 5-7. From these figures, it is clear that the element just behind the crack

tip contributes significantly to the crack opening values. The contribution of the element

immediately behind the crack tip when computing plane-strain crack opening values

using the contact stress was determined. For the C(T) specimen, approximately 85% of

the total opening value was associated with this element when using either full or reduced

integration. In contrast, this value was approximately 50% for the M(T) specimen. For

the C(T) specimen under plane-stress, a 30% value was observed. Consequently, the

element immediately behind the crack tip plays a major role in the crack opening value

computation. In cases where this role is exceedingly large, such as the C(T) specimen under plane-strain, the validity of the computed opening value become questionable. This fact, in conjugation with the observation that for the plane-strain C(T) specimen the crack surface loading is predominantly zero, suggests that plasticity-induced closure is negligible for this configuration. Lastly the effect of load ratios and stress level was studied using the contact stress method under plane-stress. Small difference was noted as shown in Figure 5-8 when compared to first node immediately behind the crack tip.
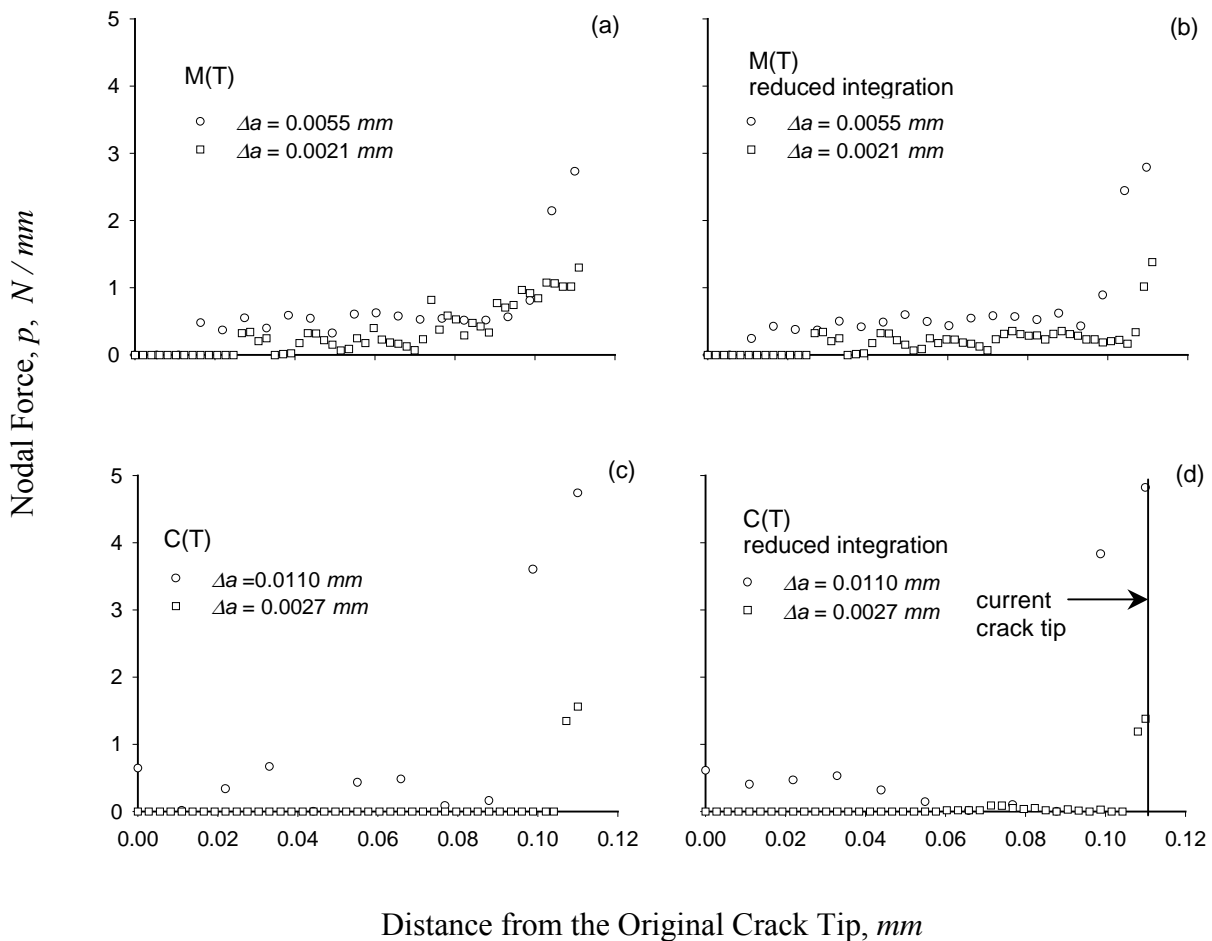
Figure 5-6 Nodal Force Distribution along the Crack Surface under Plane-strain Conditions
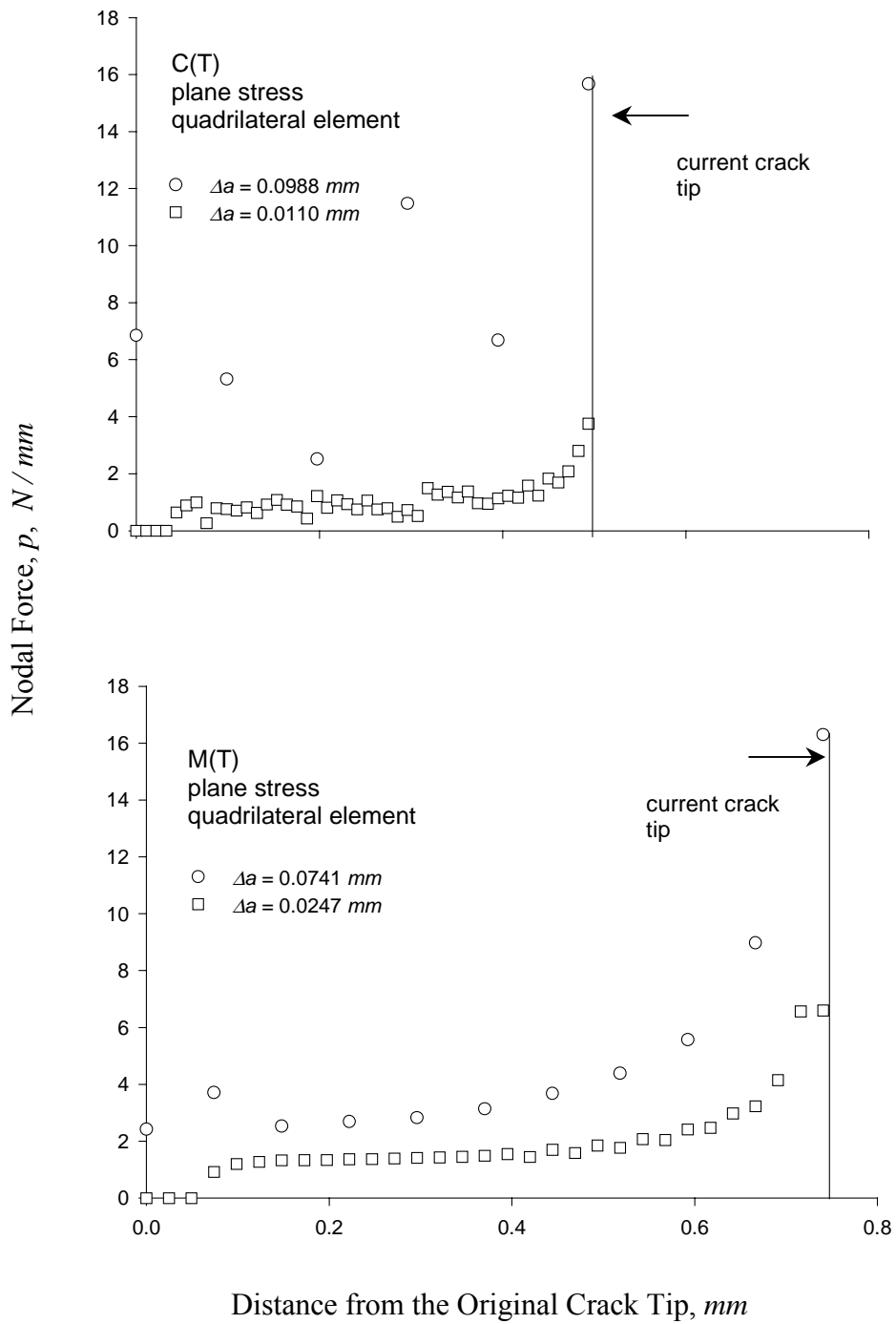
Figure 5-7 Nodal Force Distribution along the Crack Surface under Plane-stress Conditions
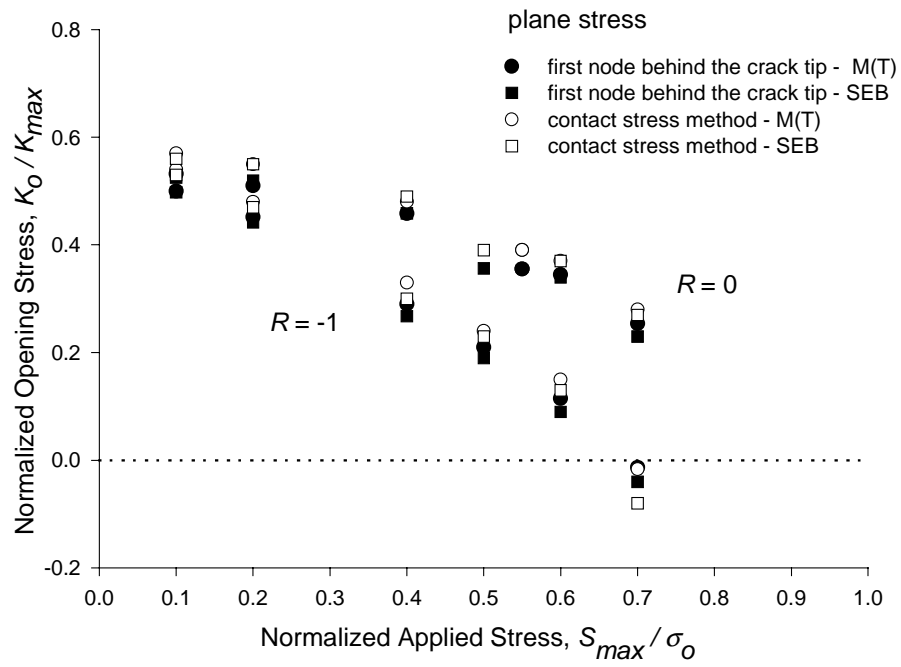
Figure 5-8 Effect of Stress Ratio on Crack Opening Values under Plane-stress

CHAPTER VI

CONCLUSION

Finite element analysis is a promising tool to simulate plasticity-induce fatigue crack closure. The modeler must consider different aspects of modeling to get better finite element crack opening values and other fracture parameters as described in this research. Modeling aspects of two-dimensional finite element analysis under plane-strain and plane-stress conditions have been well established and it is suggested that more work is needed with three-dimensional models

1. The middle-crack tension geometry crack opening stress exhibits convergence as mesh refinement is carried out under plane-strain conditions.

2. The compact tension geometry crack opening load does not exhibit convergence as mesh refinement is carried out under plane-strain conditions. This indicates that plasticity-induced closure is negligible or does not exist under plane-strain for the C(T) specimen.

3. Opening values for the compact tension, the side edge bend and middle-crack tension geometries crack exhibit convergence as mesh refinement is carried out under plane-stress conditions. This suggests that closure does exist under plane-stress.

4. Opening values vary when the initial crack tip plastic zone extends into the mesh refinement transition region and also when the crack tip is close to transition elements.

5. The middle-crack tension geometry crack opening stress does not exhibit convergence as the mesh refinement is carried out when different T-stress values with $-0.75 \leq T / S_{max} \leq 1$ are applied externally. This indicates that the level of in-plane constraint dictates the level of plasticity-induced crack closure under plane-strain.

6. Approximately 3 to 4 elements are required in the reversed plastic zone for the middle-crack tension specimen under plane-strain to obtain accurate opening values.

7. Approximately 3 to 4 elements are required in the reversed plastic zone for the compact tension, the side edge bend and middle-crack tension specimens under plane-stress to obtain accurate opening values.

8. The in-plane constraint effect on crack closure is negligible under plane-stress conditions.

9. The contact stress method of computing crack opening values was revisited and applied for the first time to finite element analyses. This global method has the advantage of not being associated with a single node and is independent of loading and unloading increment size.

10. Crack opening values computed using the contact stress method were unchanged when implementing reduced integration schemes. This suggests that the method is resistant to the effects of plane-strain locking.

11. Depending on the geometry and stress state, the element immediately behind the crack tip may play a major role in the crack opening value computation. This element is not considered in more conventional crack opening assessments.

12. Under plane-stress condition for different stress levels and load ratios, significantly lower crack opening values were found compare to those reported in literature.

13. For the three-dimensional geometry crack shape evolution can be modeled and subsequent crack growth retardation and acceleration can be predicted using FEA.

Lastly, it should be noted that while crack closure was shown either not to exist or to be negligible under plane-strain for certain levels of in-plane constraint, plane-strain is a two-dimensional idealization that cannot occur in practice. In the opinion of the author, the plane-stress condition existing at and near the free surface of a three-dimensional body will have a strong influence on the plane-strain interior, regardless of thickness of geometry.

REFERENCE

[1]   Boresi, A. P., Schmidt, R. J., and Sidebottom, O. M., "Advanced Mechanics of Materials," 5th Edition, John Wiley & Sons, Inc., New York,1993.

[2]   Stephens, R. I., Faterni, A., Stephens, R. R., and Fuchs, H. O., "Metal Fatigue in Engineering," 2nd Edition, John Wiley & Sons, Inc., New York, 2001.

[3]   Paris, P. C., and Erdogan, F., "A Critical Analysis of Crack Propagation Laws," *Journal of basic Engineering*, pp. 528-534,1963.

[4]   Elber, W., "Fatigue Crack Closure under Cyclic Tension," *Engineering Fracture Mechanics*, Volume 2, pp. 37-45, 1970.

[5]   Newman, J. C. Jr., "Advances in Finite Element Modeling of Fatigue Crack Growth and Fracture," *Fatigue '02: The Eight International Fatigue Congress*, Stockholm, Sweden, June 2-7, 2002.

[6]   Gall K., Sehitoglu H., and Kadioglu Y., "Plastic Zones and Fatigue-crack Closure under Plane-strain Double Slip," *Metallurgical and Material Transactions A*, pp. 3491-3502, 1996.

[7]   McClung, R. C., Thacker, B. H., and Roy S., "Finite Element Visualization of Fatigue Crack Closure in Plane-stress and Plane-strain," *International Journal of Fracture*, Volume 50, pp. 27-49, 1991.

[8]   Fleck, N. A., "Finite Element Analysis of Plasticity-induced Crack Closure under Plane-strain Conditions. *Engineering Fracture Mechanics*, Volume 25(4), pp. 441-449, 1986.

[9]   Fleck, N. A., and Newman, J. C., "Analysis of Crack Closure under Plane-strain Conditions," *Mechanics of Fatigue Crack Closure ASTM STP 982*, pp. 319-341, 1988.

[10]   Ogura, K., Ohji, K., and Honda, K., "Influence of Mechanical Factors on the Fatigue Crack Closure," Advances in Research on the strength and fracture of materials (Fracture 1977)., Proceeding., 4th International Conference on Fracture Mechanics., Waterloo., Canada, Volume 2B, pp. 1035-1047, 1977.

[11]   Blom, A. F., and Holm, D. K., "An Experimental and Numerical Study of Crack Closure," *Engineering Fracture Mechanics*, Volume 22, pp. 997-1101,1985.

[12]   Ashbaugh, N. E., Dattaguru, B., Khobaib, M., Nicholas, T., Prakash, R.V., Ramamurthy, T. S., Seshadri, B. R., and Sunder R., "Experimental and Analytical Estimates of Fatigue Crack Closure in an Aluminum-copper Alloy Part II: A Finite Element Analysis," *Fatigue and Facture in Engineering Materials and Structure*, Volume 20(7), pp. 963-974, 1997.

[13]   Dougherty, J. D., Padovan, J., and Srivatsan, T. S., "Fatigue Crack Propagation and Closure Behavior of Modified 1071 Steel: Finite Element Study," *Engineering Fracture Mechanics*, Volume 56(2), pp. 189-212, 1997.

[14]   McClung, R. C., "Fatigue Crack Closure and Crack Growth Outside the Small Scale-yielding Regime," Ph.D. Thesis., Department of Mechanical and Industrial Eng., Univ. of Illinois at Urbana-Champaign (1988).

[15]   Kfouri, A. F., "An Elastic Plastic Finite Element Analysis of a Compact Tension Specimen," *Journal of Strain Analysis*, Volume 18(1), pp. 69-75, 1983.

[16]   Pommier, S., "Plane Strain Crack Closure and Cyclic Hardening," *Engineering Fracture Mechanics*, Volume 69, pp. 25-44, 2001.

[17]   Sehitoglu, H., and Sun, W., "Mechanics of Crack Closure in Plane Strain and Plane Stress," *Third International Conference on Biaxial/Multiaxial Fatigue*., Stuttgart. FRG 1989.

[18]   Sehitoglu, H., and Sun, W., "Modeling of Plane Strain Fatigue Crack Closure," *Journal of Engineering Materials and Technology*, January, Volume 113, pp. 31-40, 1991.

[19]   Llorca, J., and Galvez, V. S., "Modeling Plasticity-induced Fatigue Crack Closure," *Engineering Fracture Mechanics*, Volume 37(1), pp. 185-196, 1990.

[20]   Tsukuda, H., Ogiyama, H., and Shiraishi, T., "Fatigue Crack Growth and Closure at High Stress Ratio. *Fatigue and Facture in Engineering Materials and Structure*, Volume 18(4), pp. 503-514, 1995.

[21]   Shercliff, H. R., and Fleck, N. A., "Effect of Specimen Geometry on Fatigue Crack Growth in Plane Strain I - Constant Amplitude Response," *Fatigue and Facture in Engineering Materials and Structure*, Volume 13930, pp. 287-296,1990.

[22]   Shercliff, H. R., and Fleck, N. A., "Effect of Specimen Geometry on Fatigue Crack Growth in Plane Strain II - Overload Response." *Fatigue and Facture in Engineering Materials and Structure*, Volume 13(3), pp. 297-310, 1990.

[23] Lalor, P., "Mechanics aspects of Crack Closure," M.S. Thesis., Department of Mechanical and Industrial Engineering., University of Illinois at Urbana-Champaign. Also published as Materials Engineering-Mechanical Behavior Report No. 133., UILU-ENG., College of Engineering., University of Illinois at U-C 1986:86-3610.

[24] Lalor, P., and Sehitoglu, H., "Fatigue Crack Closure Outside Small Scale Yielding Regime," *Mechanics of Fatigue Crack Closure. ASTM STP 982*, pp. 342-360, 1988.

[25] Lalor, P., Sehitoglu, H., and McClung, R. C., "Mechanics Aspects of Small Crack Growth from Notches-the Role of Crack Closure., The Behavior of Short Fatigue Cracks," EGF 1., Mechanical Engineering Publications., London, pp. 386-396, 1986.

[26] Nakagaki, M., and Atulri, S. N., "Elastic-Plastic Analysis of Fatigue Crack Closure in Modes I and II," *AIAA Journal*, Volume 18, pp. 1110-1117, 1980.

[27] Nakagaki, M., and Atluri, S. N., "Fatigue Crack Closure and Delay Effects Under Mode I Spectrum Loading: An Efficient Elastic-Plastic Analysis Procedure," *Fatigue and Facture in Engineering Materials and Structure*, Volume 1, pp. 412-429, 1979.

[28] Kiran Solanki, Daniewicz, S. R., and Newman Jr., J. C., "Finite Element Modeling of Plasticity-Induced Crack Closure with Emphasis on Geometry and Mesh Refinement Effects," submitted to *Engineering Fracture Mechanics,* 2002.

[29] Kiran Solanki., Daniewicz, S. R., and Newman Jr., J. C., "A New Methodology for Computing Crack Opening Values from Finite Element Analyses," submitted to *Engineering Fracture Mechanics*, 2002.

[30] McClung, R. C., and Sehitoglu, H., "On the Finite Element Analysis of Fatigue Crack Closure-1: Basic Modeling Issues," *Engineering Fracture Mechanics,* Volume 33(2), pp. 237-252, 1983.

[31] McClung, R. C., and Sehitoglu, H., "On the Finite Element Analysis of Fatigue Crack Closure-2: Numerical Results," *Engineering Fracture Mechanics*, Volume 33(2), pp. 253-272, 1983.

[32] Palazotto, A., and Bendnarz, E., "A Finite Element Investigation of Viscoplastic-Induced Closure of Short Cracks at High Temperatures," *ASTM STP* 1020, pp. 530-547, 1989.

[33] Kobayashi, S., and Nakamura, H., "Investigation of Fatigue Crack Closure (Analysis of Plasticity Induced Crack Closure)," Current Research on Fatigue Cracks., MRS 1., Society of Material Science., Japan, pp. 201-215, 1985.

[34] Nakamura, H., Kobayashi, S., Yanase, S., and Nakazawa, H., "Finite Element Analysis of Fatigue Crack Closure in Compact Specimen," Mechanical Behavior of

Materials (ICM4)., Forth International Conference Mechanical Behavior of Materials., Stockholm, Volume 2, pp. 817-823,1983.

[35]   Miyamoto, H., Miyoshi, T., and Fukuda, S., "An Analysis of Crack Propagation in Weld Structures: Signification of defects in welded structures," Proceedings. of Japan-U.S. Seminar., Tokyo., University of Tokyo Press, pp. 189-202, 1973.

[36]   Oliva, V., and Kunes, I., "FEM Analysis of Cyclic Deformation Around the Fatigue Crack Tip After a Single Overload," *ASTM STP 1211*, pp.77-90, 1993.

[37]   Ogura, K., and Ohji, K., "FEM Analysis of Crack Closure and Delay Effect in Fatigue Crack Growth Under Variable Amplitude Loading," *Engineering Fracture Mechanics,* Volume 9, pp. 471-480, 1977.

[38]   Ohji, K., Ogura, K., and Ohkubo, Y., "Cyclic Analyses of Propagating Crack and its Correlation with Fatigue Crack Growth," *Engineering Fracture Mechanics*, Volume 7, pp. 457-464, 1975.

[39]   Ogura, K., Ohji, K., and Ohkubo, Y., "Fatigue Crack Growth Under Biaxial Loading," *International Journal of Fracture,* Volume 10, pp. 609-610, 1974.

[40]   Ohji, K., Ogura, K., and Ohkubo, Y., "On the Closure of Fatigue Cracks Under Cyclic Tensile Loading," *International Journal of Fracture*, Volume 10, pp. 123-124, 1974.

[41]   Park, S. J., and Song, J. H., "Simulation of Fatigue Crack Closure Behavior Under Variable-Amplitude Loading by a 2D Finite Element Analysis Based on the Most Appropriate Mesh Size Concept," *ASTM STP 1343*, pp. 337-348, 1999.

[42]   McClung, R. C., "Closure and Growth of Mode I Cracks in Biaxial Fatigue," *Fatigue and Facture in Engineering Materials and Structure*, Volume 12(5), pp. 447-460, 1989.

[43]   McClung, R. C., "Finite Element Analysis of Fatigue Crack Growth, Theoretical Concepts and Numerical Analysis of Fatigue," *EMAS*, pp. 153-172, 1992.

[44]   McClung, R. C., "Finite Element Perspectives on the Mechanics of Fatigue Crack Closure," Fatigue, pp. 345-356,1996.

[45]   Newman, J. C. Jr., "Finite-Element Analysis of Crack Growth Under Monotonic and Cyclic Loading," *ASTM STP 637*, pp. 56-80,1977.

[46]   Wu, J., and Ellyin, F., "A Study of Fatigue Crack Closure by Elastic-Plastic Finite Element Analysis for Constant-Amplitude Loading," *International Journal of Fracture,* Volume 82, pp. 43-65,1996.

[47]   Park, S. J., Earmme, Y. Y., and Song, J.H., "Determination of the Most Appropriate Mesh Size for 2-D Finite Element Analysis of Fatigue Crack Closure Behavior," *Fatigue and Facture in Engineering Materials and Structure,* 20(4), pp. 533-545, 1997.

[48]   Newman, J. C. Jr., "A Finite-Element Analysis of Fatigue Crack Closure," *ASTM STP 590,* pp. 281-301, 1976.

[49]   McClung, R. C., "The Influence of Applied Stress, Crack Length, and Stress Intensity Factor on Crack Closure," Metallurgical Transactions A, Volume 22A, pp. 1559-1571, July, 1991.

[50]   McClung, R. C., "Finite Element Analysis of Specimen Geometry Effects on Fatigue Crack Closure," *Fatigue and Facture in Engineering Materials and Structure,* Volume 17(8), pp. 861-872, 1994.

[51]   Nicholas, T., Palazotto, A., and Bednarz, E., "An Analytical Investigation of Plasticity Induced Closure Involving Short Cracks," *ASTM STP 982* pp. 361-379, 1988.

[52]   Newman, J. C. Jr., "Finite Element Analysis of Fatigue Crack Propagation Including the Effects of Crack Closure," Ph.D. Thesis, Virginia Polytechnic Institute and State University, 1974.

[53]   Skinner, J. D., "Finite Element Analysis of Plasticity-Induced Fatigue Crack Closure in Three-Dimensional Cracked Geometries," MS Thesis, Department of Mechanical Engineering, Mississippi State University, 2001.

[54]   Blandford, R. S., Daniewicz, S. R., and Skinner, J. D., "Determination of the Opening Load for a Growing Crack: Evaluation of Experimental Data Reduction Techniques and Analytical Models," *Fatigue and Facture in Engineering Materials and Structure,* Volume 25(1), pp.17-26, 2002.

[55]   Roychowdhury, S., and Dodds, Jr., R. H., "Three-Dimensional Effects on Fatigue Crack Closure in the Small Scale-Yielding Regime," submitted to *Fatigue & Fracture of Engineering Materials & Structures,* 2002.

[56]   Chermahini, R. G., Shivakumar, K. N., and Newman, J. C., "Three-Dimensional Finite Element Simulation of Fatigue Crack Growth and Closure," *ASTM STP 982,* pp. 398-413, 1988.

[57]   Chermahini, R. G., and Blom, A. F., "Variation of Crack-Opening Stresses in Three-Dimensions: Finite Thickness Plate," *Theoretical and Applied Fracture Mechanics,* Volume 15, pp. 267-276, 1991.

[58] Chermahini, R. G., Palmberg, B., and Blom, A. F., "Fatigue Crack Growth and Closure Behavior of Semi-Circular and Semi-Elliptical Surface Flaws," *International Journal of Fatigue,* Volume 15(4), pp. 259-263, 1993.

[59] Zhang, J. Z., and Bowen, P., "On the Finite Element Simulation of Three-Dimensional Semi-Circular Fatigue Crack Growth and Closure," *Engineering Fracture Mechanics,* Volume 60, pp. 341-360, 1998.

[60] Skinner, J. D., and Daniewicz, S. R., "Simulation of Plasticity-Induced Fatigue Crack Closure in Part-Through Cracked Geometries Using Finite Element Analysis," *Engineering Fracture Mechanics,* Volume 69, pp. 1-11, 2002.

[61] Daniewicz, S. R., and Skinner, J. D., "Finite Element Analysis of Fatigue Crack Growth Threshold Testing Techniques," 13th European Conference on Fracture (ECF13), San Sebastian, Spain, 2000.

[62] Riddell, W. T., Piascik, R. S., Sutton, M. A., Zhao, W., McNeill, S. R., and Helm, J. D., "Determining Fatigue Crack Opening Loads From Near-Crack-Tip Displacement Measurements," *ASTM STP 1343,* Volume 2, pp. 157-74, 1999.

[63] Seshadri, B. R., "Numerical Simulation and Experimental Correlation of Crack Closure Phenomenon Under Cyclic Loading," Ph.D. Dissertation, Indian Institute of Science, Bangalore, 1995.

[64] McClung, R. C., "Finite Element Analysis of Fatigue Crack Closure: A Historical and Critical Review," Fatigue '99: The Seventh International Conference Beijing, China, June 8-12, 1999.

[65] Dawicke, D. S., Grandt, A. F. Jr., and Newman, J. C. Jr., "Three-Dimensional Crack Closure Behavior," *Engineering Fracture Mechanics*, Volume 36(1), pp. 111-121, 1990.

[66] Allison, J. E., Ku, R. C., and Pompetzki, M. A., "A Comparison of Measurement Methods and Numerical Procedures for the Experimental Characterization of Fatigue Crack Closure," *ASTM STP 982,* pp. 171-185, 1988.

[67] Ray, S. K., and Grandt, A. F., Jr., "Comparison of Methods for Measuring Fatigue Crack Closure in a Thick Specimen," *ASTM STP 982,* pp. 197-213, 1988.

[68] Donald, J. K., "A Procedure for Standardizing Crack Closure Levels," *ASTM STP 982,* pp. 222-229, 1988.

[69]   Daniewicz, S. R., and Bloom, J. M., "An Assessment of Geometry Effects on Plane Stress Fatigue Crack Closure Using a Modified Strip-Yield Model," *International Journal of Fatigue,* Volume 18(7), pp.483-490, 1996.

[70]   Nguyen, O., Repetto, E. A., Ortiz, M., and Radovitzky, R. A., "A Cohesive Model of Fatigue Crack Growth," *International Journal of Fracture,* Volume 110, pp.351-369, 2001.

[71]   Nagtegaal, J. C., Parks, D. M., and Rice, J. R., "On Numerically Accurate Finite Element Solutions in the Fully Plastic Range," *Computer Methods in Applied Mechanics and Engineering,* Volume 4, pp. 153-177, 1974.

[72]   Larsson, S. G., and Carlsson, A. J., "Influence of Non-Singular Stress Terms and Specimen Geometry on Small-Scale Yielding at the Crack Tips in Elastic-Plastic Materials," *Journal of Mechanics of Physical Solids,* Volume 21, pp.263-277, 1973.

[73]   Rice, J. R., "Limitations to Small Scale Yielding Approximation for Crack Tip Plasticity," *Journal of Mechanics of Physical Solids*, Volume 22, pp. 17-26, 1974.

[74]   Anderson, T. L., Fracture Mechanics: Fundamentals and Applications. CRC Press, LLC 2nd ed, pp. 72-75, 1994.

[75]   Sherry, A. H., France, C. C., and Goldthorpe, M. R., "Compendium of *T*-stress Solutions for Two and Three-Dimensional Cracked Geometries," *Fatigue and Facture in Engineering Materials and Structure,* Volume 18(1), pp.141-155, 1995.

[76]   Newman, J. C. Jr., "A Crack Closure Model for Predicting Fatigue Crack Growth Under Aircraft Spectrum Loading," *ASTM STP 748,* Volume 53, pp. 53-84, 1981.

[77]   Putra, I. S., and Schijve, J., "Crack Opening Stress Measurements of Surface Cracks in 7075-T6 Aluminum Alloy Plate Specimen Through Electron Fractography," *Fatigue and Facture in Engineering Materials and Structure,* Volume 15(4), pp. 323-338, 1992.

[78]   McDonald, V., and Daniewicz, S. R., "An Experimental Study of the Growth of Surface Flaws Under Cyclic Loading: Experimental uncertainty, aspect ratio evolution, and the influence of crack closure," *ASTM STP 1406,* pp. 381-396, 2001.

[79]   McDonald, V., "Growth of Surface Cracks Under Cyclic Loading," MS Thesis, Department of Mechanical Engineering, Mississippi State University, 2000.

[80]   Hughes, T. J. R., "Generalization of Selective Integration Procedures to Anisotropy and Non-Linear Media," *International Journal of Numerical Methods Engineering,* Volume 15, pp. 1413-1418, 1980.

[81]   Gall, K., Sehitoglu, H., and Kadioglu, Y., "FEM Study of Fatigue Crack Closure Under Double Slip," *Acta Metallurgica,* Volume 44(10), pp. 3955-3965, 1996.

[82]   Gall, K., Sehitoglu, H., and Kadioglu, Y., "Plastic Zone and Fatigue-Crack Closure Under Plane Strain Double slip," Metallurgical and Material Transactions A, Volume 27A, pp. 3491-3502, 1996.

[83]   Potirniche, G. P., and Daniewicz, S. R., "Finite Element Modeling of Microstructurally Small Cracks Using Single Crystal Plasticity," *International Conference on Fatigue Damage of Structural Material IV*, MA, USA, pp. 22-27, September, 2002.

[84]   ANSYS 6.1 ANSYS, Inc.

[85]   Newman, J. C., and Raju, I. S., "Stress-Intensity Factor Equations for Cracks in Three-Dimensional Finite Bodies Subjected to Tension and Bending," *Computational Methods in the Mechanics of Fracture,* Volume 2, pp. 311-334, 1986.

[86]   Rice, J. R., "Mechanics of Crack Tip Deformation and Extension by Fatigue," Fatigue Crack propagation, *ASTM STP 415,* pp. 247-309, 1967.

[87]   Daniewicz, S. R., Collins, J. A., and Houser, D. R., "An Elastic-Plastic Analytical Model for Predicting Fatigue Crack Growth in Arbitrary Edge-Cracked Two-Dimensional Geometries with Residual Stress," *International Journal of Fatigue,* Volume 16, pp. 123-133, 1999.

[88]   Dill, H. D., and Saff, C. R., "Spectrum Crack Growth Prediction Method Based on Crack Surface Displacement and Contact Analyses," *ASTM STP 595,* pp. 306-319, 1976.

[89]   Tada, H., Paris, P. C., and Irwin, G. R., The Stress Analysis of Crack Handbook. ASME Press, ASM International, pp. 3.1-5.18, 2000.

[90]   Parry, M. R., Syngellakis, S., and Sinclair, I., "Numerical modeling of combined roughness and plasticity induced crack closure effects in *Fatigue. Material Science and Engineering,* pp. 224-234, 2000.

APPENDIX A1

ANSYS INPUT FILE *APPBCS.MAC,* APPLICATION OF

BOUNDARY CONDITIONS, ANY LOAD RATIO

```
/prep7

! Element Shape Checking Off
SHPP,OFF

! Define Material Properties for Solid Elements
MP,EX,1,E
TB,BKIN,1,1,1, ,
TBMODIF,2,1,YS
!TBMODIF,3,1,HTAN




*IF,MTYPE,EQ,'SC',THEN
  ET,1,SOLID45,,,,,,
*ELSE
  !Normal Plane Element
  !ET,1,PLANE42,,,2,,

  !Reduced Iintegration Element
  ET,1,PLANE182,0,,0,,
  ! KEYOPT(3) = 0 Plane Stress
  ! KEYOPT(3) = 2 Plane Strain
  ! KEYOPT(3) = 3 Plane Stress w/ thk
*ENDIF


! Begin Building Model: Read Solid ELements from File

MAT,1
TYPE,1
REAL,1
nread,%JN%,crd
eread,%JN%,elm


*IF,MTYPE,EQ,'CT',THEN
  ! Create Linear Elastic Material Properties for Elastic "plug"
  MP,EX,2,E
  LOCAL,12,1,w,height,0,0,0,0
  NSEL,S,LOC,X,0,r
  ESLN,S,1
  EMODIF,ALL,MAT,2
  NSEL,ALL
  ESEL,ALL
  CSYS,0
*ENDIF

*IF,MTYPE,EQ,'2DCT',THEN
  ! Create Linear Elastic Material Properties for Elastic "plug"
  MP,EX,2,E
  LOCAL,12,1,w,height,0,0,0,0
  NSEL,S,LOC,X,0,r
  ESLN,S,1
  EMODIF,ALL,MAT,2
  NSEL,ALL
  ESEL,ALL
  CSYS,0
*ENDIF
```

```
*IF,MTYPE,EQ,'SEB',THEN
  ! Create Linear Elastic Material Properties for Loading Elements
  MP,EX,2,E

  !NSEL,S,LOC,Y,height
  !NSEL,R,LOC,X,0-10E-5,0+10E-5
  !ESLN,1

 ! NSEL,S,LOC,Y,height
  !*GET,SOUT,NODE,,COUNT
 ! DELT=W/(SOUT-1)
 ! NSEL,S,LOC,Y,height-delt-0.00001,height-delt-0.00001
 ! NSEL,R,LOC,X,DELT-0.00001,DELT+0.00001

 Nsel,s,loc,y,height-2,height
 nsel,r,loc,0,2
  ESLN,1

  EMODIF,ALL,MAT,2


  !NSEL,S,LOC,Y,height-delt-0.00001,height-delt-0.00001
  !NSEL,R,LOC,X,W-DELT-0.00001,W-DELT+0.00001
  Nsel,s,loc,y,height-2,height
  nsel,r,loc,w-2,w
  ESLN,1


  EMODIF,ALL,MAT,2
  NSEL,ALL
  ESEL,ALL


*ENDIF


!Constrain Nodes on Bottom Surface of Plate in the Vertical-direction
!(Constraints will be removed during crack growth)
!
!  Also, create component containing crack surface nodes (used
!  when negative loads are applied).  Assumes elliptical geometries
!  are notched, all others are not.

*IF,MTYPE,EQ,'SC',THEN
  NOTCH=NY(NODE(0,0,0))
  LOCAL,11,1,0,0,0,0,90,0,a/c
  NSEL,S,LOC,X,c,100000
  NSEL,R,LOC,Z,0,0
  NSEL,U,LOC,X,0,c-0.05*da
  D,ALL,UY,0
!Block Added for negative R,
  NSEL,S,LOC,Z,0
  NSEL,R,LOC,X,0,c
  NSEL,U,LOC,X,c-0.3*da,c+0.3*da
  CSYS,0
  NSEL,A,LOC,Y,NOTCH
  CM,CSNODES,NODE
!End of Block
*ELSE
```

```
  NSEL,S,LOC,Y,0
  NSEL,R,LOC,X,c,100000
  NSEL,U,LOC,X,0,c-da*0.25
  D,ALL,UY,0
!Block Added for negative R,
  NSEL,S,LOC,Y,0
  NSEL,R,LOC,X,0,c
  NSEL,U,LOC,X,c-0.3*da,c+0.3*da
  CM,CSNODES,NODE
!End of Block
*ENDIF


!Apply Appropriate Conditions in X-direction:

*IF,MTYPE,EQ,'CT',THEN
  NSEL,S,LOC,Y,0
  NSEL,R,LOC,Z,0
  NSEL,R,LOC,X,3.75
  D,ALL,UX,0
  NSEL,ALL
*ENDIF

*IF,MTYPE,EQ,'MT',THEN
  NSEL,S,LOC,X,0
  D,ALL,UX,0
  NSEL,ALL
*ENDIF

*IF,MTYPE,EQ,'SC',THEN
  NSEL,S,LOC,X,0
  D,ALL,UX,0
  NSEL,ALL
*ENDIF

*IF,MTYPE,EQ,'2DCT',THEN
  NDLOC=0
  NSEL,S,LOC,Y,0
  *GET,MINnode,NODE,,NUM,MIN
  NODEno=MINnode
  NDLOC=nx(NODEno)
  *GET,NSNODES,NODE,,COUNT
  *DO,L,1,NSNODES-1
    NODEno=NDNEXT(NODEno)
    NDLOC1=NX(NODEno)
    *IF,NDLOC1,GT,NDLOC,THEN
      NDLOC=NDLOC1
      MAXnode=NODEno
    *ENDIF
  *ENDDO
  NSEL,R,,,MAXnode
  D,ALL,UX,0
  NSEL,ALL
*ENDIF

*IF,MTYPE,EQ,'SEB',THEN
  NDLOC=0
  NSEL,S,LOC,Y,0
  *GET,MINnode,NODE,,NUM,MIN
  NODEno=MINnode
```

```
    NDLOC=nx(NODEno)
   *GET,NSNODES,NODE,,COUNT
   *DO,L,1,NSNODES-1
     NODEno=NDNEXT(NODEno)
     NDLOC1=NX(NODEno)
    *IF,NDLOC1,GT,NDLOC,THEN
      NDLOC=NDLOC1
      MAXnode=NODEno
    *ENDIF
   *ENDDO
   NSEL,R,,,MAXnode
   D,ALL,UX,0
   NSEL,ALL
 *ENDIF




!Apply Symetry BC's at Z=0 plane
*IF,MTYPE,EQ,'SC',THEN
  NSEL,S,LOC,Y,0
  NSEL,R,LOC,X,0
  NSEL,R,LOC,Z,t
  D,ALL,UZ,0
  NSEL,ALL
*ENDIF


*IF,MTYPE,EQ,'2DCT',THEN
  NSEL,S,LOC,Z,0
  D,ALL,UZ,0
  NSEL,ALL
*ENDIF


!Select Crack Mouth Node...Create Component CMNODES

NSEL,S,LOC,X,0
NSEL,R,LOC,Y,0
CM,CMNODES,NODE

CMSEL,ALL
NSEL,ALL
ESEL,ALL

WSORT,ALL,0         !Sort Elements to minimize wavefront

SAVE
FINISH
```

APPENDIX A2

ANSYS INPUT FILE *StrtCyc.MAC,* CONTROL OF

CYCLIC LOADING, ANY LOAD RATIO

```
FirstLoad
ClearRST,BDrive,BDir,MaxDir

*DO,I,1,NLC
  AdvanceCrack,I
  ClearRST,BDrive,BDir,''
  UnloadCrack,I
  ClearRST,BDrive,BDir,MinDir
  LoadCrack,I
  ClearRST,BDrive,BDir,MaxDir
*ENDDO
```

APPENDIX A3

ANSYS INPUT FILE *FIRSTLOAD.MAC,* APPLICATION OF

FIRST LOAD, ANY LOAD RATIO

```
! Apply Maximum Load on First Cycle:



/SOLU
Appload,height,StrsMax
AUTOTS,ON
NSUBST,5,10000,5,ON
TIME,0.45
SOLVE
SAVE
```

APPENDIX A4

ANSYS INPUT FILE *ADVANCECRACK.MAC,* INCREMENTALLY

ADVANCE THE CRACK TIP, ANY LOAD RATIO

```
! AdvanceCrack.mac
! Macro File to advance crack uniformly one element
!
! Should be executed as:
!
! AdvanceCrack,LoadCycleNumber
!

AUTOTS,OFF
NSUBST,1,1,1

/PREP7
SelCTNodes,arg1
*GET,NNODES,NODE,,COUNT
NODNO=0
*DO,JJ,1,NNODES
  NODNO=NDNEXT(NODNO)
   *GET,NODERF,NODE,NODNO,RF,FY
   DDELE,NODNO,UY
   F,NODNO,FY,NODERF
*ENDDO
NSEL,ALL
ESEL,ALL
/SOLU
ANTYPE,,REST

TimeVar=0.45+0.05/(NCGECut+1)+(arg1-1)
Time,TimeVar
SOLVE
SAVE

*DO,J,1,NCGECut-1
  /PREP7
  SelCTNodes,arg1
  NODNO=0
  *DO,JJ,1,NNODES
      NODNO=NDNEXT(NODNO)
       *GET,NODERF,NODE,NODNO,F,FY
       F,NODNO,FY,NODERF/CGERF
  *ENDDO
  NSEL,ALL
  ESEL,ALL
  /SOLU
  ANTYPE,,REST
  TimeVar=0.45+(J+1)*0.05/(NCGECut+1)+(arg1-1)
  Time,TimeVar
  SOLVE
  SAVE
*ENDDO

/PREP7
SelCTNodes,arg1
NODNO=0
*DO,JJ,1,NNODES
   NODNO=NDNEXT(NODNO)
    *GET,NODERF,NODE,NODNO,F,FY
    FDELE,NODNO,FY
*ENDDO
NSEL,ALL
```

```
ESEL,ALL
/SOLU
ANTYPE,,REST
TimeVar=arg1-0.5
Time,TimeVar
SOLVE
SAVE
```

APPENDIX A5

ANSYS INPUT FILE *UNLOADCRACK.MAC,*UNLOAD MODEL,

ANY LOAD RATIO

```
AUTOTS,ON
NSUBST,1,100,1,OFF
*CFOPEN,%JN%_unload_%arg1%,dat
!*VWRITE
! ("NODE#   Node r       NodeAng  S/Smax    UY             OStat Remote Stress")
CurrLInc=UIBCC
StrsLvl=StrsMax/StrsMax
RStrs=StrsMax
*DO,JJ,1,arg1
  SelCTNodes,JJ
  NSEL,U,D,UY,0
  *GET,NSNODES,NODE,,COUNT
  *IF,NSNODES,GT,0,THEN
    NODNO=0
    *DO,JJJ,1,NSNODES
       NODNO=NDNEXT(NODNO)
       NODYSTRS=UY(NODNO)
       *IF,MTYPE,EQ,'SC',THEN
         CSYS,11
         NDANG=NY(NODNO)
         NXLOC=NX(NODNO)
         CSYS,0
       *ELSE
         NDANG=NZ(NODNO)
         NXLOC=NX(NODNO)
       *ENDIF
       NodeStat=0
       *VWRITE,NODNO,NXLOC,NDANG,StrsLvl,NODYSTRS,NODESTAT,RSTRS
          (F6.0,2X,E12.6,2X,E10.4,2X,F8.6,2X,E12.6,2X,F4.0,2X,E12.6)
    *ENDDO
  *ENDIF
*ENDDO

*DO,J,1,1/UIDCC
  TimeVar=TimeVar+CurrLInc*0.5
  RStrs=StrsMax-(StrsMax-StrsMin)*(TimeVar+0.5-arg1)/0.5
  *IF,TimeVar,GE,arg1,Then
    RStrs=StrsMin
    TimeVar=arg1
    Time,TimeVar
    AppLoad,height,RStrs
    SOLVE
    SAVE
    *EXIT
  *ENDIF
  Time,TimeVar
  StrsLvl=RStrs/StrsMax
  AppLoad,height,RStrs
  SOLVE
  SAVE
  ClearRST,BDrive,BDir,''
  OPENSTAT=0
  OpnRwCnt=0
  *DO,JJ,1,arg1
    SelCTNodes,JJ
    NSEL,U,D,UY,0
    *GET,NSNODES,NODE,,COUNT
    *IF,NSNODES,GT,0,THEN
      NODNO=0
```

```
    *DO,JJJ,1,NSNODES
      NodeStat=0
      NODNO=NDNEXT(NODNO)
      NODYSTRS=UY(NODNO)
      *IF,MTYPE,EQ,'SC',THEN
        CSYS,11
        NDANG=NY(NODNO)
        NXLOC=NX(NODNO)
        CSYS,0
      *ELSE
        NDANG=NZ(NODNO)
        NXLOC=NX(NODNO)
      *ENDIF
      *IF,NodYStrs*1e10,LT,0,THEN
        CurrLInc=UIDCC
        OPENSTAT=1
        NODESTAT=1
        D,NODNO,UY,0
      *ENDIF
      *VWRITE,NODNO,NXLOC,NDANG,StrsLvl,NODYSTRS,NodeStat,RStrs
          (F6.0,2X,E12.6,2X,E10.4,2X,F8.6,2X,E12.6,2X,F4.0,2X,E12.6)
    *ENDDO
  *ELSEIF,NSNODES,EQ,0,THEN
    OpnRwCnt=OpnRwCnt+1
  *ENDIF
  *ENDDO
  NSEL,ALL

!  Close Crack surface nodes if negative load applied
!  Added for negative R -1
  *IF,RStrs,LE,0,THEN
    CMSEL,S,CSNODES
    NSEL,U,D,UY,0
    *GET,NSNODES,NODE,,COUNT
    *IF,NSNODES,GT,0,THEN
      NODNO=0
      *DO,JJJ,1,NSNODES
        NODNO=NDNEXT(NODNO)
        NODYSTRS=UY(NODNO)
        *IF,NodYStrs*1e10,LT,0,THEN
          OPENSTAT=1
          D,NODNO,UY,0
        *ENDIF
      *ENDDO
    *ENDIF
    NSEL,ALL
  *ENDIF
!  End of Block
  *IF,OPENSTAT,EQ,1,THEN
    Time,Timevar+CurrLInc*0.01
    SOLVE
    SAVE
    ClearRST,BDrive,BDir,''
  *ENDIF
  *IF,OpnRwCnt,EQ,arg1,THEN
    CurrLInc=UIACC
  *ENDIF
*ENDDO
*CFCLOSE
ContactStress,arg1
```

APPENDIX A6

ANSYS INPUT FILE *ContactStress.MAC,* CONTACT STRESS

METHOD, ANY LOAD RATIO

```
!   contact stress method


NSEL,ALL
ESEL,ALL
NODY1=0
NODY2=0

K=0
*CFOPEN,K1_%JN%_%arg1%,txt

PI=acos(-1)

SELCTNODES,(arg1+1)

*GET,FON,NODE,,NUM,MAX
AA=NX(FON)
NSEL,ALL

*IF,MTYPE,EQ,'2D',THEN
   NSEL,S,LOC,Y,0
   NSEL,R,LOC,X,0-(da*0.00001),AA+(da*0.00001)
   *GET,TNODE,NODE,,COUNT
   NSEL,S,LOC,Y,0
   NSEL,R,LOC,X,0-10e-5,0+10e-5
   *GET,FON1,NODE,,NUM,MAX
   A1=NX(FON1)
   NSEL,S,LOC,Y,0
   NSEL,R,LOC,X,0-(da*0.00001),AA+(da*0.00001)
   *DO,II,2,TNODE
      FON2=NNEAR(FON1)
      A2=NX(FON2)
      *GET,NODY1,NODE,FON1,RF,FY
      *GET,NODY2,NODE,FON2,RF,FY
      !CONVERSTION OF NODAL FORCE IN TO ELEMENT STRESS
      NODY1=NODY1/da
      NODY2=NODY2/da
      !FIND KMAX FOR MT SPECIMEN
      F=(1-(0.025*((aa/w)**2))+(0.06*((aa/w)**4)))*sqrt(1/cos((PI*aa)/(2*w)))
      KMAX=StrsMax*sqrt(PI*aa)*F
      !FIND KOPENING FOR MT SPECIMEN MODEL
      !AS INFINITE PLATE WITH A FINITE CRACK
      !WITH LINEAR ELEMENT STRESS DISTRIBUTION
      !MORE REFERENCE ORIGINAL PAPER
      !BY KIRAN SOLANKI, S.R.DANIEWICZ, J.C. NEWMAN JR.
      BB=A1
      CC=A2
      C1=(NODY2*BB-NODY1*CC)/(BB-CC)
      C2=(NODY1-NODY2)/(BB-CC)
      tem=asin(cc/aa)
      J1=(tem*C1)-(asin(BB/AA)*C1)+(C2*((sqrt(AA**2-bb**2))-(sqrt(AA**2-
cc**2))))
      K=((2*(sqrt(1/(AA*PI)))*(J1))/KMAX)+K
      NSEL,U,LOC,X,0-(da*0.00001),a1+(da*0.00001)
      FON1=FON2
      A1=A2
      NODY1=NODY1*da
```

```
      NODY2=NODY2*da
      !OUTPUT FOR THE FILE READ AS
      !NODE NO, NODE LOCATION, NODAL FORCE 1,
      !KOPEN/KMAX, DISTANCE FROM THE CRACK TIP, NODALFORCE 2
      *VWRITE,FON1,NXLOC,NODY1,K,BB,NODY2
            (F6.0,2X,E12.6,2X,E12.6,2X,E12.6,2X,F8.6,2x,E12.6)
      NSEL,U,LOC,X,0-(da*0.00001),a1+(da*0.00001)
      FON1=FON2
      A1=A2
      NODY1=0
      NODY2=0
    *ENDDO
*ENDIF

*IF,MTYPE,EQ,'2DCT',THEN
    !FIND KMAX FOR CT/SEB SPECIMENS
    AW=AA/w    !A/W RATIO
    B=1        !THICKNESS
    F=((2+AW)/((1-AW)**1.5))*(0.886+4.64*AW-13.32*(AW**2)+14.72*(AW**3)-
5.6*(AW**4))
    KMAX=F*StrsMax/(sqrt(W)*B)
    !FIND KOPENING FOR CT SPECIMEN MODEL
    !AS INFINITE PLATE WITH A SEMI-INFINITE CRACK
    !WITH LINEAR ELEMENT STRESS DISTRIBUTION
    !MORE REFERENCE ORIGINAL PAPER
    !BY KIRAN SOLANKI, S.R.DANIEWICZ, J.C. NEWMAN JR.
    NSEL,S,LOC,Y,0
    NSEL,R,LOC,X,0-(da*0.00001),AA+(da*0.00001)
    *GET,TNODE,NODE,,COUNT
    NODN=0
    NODN=NDNEXT(NODN)
    NX1=NX(NODN)
    FON1=NODN
    *DO,Z,2,TNODE
       NODN=NDNEXT(NODN)
       NX2=NX(NODN)
       *IF,NX2,LT,NX1,THEN
          NX1=NX2
          FON1=NODN
       *ENDIF
    *ENDDO
    NSEL,S,LOC,Y,0
    A1=AA-NX1
    NSEL,S,LOC,Y,0
    NSEL,R,LOC,X,0-(da*0.00001),AA+(da*0.00001)
    *DO,II,2,TNODE
        FON2=NNEAR(FON1)
        A2=NX(FON2)
        A2=AA-A2
        *GET,NODY1,NODE,FON1,RF,FY
        *GET,NODY2,NODE,FON2,RF,FY
        !CONVERSTION OF NODAL FORCE IN TO ELEMENT STRESS
        NODY1=NODY1/da
        NODY2=NODY2/da
        !Find Kopening FOR CT/SEB Models
        !As Infinite Plate With A Semi-infinite Crack
        !With Linear Element Stress Distribution
        !More Reference Original Paper
        !By Kiran Solanki, S.R.Daniewicz, J.C. Newman JR.
```

```
        BB=A1
        CC=A2
        C1=(NODY2*BB-NODY1*CC)/(BB-CC)
        C2=(NODY1-NODY2)/(BB-CC)
        K=((2/3)*sqrt(2/PI)*((sqrt(CC)*(3*C1+CC*C2))-
(sqrt(BB)*(3*C1+BB*C2))))/KMAX+K

        NODY1=NODY1*da
        NODY2=NODY2*da
        !OUTPUT FOR THE FILE READ AS
        !NODE NO, NODE LOCATION, NODAL FORCE 1,
        !KOPEN/KMAX, DISTANCE FROM THE CRACK TIP, NODALFORCE 2
        *VWRITE,FON1,NXLOC,NODY1,K,BB,NODY2
              (F6.0,2X,E12.6,2X,E12.6,2X,E12.6,2X,F8.6,2x,E12.6)
        NSEL,U,LOC,X,0-(da*0.00001),a1+(da*0.00001)
        FON1=FON2
        A1=A2
        NODY1=0
        NODY2=0
   *ENDDO
 *ENDIF


 *IF,MTYPE,EQ,'SEB',THEN
    !FIND KMAX FOR CT/SEB SPECIMENS
    AW=AA/w    !A/W RATIO
    B=1        !THICKNESS
    F=((2+AW)/((1-AW)**1.5))*(0.886+(4.64*AW)-(13.32*(AW**2))+(14.72*(AW**3))-
(5.6*(AW**4)))
    KMAX=F*(StrsMax/(sqrt(W)*B))
    !FIND KOPENING FOR CT SPECIMEN MODEL
    !AS INFINITE PLATE WITH A SEMI-INFINITE CRACK
    !WITH LINEAR ELEMENT STRESS DISTRIBUTION
    !MORE REFERENCE ORIGINAL PAPER
    !BY KIRAN SOLANKI, S.R.DANIEWICZ, J.C. NEWMAN JR.
    NSEL,S,LOC,Y,0
    NSEL,R,LOC,X,0-(da*0.00001),AA+(da*0.00001)
    *GET,TNODE,NODE,,COUNT
    NODN=0
    NODN=NDNEXT(NODN)
    NX1=NX(NODN)
    FON1=NODN
    *DO,Z,2,TNODE
       NODN=NDNEXT(NODN)
       NX2=NX(NODN)
       *IF,NX2,LT,NX1,THEN
          NX1=NX2
          FON1=NODN
       *ENDIF
    *ENDDO
    a4=nx1
    A1=AA-NX1
    NSEL,S,LOC,Y,0
    NSEL,R,LOC,X,0-(da*0.00001),AA+(da*0.00001)
    *DO,II,2,TNODE
        FON2=NNEAR(FON1)
        A3=NX(FON2)
        A2=AA-A3
        *GET,NODY1,NODE,FON1,RF,FY
        *GET,NODY2,NODE,FON2,RF,FY
```

```
        !CONVERSTION OF NODAL FORCE IN TO ELEMENT STRESS
        NODY1=NODY1/da
        NODY2=NODY2/da
        !Find Kopening FOR CT/SEB Models
        !As Infinite Plate With A Semi-infinite Crack
        !With Linear Element Stress Distribution
        !More Reference Original Paper
        !By Kiran Solanki, S.R.Daniewicz, J.C. Newman JR.

        BB=A1
        CC=A2
        C1=((NODY2*BB)-(NODY1*CC))/(BB-CC)
        C2=(NODY1-NODY2)/(BB-CC)
        t1=3*C1*(sqrt(bb)-sqrt(cc))
        t2=C2*((sqrt(BB)*BB)-(sqrt(CC)*CC))
        tem=sqrt(2/PI)*(2/3)*(t1+t2)
        K=(tem/kmax)+K

        NODY1=NODY1*da
        NODY2=NODY2*da
        !OUTPUT FOR THE FILE READ AS
        !NODE NO, NODE LOCATION, NODAL FORCE 1,
        !KOPEN/KMAX, DISTANCE FROM THE CRACK TIP, NODALFORCE 2
        *VWRITE,FON1,NXLOC,NODY1,K,BB,NODY2
              (F6.0,2X,E12.6,2X,E12.6,2X,E12.6,2X,F8.6,2x,E12.6)
        NSEL,U,LOC,X,0-(da*0.00001),a4+(da*0.00001)
        FON1=FON2
        A1=A2
        NODY1=0
        NODY2=0
        a4=a3
    *ENDDO
*ENDIF
```

APPENDIX A7

ANSYS INPUT FILE *LOADCRACK.MAC,* LOAD

MODEL, ANY LOAD RATIO

```
AUTOTS,ON
NSUBST,1,100,1,OFF
*CFOPEN,%JN%_load_%arg1%,dat

!*VWRITE
! ("NODE#   Node r       NodeAng  S/Smax    SY              OStat Remote Stress")

CurrLInc=LIBCO
StrsLvl=StrsMin/StrsMax
RStrs=StrsMin
*DO,JJ,1,arg1
  SelCTNodes,JJ
  NSEL,R,D,UY,0
  *GET,NSNODES,NODE,,COUNT
  *IF,NSNODES,GT,0,THEN
    NODNO=0
    *DO,JJJ,1,NSNODES
      NODNO=NDNEXT(NODNO)
      *GET,NODYSTRS,NODE,NODNO,S,Y
      *IF,MTYPE,EQ,'SC',THEN
        CSYS,11
        NDANG=NY(NODNO)
        NXLOC=NX(NODNO)
        CSYS,0
      *ELSE
        NDANG=NZ(NODNO)
        NXLOC=NX(NODNO)
      *ENDIF
      NodeStat=0
      *VWRITE,NODNO,NXLOC,NDANG,StrsLvl,NODYSTRS,NODESTAT,RSTRS
        (F6.0,2X,E12.6,2X,E10.4,2X,E12.6,2X,E12.6,2X,F4.0,2X,E12.6)


!(F6.0,2X,E12.6,2X,E10.4,2X,F8.6,2X,E12.6,2X,F4.0,2X,E12.6)
    *ENDDO
  *ENDIF
*ENDDO
*DO,J,1,1/LIDCO
  TimeVar=TimeVar+CurrLInc*0.45
  RStrs=(StrsMax-StrsMin)*(TimeVar-arg1)/0.45+StrsMin
  *IF,TimeVar,GE,arg1+0.45,Then
    RStrs=StrsMax
    TimeVar=arg1+0.45
    Time,TimeVar
    AppLoad,height,RStrs
    SOLVE
    SAVE
    *EXIT
  *ENDIF
  Time,TimeVar
  StrsLvl=RStrs/StrsMax
  AppLoad,height,RStrs
  SOLVE
  SAVE
  ClearRST,BDrive,BDir,''
  OPENSTAT=0
  OpnRwCnt=0
```

```
    *DO,JJ,1,arg1
      SelCTNodes,JJ
      NSEL,R,D,UY,0
      *GET,NSNODES,NODE,,COUNT
      *IF,NSNODES,GT,0,THEN
        NODNO=0
        *DO,JJJ,1,NSNODES
          NodeStat=0
          NODNO=NDNEXT(NODNO)
          *GET,NodYStrs,NODE,NODNO,S,Y
          *IF,MTYPE,EQ,'SC',THEN
            CSYS,11
            NDANG=NY(NODNO)
            NXLOC=NX(NODNO)
            CSYS,0
          *ELSE
            NDANG=NZ(NODNO)
            NXLOC=NX(NODNO)
          *ENDIF
          *IF,NodYStrs*1e10,GT,0,THEN
            CurrLInc=LIDCO
            OPENSTAT=1
            NODESTAT=1
            DDELE,NODNO,UY
          *ENDIF
          *VWRITE,NODNO,NXLOC,NDANG,StrsLvl,NODYSTRS,NodeStat,RStrs
            (F6.0,2X,E12.6,2X,E10.4,2X,E12.6,2X,E12.6,2X,F4.0,2X,E12.6)
        *ENDDO
      *ELSEIF,NSNODES,EQ,0,THEN
        OpnRwCnt=OpnRwCnt+1
      *ENDIF
    *ENDDO
    NSEL,ALL

! Block Added for negative R,

    CMSEL,S,CSNODES
    NSEL,R,D,UY,0
    *GET,NSNODES,NODE,,COUNT
    *IF,NSNODES,GT,0,THEN
      NODNO=0
      *DO,JJJ,1,NSNODES
        NODNO=NDNEXT(NODNO)
        *GET,NodYStrs,NODE,NODNO,S,Y
        *IF,NodYStrs*1e10,GT,0,THEN
          OPENSTAT=1
          DDELE,NODNO,UY
        *ENDIF
      *ENDDO
    *ENDIF
    NSEL,ALL

! End of New Block

    *IF,OPENSTAT,EQ,1,THEN
      Time,Timevar+CurrLInc*0.01
      SOLVE
      SAVE
      ClearRST,BDrive,BDir,''
    *ENDIF
```

```
  *IF,OpnRwCnt,EQ,arg1,THEN
    CurrLInc=LIACO
  *ENDIF
*ENDDO
*CFCLOSE
```

APPENDIX A8

ANSYS INPUT FILE *SELCTNODES.MAC,* SELECT CRACK

TIP NODE, ANY LOAD RATIO

```
! SelCTNodes.mac
! Macro to Select the Crack tip nodes for load cycle "N"
!
! Executed as follows:
!     SelCTNodes,N
!
!Set Coordinate System to Elliptical


*IF,MTYPE,EQ,'SC',THEN
  ! The following are for a surface crack: (Using Faleskog Numbering Scheme)
  LOCAL,11,1,0,0,0,0,90,0,a/c
  NSEL,S,LOC,X,c-0.3*da,c+0.3*da
  NSEL,R,LOC,Z,0
  *GET,FNODNO,NODE,,NUM,MIN
  *GET,LNODNO,NODE,,NUM,MAX
  DELTANN=NDNEXT(FNODNO)-FNODNO
  *GET,NODCNT,NODE,,COUNT
  NSEL,S,NODE,,FNODNO+(arg1-1),LNODNO+(arg1-1),DELTANN
  CSYS,0
*ELSE
  NSEL,S,LOC,Y,0
  NSEL,R,LOC,X,c+da*(arg1-1.25),c+da*(arg1-0.75)
*ENDIF

!LOCAL,11,1,0,0,0,0,90,0,(a+da*(arg1-1))/(c+da*(arg1-1))
!NSEL,S,LOC,X,c+(arg1-1.45)*da,c+(arg1-0.55)*da
!NSEL,R,LOC,Z,0
!CSYS,0
```

APPENDIX A9

ANSYS INPUT FILE *CLEARRST.MAC,* DELETE UNNECESSARY

OUTPUT FILES, ANY LOAD RATIO

```
!  This Macro Saves Disk Space by deleting 'jobname'.rst
!  It also provides a tool for stopped jobs by saving the
!  db and rst from the last completed loadstep to a backup
!  directory
!  Execution of this macro should be done with the following command:
!  ClearRST,BDrive,Bdir1,Bdir2
!
!  If Bdir2 is unneccessary, '' should be input
!
!  Modified 1/28/2000

SAVE
FINISH
!pltpzone
!/COPY,,RST,,,,%arg1%%arg2%%arg3%

!/COPY,,EMAT,,,,%arg1%%arg2%%arg3%
/COPY,,OSAV,,,,%arg1%%arg2%%arg3%
/COPY,,ESAV,,,,%arg1%%arg2%%arg3%
/COPY,,MNTR,,,,%arg1%%arg2%%arg3%
/COPY,,DB,,,,%arg1%%arg2%%arg3%
!/COPY,,DB,,%jn%_%arg4%,,%arg1%%arg2%%arg3%
/DELETE,,RST
/SOLU
ANTYPE,,REST
```

APPENDIX A10

ANSYS INPUT FILE *APPLOAD.MAC,* APPLICATION OF

LOAD, ANY LOAD RATIO

```
! This macro is used to apply Surface Pressure

! along the top of the hole in the CT model
!
! The center of the hole should be at coordinates
! x = w, y = h
!
! Use should be as follows:
! SCappLoad,height,Pressure



*IF,MTYPE,EQ,'CT',THEN
   NSEL,S,LOC,X,w
   NSEL,R,LOC,Y,arg1
   NSEL,R,LOC,Z,0
   F,ALL,FY,arg2
   NSEL,ALL
*ENDIF

*IF,MTYPE,EQ,'2DCT',THEN
   NSEL,S,LOC,X,w
   NSEL,R,LOC,Y,arg1
   NSEL,R,LOC,Z,0
   F,ALL,FY,arg2
   NSEL,ALL
*ENDIF

*IF,MTYPE,EQ,'SEB',THEN
   NSEL,S,LOC,Y,height
   NSEL,R,LOC,X,0-10E-5,0+10E-5
   F,ALL,FY,arg2
   NSEL,S,LOC,Y,height
   NSEL,R,LOC,X,W
   F,ALL,FY,-arg2
   Nsel,all
*ENDIF

*IF,MTYPE,EQ,'SC',THEN
   NSEL,S,LOC,Y,arg1
   !D,ALL,UY,arg2
   SF,ALL,PRES,-arg2
   NSEL,ALL
*ENDIF


*IF,MTYPE,EQ,'MT',THEN
   NSEL,S,LOC,Y,arg1
   !D,ALL,UY,arg2
   SF,ALL,PRES,-arg2
   NSEL,ALL
*ENDIF
```

APPENDIX A11

ANSYS INPUT FILE *APPLOAD.MAC,* APPLICATION

OF LOAD, T-STRESS

```
! This macro is used to apply Surface Pressure

! along the top of the hole in the CT model
!
! The center of the hole should be at coordinates
! x = w, y = h
!
! Use should be as follows:
! SCappLoad,height,Pressure
!
!

*IF,MTYPE,EQ,'CT',THEN
   NSEL,S,LOC,X,w
   NSEL,R,LOC,Y,arg1
   NSEL,R,LOC,Z,0
   F,ALL,FY,arg2
   NSEL,ALL
*ELSEIF,MTYPE,EQ,'2DCT'
   NSEL,S,LOC,X,w
   NSEL,R,LOC,Y,arg1
   NSEL,R,LOC,Z,0

   !nsel,s,,,bon

   F,ALL,FY,arg2
   NSEL,ALL
*ELSEIF,MTYPE,EQ,'2D'
   NSEL,S,LOC,Y,arg1
!   D,ALL,UY,arg2
  SF,ALL,PRES,-arg2
   NSEL,ALL
!T-STRESS
NSEL,S,LOC,X,w
SF,ALL,PRES,-arg2
NSEL,ALL
*ELSE
   NSEL,S,LOC,Y,arg1
!   D,ALL,UY,arg2
  SF,ALL,PRES,-arg2
   NSEL,ALL

*ENDIF
```

APPENDIX A12

ANSYS INPUT FILE *LOADCRACK.DAT,* LOAD MODEL, T-STRESS

```
AUTOTS,ON
NSUBST,1,100,1,OFF
*CFOPEN,%JN%_load_%arg1%,dat

!*VWRITE
! ("NODE#   Node r      NodeAng  S/Smax   SY          OStat Remote Stress")

CurrLInc=LIBCO
StrsLvl=StrsMin/StrsMax
RStrs=StrsMin
*DO,JJ,1,arg1
  SelCTNodes,JJ
  NSEL,R,D,UY,0
  *GET,NSNODES,NODE,,COUNT
  *IF,NSNODES,GT,0,THEN
    NODNO=0
    *DO,JJJ,1,NSNODES
       NODNO=NDNEXT(NODNO)
       *GET,NODYSTRS,NODE,NODNO,S,Y
       *IF,MTYPE,EQ,'SC',THEN
         CSYS,11
         NDANG=NY(NODNO)
         NXLOC=NX(NODNO)
         CSYS,0
       *ELSE
         NDANG=NZ(NODNO)
         NXLOC=NX(NODNO)
       *ENDIF
       NodeStat=0
       *VWRITE,NODNO,NXLOC,NDANG,StrsLvl,NODYSTRS,NODESTAT,RSTRS
          (F6.0,2X,E12.6,2X,E10.4,2X,F8.6,2X,E12.6,2X,F4.0,2X,E12.6)
    *ENDDO
  *ENDIF
*ENDDO
*DO,J,1,1/LIDCO
  TimeVar=TimeVar+CurrLInc*0.45
  RStrs=(StrsMax-StrsMin)*(TimeVar-arg1)/0.45+StrsMin
  *IF,TimeVar,GE,arg1+0.45,Then
    RStrs=StrsMax
    TimeVar=arg1+0.45
    Time,TimeVar
    AppLoad,height,RStrs
    SOLVE
    SAVE
    *EXIT
  *ENDIF
  Time,TimeVar
  StrsLvl=RStrs/StrsMax
  AppLoad,height,RStrs
  SOLVE
  SAVE
  ClearRST,BDrive,BDir,''
  OPENSTAT=0
  OpnRwCnt=0
  *DO,JJ,1,arg1
    SelCTNodes,JJ
    NSEL,R,D,UY,0
    *GET,NSNODES,NODE,,COUNT
    *IF,NSNODES,GT,0,THEN
      NODNO=0
```

```
        *DO,JJJ,1,NSNODES
          NodeStat=0
          NODNO=NDNEXT(NODNO)
          *GET,NodYStrs,NODE,NODNO,S,Y
          *IF,MTYPE,EQ,'SC',THEN
            CSYS,11
            NDANG=NY(NODNO)
            NXLOC=NX(NODNO)
            CSYS,0
          *ELSE
            NDANG=NZ(NODNO)
            NXLOC=NX(NODNO)
          *ENDIF
          *IF,NodYStrs*1e10,GT,0,THEN
            CurrLInc=LIDCO
            OPENSTAT=1
            NODESTAT=1
            DDELE,NODNO,UY
          *ENDIF
          *VWRITE,NODNO,NXLOC,NDANG,StrsLvl,NODYSTRS,NodeStat,RStrs
              (F6.0,2X,E12.6,2X,E10.4,2X,F8.6,2X,E12.6,2X,F4.0,2X,E12.6)
        *ENDDO
      *ELSEIF,NSNODES,EQ,0,THEN
        OpnRwCnt=OpnRwCnt+1
      *ENDIF
    *ENDDO
    NSEL,ALL
    *IF,OPENSTAT,EQ,1,THEN
      Time,Timevar+CurrLInc*0.01
      SOLVE
      SAVE
      ClearRST,BDrive,BDir,''
    *ENDIF
    *IF,OpnRwCnt,EQ,arg1,THEN
      CurrLInc=LIACO
    *ENDIF
  *ENDDO
  *CFCLOSE
```

APPENDIX A13

ANSYS INPUT FILE *UNLOADCRCAK.DAT,* UNLOAD MODEL, T-STRESS

```
AUTOTS,ON
NSUBST,1,100,1,OFF
*CFOPEN,%JN%_unload_%arg1%,dat
!*VWRITE
! ("NODE#   Node r      NodeAng  S/Smax   UY          OStat Remote Stress")
CurrLInc=UIBCC
StrsLvl=StrsMax/StrsMax
RStrs=StrsMax
*DO,JJ,1,arg1
  SelCTNodes,JJ
  NSEL,U,D,UY,0
  *GET,NSNODES,NODE,,COUNT
  *IF,NSNODES,GT,0,THEN
    NODNO=0
    *DO,JJJ,1,NSNODES
       NODNO=NDNEXT(NODNO)
       NODYSTRS=UY(NODNO)
       *IF,MTYPE,EQ,'SC',THEN
         CSYS,11
         NDANG=NY(NODNO)
         NXLOC=NX(NODNO)
         CSYS,0
       *ELSE
         NDANG=NZ(NODNO)
         NXLOC=NX(NODNO)
       *ENDIF
       NodeStat=0
       *VWRITE,NODNO,NXLOC,NDANG,StrsLvl,NODYSTRS,NODESTAT,RSTRS
          (F6.0,2X,E12.6,2X,E10.4,2X,F8.6,2X,E12.6,2X,F4.0,2X,E12.6)
    *ENDDO
  *ENDIF
*ENDDO

*DO,J,1,1/UIDCC
  TimeVar=TimeVar+CurrLInc*0.5
  RStrs=StrsMax-(StrsMax-StrsMin)*(TimeVar+0.5-arg1)/0.5
  *IF,TimeVar,GE,arg1,Then
    RStrs=StrsMin
    TimeVar=arg1
    Time,TimeVar
    AppLoad,height,RStrs
    SOLVE
    SAVE
!modified
    *DO,JJ,1,arg1
    SelCTNodes,JJ
    NSEL,U,D,UY,0
    *GET,NSNODES,NODE,,COUNT
    *IF,NSNODES,GT,0,THEN
      NODNO=0
      *DO,JJJ,1,NSNODES
        NodeStat=0
        NODNO=NDNEXT(NODNO)
        NODYSTRS=UY(NODNO)
        *IF,MTYPE,EQ,'SC',THEN
          CSYS,11
          NDANG=NY(NODNO)
          NXLOC=NX(NODNO)
          CSYS,0
```

```
            *ELSE
              NDANG=NZ(NODNO)
              NXLOC=NX(NODNO)
            *ENDIF
            *IF,NodYStrs*1e10,LT,0,THEN
              CurrLInc=UIDCC
              OPENSTAT=1
              NODESTAT=1
              D,NODNO,UY,0
            *ENDIF
            *VWRITE,NODNO,NXLOC,NDANG,StrsLvl,NODYSTRS,NodeStat,RStrs
                (F6.0,2X,E12.6,2X,E10.4,2X,F8.6,2X,E12.6,2X,F4.0,2X,E12.6)
        *ENDDO
        *endif
        *enddo
!end of modification
      *EXIT
    *ENDIF
    Time,TimeVar
    StrsLvl=RStrs/StrsMax
    AppLoad,height,RStrs
    SOLVE
    SAVE
    ClearRST,BDrive,BDir,''
    OPENSTAT=0
    OpnRwCnt=0
    *DO,JJ,1,arg1
      SelCTNodes,JJ
      NSEL,U,D,UY,0
      *GET,NSNODES,NODE,,COUNT
      *IF,NSNODES,GT,0,THEN
        NODNO=0
        *DO,JJJ,1,NSNODES
          NodeStat=0
          NODNO=NDNEXT(NODNO)
          NODYSTRS=UY(NODNO)
          *IF,MTYPE,EQ,'SC',THEN
            CSYS,11
            NDANG=NY(NODNO)
            NXLOC=NX(NODNO)
            CSYS,0
          *ELSE
            NDANG=NZ(NODNO)
            NXLOC=NX(NODNO)
          *ENDIF
          *IF,NodYStrs*1e10,LT,0,THEN
            CurrLInc=UIDCC
            OPENSTAT=1
            NODESTAT=1
            D,NODNO,UY,0
          *ENDIF
          *VWRITE,NODNO,NXLOC,NDANG,StrsLvl,NODYSTRS,NodeStat,RStrs
              (F6.0,2X,E12.6,2X,E10.4,2X,F8.6,2X,E12.6,2X,F4.0,2X,E12.6)
        *ENDDO
      *ELSEIF,NSNODES,EQ,0,THEN
        OpnRwCnt=OpnRwCnt+1
      *ENDIF
    *ENDDO
    NSEL,ALL
    *IF,OPENSTAT,EQ,1,THEN
```

```
      Time,Timevar+CurrLInc*0.01
      SOLVE
      SAVE
      ClearRST,BDrive,BDir,''
   *ENDIF
   *IF,OpnRwCnt,EQ,arg1,THEN
      CurrLInc=UIACC
   *ENDIF
*ENDDO
save
*CFCLOSE
```

APPENDIX A14

ANSYS INPUT FILE *StrtCyc.MAC,* CONTROL OF CYCLIC

LOADING, MIN LOAD RELEASE SHCEME

```
FirstLoad
ClearRST,BDrive,BDir,MaxDir


*DO,I,1,NLC
  UnloadCrack,I
  ClearRST,BDrive,BDir,MinDir
  LoadCrack,I
  ClearRST,BDrive,BDir,MaxDir
*ENDDO
```

APPENDIX B1

ANSYS INPUT FILE *SEB.DAT,* INPUT FILE FOR SEB SPECIMEN

```
/BATCH
! This runs the script "SCmodel.dat"  to import the Solid
! Elements and Nodes from the files "jobname.crd" & "jobname.elm",
! and applies necessary boundary conditions for Crack Growth
! It then calls "SCLoadfile.dat"  to run growth analysis.
!

!Note all lengths are in in, and pressures in Psi

/CONFIG,NPROC,1

!Loading information:

StrsMax=314.385          ! Maximum Applied Stress
StrsMin=0               ! Minimum Applied Stress
!NLC=1
NLC=40                  ! Total Number of Loading Cycles to execute

!Geometry Information:

MTYPE='SEB'

t=0                     ! Thickness of plate
w=20                    ! Plate Half-Width
height=40                ! Model Height
c=2            ! Initial Crack half-length initial craktip node number 362
a=0            ! Initial Depth of Surface Crack
da=0.0185185            ! Crack Growth Increment

!Material Properties:

E=200e3                 ! Young's Modulus
YS=230                  ! Yield Stress

!Matrix Element Properties:

KCGELE=10**12           ! Crack Growth Element Stiffness
NCGECut=10               ! Number of bisections to matrix stiffness before
CGERF=2                  ! Crack Growth Element Stiffness Reduction Factor

*get,JN,ACTIVE,,JOBNAM
/TITLE, Plasticity Induced Closure of model %JN%

AppBCs

BDrive='d:'           ! Drive for file backups
BDir='\backup'        ! Directory for file backups
MaxDir='\maxload'     ! Directory for backup at Max Load
MinDir='\minload'     ! Directory for Backup at Min Load

!Solution Information:

/SOLU                  ! Enter Solution Processor

LIBCO=0.0125            ! Loading Increment before crack opening
LIDCO=0.0125            ! Loading Increment during crack opening
LIACO=0.01250           ! Loading Increment after crack opening
UIBCC=0.0125            ! Un-load Increment before crack closing
```

```
UIDCC=0.0125              ! Un-load Increment during crack closing
UIACC=0.0125               ! Un-load Increment after crack closing


NSUB,1
NEQIT,8                   ! Number of Equillibrium Iterations before bisection
NROPT,FULL,,ON            ! Full Newton Rapson Option, Adaptive Descent ON
EQSLV,PCG,1.0e-8          ! Use the Pre-Conditioned Conjugate Solver (In Core)


RESCONTROL,DEFINE,NONE,NONE,0
StrtCyc
```

APPENDIX B2

ANSYS INPUT FILE *MT.DAT,* INPUT FILE FOR M(T) SPECIMEN

```
/BATCH

! This runs the script "SCmodel.dat"  to import the Solid
! Elements and Nodes from the files "jobname.crd" & "jobname.elm",
! and applies necessary boundary conditions for Crack Growth
! It then calls "SCLoadfile.dat"  to run growth analysis.
!

!Note all lengths are in in, and pressures in Psi

/CONFIG,NPROC,1

!Loading information:

StrsMax=0.2*230             ! Maximum Applied Stress
StrsMin=-0.2*230             ! Minimum Applied Stress

NLC=45                   ! Total Number of Loading Cycles to execute

!Geometry Information:

MTYPE='MT'

t=0                 ! Thickness of plate
w=40                 ! Plate Half-Width
height=40              ! Model Height
c=4            ! Initial Crack half-length initial craktip node number 362
a=0            ! Initial Depth of Surface Crack
da=0.005486968             ! Crack Growth Increment

!Material Properties:

E=200e3             ! Young's Modulus
YS=230              ! Yield Stress

!Matrix Element Properties:

KCGELE=10**12           ! Crack Growth Element Stiffness
NCGECut=5             ! Number of bisections to matrix stiffness before
CGERF=2              ! Crack Growth Element Stiffness Reduction Factor

*get,JN,ACTIVE,,JOBNAM
/TITLE, Plasticity Induced Closure of model %JN%

AppBCs

BDrive='c:'           ! Drive for file backups
BDir='\backup'        ! Directory for file backups
MaxDir='\maxload'     ! Directory for backup at Max Load
MinDir='\minload'     ! Directory for Backup at Min Load

!Solution Information:

/SOLU                 ! Enter Solution Processor

LIBCO=0.0125           ! Loading Increment before crack opening
LIDCO=0.0125           ! Loading Increment during crack opening
LIACO=0.01250          ! Loading Increment after crack opening
UIBCC=0.0125           ! Un-load Increment before crack closing
UIDCC=0.0125           ! Un-load Increment during crack closing
```

```
      UIACC=0.01250                 ! Un-load Increment after crack closing


      NSUB,1
      NEQIT,8                       ! Number of Equillibrium Iterations before bisection
      NROPT,FULL,,ON                ! Full Newton Rapson Option, Adaptive Descent ON
      EQSLV,PCG,1.0e-8              ! Use the Pre-Conditioned Conjugate Solver (In Core)


      RESCONTROL,DEFINE,NONE,NONE,0
      StrtCyc
```

APPENDIX B3

ANSYS INPUT FILE *MT.DAT,* INPUT FILE FOR M(T) SPECIMEN, T-STRESS

```
/BATCH
! This is the input file for schiv_15.dat
! This runs the script "SCmodel.dat"  to import the Solid
! Elements and Nodes from the files "jobname.crd" & "jobname.elm",
! and applies necessary boundary conditions for Crack Growth
! It then calls "SCLoadfile.dat"  to run growth analysis.
!
!
!Note all lengths are in in, and pressures in Psi

/CONFIG,NPROC,1

!Loading information:

StrsMax=69            ! Maximum Applied Stress
StrsMin=0             ! Minimum Applied Stress
!t stress for MT t=0.435
tstress=99
NLC=36                    ! Total Number of Loading Cycles to execute

!Geometry Information:

MTYPE='MT'

t=0                   ! Thickness of plate
w=40                  ! Plate Half-Width
height=40                ! Model Height
c=4           ! Initial Crack half-length initial craktip node number 362
a=0           ! Initial Depth of Surface Crack
da=0.0030864           ! Crack Growth Increment

!Material Properties:

E=200e3               ! Young's Modulus
YS=230                ! Yield Stress

!Matrix Element Properties:

KCGELE=10**12            ! Crack Growth Element Stiffness
NCGECut=10                ! Number of bisections to matrix stiffness before
CGERF=2                  ! Crack Growth Element Stiffness Reduction Factor

*get,JN,ACTIVE,,JOBNAM
/TITLE, Plasticity Induced Closure of model %JN%

AppBCs

BDrive='E:'           ! Drive for file backups
BDir='\backup'        ! Directory for file backups
MaxDir='\maxload'     ! Directory for backup at Max Load
MinDir='\minload'     ! Directory for Backup at Min Load

!Solution Information:

/SOLU                 ! Enter Solution Processor

LIBCO=0.05            ! Loading Increment before crack opening
LIDCO=0.025           ! Loading Increment during crack opening
```

```
LIACO=0.10               ! Loading Increment after crack opening
UIBCC=0.05               ! Un-load Increment before crack closing
UIDCC=0.025              ! Un-load Increment during crack closing
UIACC=0.10               ! Un-load Increment after crack closing
SOLCONTROL,ON
NSUB,1
NEQIT,8                  ! Number of Equillibrium Iterations before bisection
NROPT,FULL,,ON           ! Full Newton Rapson Option, Adaptive Descent ON
EQSLV,PCG,1.0e-8         ! Use the Pre-Conditioned Conjugate Solver (In Core)


RESCONTROL,DEFINE,NONE,NONE,0


StrtCyc
```

APPENDIX C1

ANSYS INPUT FILE *APPBCS.MAC,* APPLICATION OF BOUNDARY

CONDITIONS, SPIKE OVERLOAD

```
/prep7

! Element Shape Checking Off
SHPP,OFF

! Define Material Properties for Solid Elements
MP,EX,1,E
TB,BKIN,1,1,1, ,
TBMODIF,2,1,YS
!TBMODIF,3,1,HTAN

*IF,MTYPE,EQ,'2D',THEN
  ET,1,PLANE42,,,2,,
   ! KEYOPT(3) = 0 Plane Stress
   ! KEYOPT(3) = 2 Plane Strain
   ! KEYOPT(3) = 3 Plane Stress w/ thk
*ELSE
  ET,1,SOLID45,,,,,,
*ENDIF

! Begin Building Model: Read Solid ELements from File

MAT,1
TYPE,1
REAL,1
nread,%JN%,crd
eread,%JN%,elm

*IF,MTYPE,EQ,'CT',THEN
  ! Create Linear Elastic Material Properties for Elastic "plug"
  MP,EX,2,E
  LOCAL,12,1,w,height,0,0,0,0
  NSEL,S,LOC,X,0,r
  ESLN,S,1
  EMODIF,ALL,MAT,2
  NSEL,ALL
  ESEL,ALL
  CSYS,0
*ENDIF

!Constrain Nodes on Bottom Surface of Plate in the Vertical-direction
!(Constraints will be removed during crack growth)
!
!  Also, create component containing crack surface nodes (used
!  when negative loads are applied).  Assumes elliptical geometries
!  are notched, all others are not.

*IF,MTYPE,EQ,'SC',THEN
  LOCAL,11,1,0,0,0,0,90,0,a/c
  NSEL,S,LOC,X,c,100000
  NSEL,R,LOC,Z,0,0
  NSEL,U,LOC,X,0,c-0.05*da
  D,ALL,UY,0

  CSYS,0


*ELSE
  NSEL,S,LOC,Y,0
  NSEL,R,LOC,X,c,100000
```

```
  NSEL,U,LOC,X,0,c-da*0.25
  D,ALL,UY,0

*ENDIF

!Apply Appropriate Conditions in X-direction:
*IF,MTYPE,EQ,'CT',THEN
  NSEL,S,LOC,Y,0
  NSEL,R,LOC,Z,0
  NSEL,R,LOC,X,3.75
  D,ALL,UX,0
  NSEL,ALL
*ELSE
  NSEL,S,LOC,X,0
  D,ALL,UX,0
  NSEL,ALL
*ENDIF

!Apply Symetry BC's at Z=0 plane
*IF,MTYPE,EQ,'SC',THEN
  NSEL,S,LOC,Y,0
  NSEL,R,LOC,X,0
  NSEL,R,LOC,Z,t
  D,ALL,UZ,0
  NSEL,ALL
*ELSE
  NSEL,S,LOC,Z,0
  D,ALL,UZ,0
  NSEL,ALL
*ENDIF

!Select Crack Mouth Node...Create Component CMNODES

NSEL,S,LOC,X,0
NSEL,R,LOC,Y,0
CM,CMNODES,NODE

CMSEL,ALL
NSEL,ALL
ESEL,ALL

WSORT,ALL,0          !Sort Elements to minimize wavefront

SAVE
FINISH
```

APPENDIX C2

ANSYS INPUT FILE *StrtCyc.MAC,* CONTROL OF CYCLIC

LOADING, SPIKE OVERLOAD

```
TimeVar=0.45
FirstLoad
ClearRST,BDrive,BDir,MaxDir

PE=0
SPAC=0
POP=0

*DO,I,1,NLC

 *IF,PE,NE,0,THEN
  I=PE+1
 *ENDIF
 *IF,I,EQ,1,THEN
  UnloadCrack,I
  ClearRST,BDrive,BDir,MinDir
  *DO,O,1,I
   JK_%O%=1
  *ENDDO
  LoadCrack,I
  ClearRST,BDrive,BDir,MaxDir
  SU=I
  SU_%I%=I
  POP=POP+1
  POP_%POP%=I
  PE=I

 *ELSE

  *IF,spike,EQ,I,THEN
!sort the array in ascENDing ORDEr
   *MOPER,ORDE(1),JUNK_%SU%(1,1),sort,JUNK_%SU%(1,1)
   VES=JUNK_%SU%(nodeNO,1)
   FUNI=SU+VES
   VES_%FUNI%=VES
!rearranging the array
   *MOPER,ORDE(1),JUNK_%SU%(1,1),sort,ORDE(1,1)
   JUMP=1
   JUMP_%I%=1

   *DO,TEE,1,VES

    *IF,TEE,GT,1,THEN
     I=I+1
     JUMP_%I%=JUMP+1
     JUMP=JUMP+1
     *IF,TEE,EQ,VES,THEN
      JUMP_%I%=0
     *ENDIF
    *ENDIF
    *IF,TEE,EQ,VES,THEN
     JUMP_%I%=0
     POP_%I-TEE+1%=I
     POP=I-TEE+1
     *ENDIF
    StrsMax=spmax
    UnloadCrack,I
    ClearRST,BDrive,BDir,MinDir
    *DO,O,1,I
     JK_%O%=1
```

```
 *ENDDO
 LoadCrack,I
 ClearRST,BDrive,BDir,MaxDir
*ENDDO
TEE=VES
NLC=NLC+TEE-1
SU=I
POP=POP+1
POP_%I-TEE+1%=I
JUMP=1
SU_%I%=I
PE=I
SPAC=1
save
*ELSE
StrsMax=smax
*MOPER,ORDE(1),JUNK_%SU%(1,1),sort,JUNK_%SU%(1,1)
VES=JUNK_%SU%(nodeNO,1)
FUNI=SU+VES
VES_%FUNI%=VES
!rearranging the array
*MOPER,ORDE(1),JUNK_%SU%(1,1),sort,ORDE(1,1)
JUMP=1
JUMP_%I%=1
*DO,TEE,1,VES
 *IF,TEE,EQ,1,THEN
  *IF,SPAC,EQ,0,THEN
   spike=spike+VES-1
  *ENDIF
 *ENDIF
 *IF,TEE,GT,1,THEN
  I=I+1
  JUMP_%I%=JUMP+1
  JUMP=JUMP+1
  *IF,TEE,EQ,VES,THEN
   JUMP_%I%=0
  *ENDIF
 *ENDIF
 *IF,TEE,EQ,VES,THEN
  POP=POP+1
  POP_%POP%=I
  JUMP_%I%=0
 *ENDIF
 UnloadCrack,I
 ClearRST,BDrive,BDir,MinDir
 *DO,O,1,I
  JK_%O%=1
 *ENDDO
 LoadCrack,I
 ClearRST,BDrive,BDir,MaxDir
*ENDDO
TEE=VES
NLC=NLC+TEE-1
SU=I
JUMP=1
SU_%I%=I
PE=I
*ENDIF
*ENDIF
SAVE
```

```
 *IF,PE,EQ,nlc,exit
*ENDDO
```

APPENDIX C3

ANSYS INPUT FILE *RAJU.MAC,* NEWMAN-RAJU

CONSTANT, SPIKE OVERLOAD

```
!CONSTANTS FOR NEWMAN-RAJU EQUATION

PI=(1989/22+7)**0.25

M1=1.13-(0.09*(a/c))

M2=-0.54+(0.89/(0.2+(a/c)))

M3=0.5-(1.0/(0.65+(a/c)))+14*((1-(a/c))**24)

QW=1+(1.464*((a/c)**1.65))

FW=sqrt(cos(((pi*c)/(2*w))*sqrt(a/t)))


StrtCyc
```

APPENDIX C4

ANSYS INPUT FILE *SELCTNODES.MAC,* SELECT

CRACK FRONT, SPIKE OVERLOAD

```
! SelCTNodes.mac
! Macro to Select the Crack tip nodes for load cycle "N"
!
! Executed as follows:
!     SelCTNodes,N
!
!Set Coordinate System to Elliptical




*IF,arg1,EQ,1,THEN
  !for first cycle
  LOCAL,11,1,0,0,0,0,90,0,a/c
  NSEL,S,LOC,X,c-0.3*da,c+0.3*da
  NSEL,R,LOC,Z,0
  *GET,FNODNO,NODE,,NUM,MIN
  *GET,LNODNO,NODE,,NUM,MAX
  DELTANN=NDNEXT(FNODNO)-FNODNO
  *GET,NODCNT,NODE,,COUNT
  nodeNO=((LNODNO-FNODNO)/DELTANN)+1
  NSEL,S,NODE,,FNODNO+(arg1-1),LNODNO+(arg1-1),DELTANN
  CSYS,0
*ENDIF



*IF,JUMP_%arg1%,GE,1,THEN
  *IF,arg1,NE,1,THEN
    !selction of node
    LOCAL,11,1,0,0,0,0,90,0,a/c
    NSEL,S,LOC,X,c-0.3*da,c+0.3*da
    NSEL,R,LOC,Z,0
    NSEL,S,NODE,,JUNK_%arg1%(1,3)+JUMP_%arg1%,JUNK_%arg1%(1,3)+JUMP_%arg1%,1
    *DO,QP,2,DD_%arg1%

nsel,a,NODE,,JUNK_%arg1%(QP,3)+JUMP_%arg1%,JUNK_%arg1%(QP,3)+JUMP_%arg1%,1
    *ENDDO
    CSYS,0
  *ENDIF
*ENDIF



*IF,JUMP_%arg1%,EQ,0,THEN
  *IF,arg1,NE,1,THEN
    !selction of node
    LOCAL,11,1,0,0,0,0,90,0,a/c
    NSEL,S,LOC,X,c-0.3*da,c+0.3*da
    NSEL,R,LOC,Z,0
    KII=VES_%arg1%
    nsel,s,,,JUNK_%arg1-KII%(1,3)+JUNK_%arg1-KII%(1,1),JUNK_%arg1-
KII%(1,3)+JUNK_%arg1-KII%(1,1),1
    *DO,K,2,nodeNO
      nsel,a,,,JUNK_%arg1-KII%(K,3)+JUNK_%arg1-KII%(K,1),JUNK_%arg1-
KII%(K,1)+JUNK_%arg1-KII%(K,3),1
      CSYS,0
    *ENDDO
```

```
      KIR_%arg1%=arg1
      KIR=arg1
    *ENDIF
  *ENDIF
```

APPENDIX C5

ANSYS INPUT FILE *LOADCRACK.MAC,* LOAD MODEL, SPIKE OVERLOAD

```
AUTOTS,ON
NSUBST,1,100,1,OFF
*CFOPEN,%JN%_load_%arg1%,dat

!*VWRITE
! ("NODE#   Node r      NodeAng  S/Smax    SY          OStat Remote StreSS")
!modIFication

*DO,JK,1,arg1-1
 *DO,KJ,1,K_%JK%
  NEXT_%JK%(KJ,2)=0
 *ENDDO
*ENDDO

SelCTNodes,arg1
NSEL,R,D,UY,0
*GET,NSNODES,NODE,,COUNT
*DIM,NEXT_%arg1%,array,NSNODES,4
nsel,all
CurrLInc=LIBCO
StrsLvl=StrsMin/StrsMax
RStrs=StrsMin


*DO,JJ,1,arg1
  SelCTNodes,JJ
  NSEL,R,D,UY,0
  *GET,NSNODES,NODE,,COUNT
  *DIM,PRE_%JJ%,array,NSNODES,3
  KA_%JJ%=NSNODES
!storing the no. of node for NEXT cycle
  *IF,JJ,EQ,arg1,THEN
   *GET,FNO,NODE,,NUM,MIN
   *GET,LNO,NODE,,NUM,MAX
   K_%JJ%=NSNODES
  *ENDIF

  *IF,NSNODES,GT,0,THEN
    NODNO=0
    *DO,JJJ,1,NSNODES
       NODNO=NDNEXT(NODNO)
       *GET,NODYSTRS,NODE,NODNO,S,Y
       *IF,MTYPE,EQ,'SC',THEN
         CSYS,11
         NDANG=NY(NODNO)
         NXLOC=NX(NODNO)
         CSYS,0
       *ELSE
         NDANG=NZ(NODNO)
         NXLOC=NX(NODNO)
       *ENDIF
       NodeStat=0
        *IF,NodYStrs*1e10,GT,0,THEN
          CurrLInc=LIDCO
          OPENSTAT=1
          NODESTAT=1
          DDELE,NODNO,UY
        *ENDIF
       *VWRITE,NODNO,NXLOC,NDANG,StrsLvl,NODYSTRS,NODESTAT,RSTRS
         (F6.0,2X,E12.6,2X,E10.4,2X,F8.6,2X,E12.6,2X,F4.0,2X,E12.6)
```

```
        *IF,NodeStat,EQ,1,THEN
             *IF,JJ,LT,arg1,THEN
              *DO,RS,1,K_%JJ%
               *IF,nodno,EQ,NEXT_%JJ%(RS,3),THEN
            NEXT_%JJ%(RS,2)=StrsMin/StrsMax
                *ENDIF
               *ENDDO
              *ELSE
              NEXT_%JJ%(JK_%JJ%,4)=NDANG
            NEXT_%JJ%(JK_%JJ%,3)=NODNO
            NEXT_%JJ%(JK_%JJ%,2)=StrsMin/StrsMax
            JK_%JJ%=JK_%JJ%+1
               *ENDIF
        *ELSE
             PRE_%JJ%(JJJ,3)=NODNO
             PRE_%JJ%(JJJ,2)=StrsLvl
             PRE_%JJ%(JJJ,1)=NODYSTRS
        *ENDIF
      *ENDDO
   *ENDIF
 *ENDDO




*DO,J,1,1/LIDCO
  TimeVar=TimeVar+CurrLInc*0.45
  RStrs=(StrsMax-StrsMin)*(TimeVar-arg1)/0.45+StrsMin
  *IF,TimeVar,GE,arg1+0.45,THEN
    RStrs=StrsMax
    TimeVar=arg1+0.45
    Time,TimeVar
    AppLoad,height,RStrs
    SOLVE
    SAVE
    *EXIT
  *ENDIF
  Time,TimeVar
  StrsLvl=RStrs/StrsMax
  AppLoad,height,RStrs
  SOLVE
  SAVE
  ClearRST,BDrive,BDir,''
  OPENSTAT=0
  OpnRwCnt=0
  *DO,JJ,1,arg1
    SelCTNodes,JJ
    NSEL,R,D,UY,0
    *GET,NSNODES,NODE,,COUNT
    *IF,NSNODES,GT,0,THEN
      NODNO=0
      *DO,JJJ,1,NSNODES
        NodeStat=0
        NODNO=NDNEXT(NODNO)
        *GET,NodYStrs,NODE,NODNO,S,Y
        *IF,MTYPE,EQ,'SC',THEN
          CSYS,11
          NDANG=NY(NODNO)
          NXLOC=NX(NODNO)
          CSYS,0
```

```
        *ELSE
          NDANG=NZ(NODNO)
          NXLOC=NX(NODNO)
        *ENDIF
        *IF,NodYStrs*1e10,GT,0,THEN
          CurrLInc=LIDCO
          OPENSTAT=1
          NODESTAT=1
          DDELE,NODNO,UY
        *ENDIF
        *VWRITE,NODNO,NXLOC,NDANG,StrsLvl,NODYSTRS,NodeStat,RStrs
          (F6.0,2X,E12.6,2X,E10.4,2X,F8.6,2X,E12.6,2X,F4.0,2X,E12.6)
      *IF,NodeStat,EQ,1,THEN
        *IF,JJ,LT,arg1,THEN
        *DO,L,1,KA_%JJ%
          *IF,nodno,EQ,PRE_%JJ%(l,3),THEN
            JUNK=(NODYSTRS-PRE_%JJ%(L,1))
            Q1=PRE_%JJ%(L,2)
            *DO,RS,1,K_%JJ%
             *IF,nodno,EQ,NEXT_%JJ%(RS,3),THEN
               NEXT_%JJ%(RS,2)=((NODYSTRS*Q1)-(PRE_%JJ%(L,1)*StrsLvl))/JUNK
             *ENDIF
            *ENDDO
          *ENDIF
        *ENDDO
        *ELSE
        NEXT_%JJ%(JK_%JJ%,4)=NDANG
          NEXT_%JJ%(JK_%JJ%,3)=NODNO
        *DO,L,1,K_%JJ%
         *IF,NODNO,eq,PRE_%JJ%(L,3),THEN
          JUNK=(NODYSTRS-PRE_%JJ%(L,1))
            Q1=PRE_%JJ%(L,2)
            NEXT_%JJ%(JK_%JJ%,2)=((NODYSTRS*Q1)-(PRE_%JJ%(L,1)*StrsLvl))/JUNK
         *ENDIF
        *ENDDO
        JK_%JJ%=JK_%JJ%+1
       *ENDIF
      *ELSE
        *DO,L,1,KA_%JJ%
         *IF,PRE_%JJ%(L,3),EQ,NODNO,THEN
           PRE_%JJ%(L,3)=NODNO
           PRE_%JJ%(L,2)=StrsLvl
           PRE_%JJ%(L,1)=NODYSTRS
         *ENDIF
        *ENDDO
      *ENDIF
      *ENDDO
    *ELSEIF,NSNODES,EQ,0,THEN
      OpnRwCnt=OpnRwCnt+1
    *ENDIF
  *ENDDO
NSEL,ALL
*IF,OPENSTAT,EQ,1,THEN
  Time,Timevar+CurrLInc*0.01
  SOLVE
  SAVE
  ClearRST,BDrive,BDir,''
*ENDIF
*IF,OpnRwCnt,EQ,arg1,THEN
  CurrLInc=LIACO
```

```
   *ENDIF
*ENDDO
*CFCLOSE




*IF,arg1,EQ,1,THEN
!Newman Raju Equation to find SIF
  *DIM,TEMPI,array,nodeNO
  *DIM,FA,array,nodeNO
  *DIM,G,array,nodeNO
  *DIM,F,array,nodeNO
  *DIM,KMAX,array,nodeNO
  *DIM,KOPEN,array,nodeNO
  *DIM,CONS,array,nodeNO

  *DO,JJJ,1,nodeNO
   TEMPI(JJJ)=NEXT_%arg1%(JJJ,4)*(PI/180)
   AA=NZ(FNO)
   CC=NX(LNO)
   CONS(JJJ)=(8.1932965e-9)*TEMPI(JJJ)+1.503e-8
   FA(JJJ)=((((AA/CC)**2)*(cos(TEMPI(JJJ))**2))+(sin(TEMPI(JJJ))**2))**0.25
   G(JJJ)=1+((0.1+0.35*((AA/t)**2))*((1-sin(TEMPI(JJJ)))**2))
   f(JJJ)=(m1+(m2*((AA/t)**2))+(m3*((AA/t)**4)))*FA(JJJ)*g(JJJ)*FW
   KMAX(JJJ)=strsMax*sqrt(PI*(AA/QW))*F(JJJ)
   KOPEN(JJJ)=NEXT_%arg1%(JJJ,2)*strsMax*sqrt(PI*(AA/QW))*F(JJJ)
   NEXT_%arg1%(JJJ,1)=((KMAX(JJJ)-KOPEN(JJJ))**2.881)*CONS(JJJ)
  *ENDDO

!sort the array in ascENDing order
  *DIM,ORDE,,nodeNO
  *MOPER,ORDE(1),NEXT_%arg1%(1,1),sort,NEXT_%arg1%(1,1)

!Delta k effective
  *DO,JJJ,2,nodeNO
   NEXT_%arg1%(JJJ,1)=NINT(NEXT_%arg1%(JJJ,1)/NEXT_%arg1%(1,1))
  *ENDDO

!min. delta K effective
  NEXT_%arg1%(1,1)=1
  PQP=NEXT_%arg1%(nodeNO,1)
!rearranging the array
  *MOPER,ORDE(1),NEXT_%arg1%(1,1),sort,ORDE(1,1)


!Exchange of the matrix values to store permanently

  *DIM,JUNK_%arg1%,array,nodeNO,4
  *DO,JJJ,1,nodeNO
   JUNK_%arg1%(JJJ,1)=NEXT_%arg1%(JJJ,1)
   JUNK_%arg1%(JJJ,2)=NEXT_%arg1%(JJJ,2)
   JUNK_%arg1%(JJJ,3)=NEXT_%arg1%(JJJ,3)
   JUNK_%arg1%(JJJ,4)=NEXT_%arg1%(JJJ,4)
  *ENDDO

  *IF,PQP,GT,1,THEN
   *DO,PPQ,2,PQP
    DD_%PPQ%=0
```

```
   *DO,QA,1,nodeNO
    *IF,JUNK_%arg1%(QA,1),GE,PPQ,THEN
     DD_%PPQ%=DD_%PPQ%+1
    *ENDIF
   *ENDDO
  *ENDDO
 *ENDIF

 *IF,PQP,GT,1,THEN
  *DO,PPQ,2,PQP
   QQQ=1
   *DIM,JUNK_%PPQ%,array,DD_%PPQ%,4
   *DO,QA,1,nodeNO
    *IF,JUNK_%arg1%(QA,1),GE,PPQ,THEN
     JUNK_%PPQ%(QQQ,1)=JUNK_%arg1%(QA,1)
     JUNK_%PPQ%(QQQ,2)=JUNK_%arg1%(QA,2)
     JUNK_%PPQ%(QQQ,3)=JUNK_%arg1%(QA,3)
     JUNK_%PPQ%(QQQ,4)=JUNK_%arg1%(QA,4)
     QQQ=1+QQQ
    *ENDIF
   *ENDDO
  *ENDDO
 *ENDIF
 !write array in to file
 *CFOPEN,%JN%_mat_%arg1%,dat
 *vwrite,JUNK_%arg1%(1,1),JUNK_%arg1%(1,2),JUNK_%arg1%(1,3),JUNK_%arg1%(1,4)
   (F8.6,2X,E12.6,2X,F6.0,2X,E12.6,2X)
 *CFCLOSE

*ELSE

 !swap the required matrix
 *IF,JUMP,EQ,VES,THEN
  *DIM,JUNK_%arg1%,array,nodeNO,4
  *DO,KO,1,nodeNO
   JUNK_%arg1%(KO,1)=NEXT_%arg1%(KO,1)
   JUNK_%arg1%(KO,2)=NEXT_%arg1%(KO,2)
   JUNK_%arg1%(KO,3)=NEXT_%arg1%(KO,3)
   JUNK_%arg1%(KO,4)=NEXT_%arg1%(KO,4)
  *ENDDO

 !SPike overload modIFication- for cycles after SPike

 *IF,spac,EQ,1,THEN
  *DIM,SPIK_%arg1%,array,nodeno,6
  !up to second cycle
  DE=POP_2
  *DO,SP,1,K_%DE%
   *DO,SPS,1,K_1
    *IF,NEXT_1(SPS,3)+NEXT_1(SPS,1),EQ,NEXT_%DE%(SP,3),THEN
     *IF,NEXT_1(SPS,2),LT,NEXT_%DE%(SP,2),THEN
      SPIK_%arg1%(SP,1)=NEXT_%DE%(SP,1)
      SPIK_%arg1%(SP,2)=NEXT_%DE%(SP,2)
      SPIK_%arg1%(SP,3)=NEXT_%DE%(SP,3)
      SPIK_%arg1%(SP,4)=NEXT_%DE%(SP,4)
      SPIK_%arg1%(SP,5)=NEXT_%DE%(SP,1)
      SPIK_%arg1%(SP,6)=NEXT_%DE%(SP,3)
     *ELSE
      SPIK_%arg1%(SP,1)=NEXT_1(SPS,1)
      SPIK_%arg1%(SP,2)=NEXT_1(SPS,2)
```

```
        SPIK_%arg1%(SP,3)=NEXT_1(SPS,3)
        SPIK_%arg1%(SP,4)=NEXT_1(SPS,4)
        SPIK_%arg1%(SP,5)=NEXT_%DE%(SP,1)
        SPIK_%arg1%(SP,6)=NEXT_%DE%(SP,3)
      *ENDIF
     *ENDIF
    *ENDDO
   *ENDDO

    *DO,SP,3,POP-1
     SS=POP_%SP%
    *DO,SPSS,1,K_%SS%
     *DO,SPP,1,K_%SS%
      *IF,NEXT_%SS%(SPSS,3),EQ,SPIK_%arg1%(SPP,5)+SPIK_%arg1%(SPP,6),THEN
     *IF,NEXT_%SS%(SPSS,2),LT,SPIK_%arg1%(SPP,2),THEN
      SPIK_%arg1%(SPP,5)=NEXT_%SS%(SPSS,1)
      SPIK_%arg1%(SPP,6)=NEXT_%SS%(SPSS,3)
     *ELSE
      SPIK_%arg1%(SPP,1)=NEXT_%SS%(SPSS,1)
      SPIK_%arg1%(SPP,2)=NEXT_%SS%(SPSS,2)
      SPIK_%arg1%(SPP,3)=NEXT_%SS%(SPSS,3)
        SPIK_%arg1%(SPP,4)=NEXT_%SS%(SPSS,4)
      SPIK_%arg1%(SPP,5)=NEXT_%SS%(SPSS,1)
      SPIK_%arg1%(SPP,6)=NEXT_%SS%(SPSS,3)
       *ENDIF
      *ENDIF
     *ENDDO
    *ENDDO
   *ENDDO

! for current cycle

    *DO,SP,1,K_1
     *DO,SPS,1,K_1
      *IF,SPIK_%arg1%(SPS,5)+SPIK_%arg1%(SPS,6),EQ,JUNK_%arg1%(SP,3),THEN
       *IF,SPIK_%arg1%(SPS,2),LT,JUNK_%arg1%(SP,2),THEN
        SPIK_%arg1%(SPS,2)=JUNK_%arg1%(SP,2)
        SPIK_%arg1%(SPS,3)=JUNK_%arg1%(SP,3)
        SPIK_%arg1%(SPS,4)=JUNK_%arg1%(SP,4)
       *ENDIF
      *ENDIF
     *ENDDO
    *ENDDO


!END of modIFication

!Newman Raju Equation to find SIF

    *DO,JJJ,1,nodeNO
     AA=NZ(fno)
     CC=NX(lno)
     TEMPI(JJJ)=SPIK_%arg1%(JJJ,4)*(PI/180)
     CONS(JJJ)=(8.1932965e-9)*TEMPI(JJJ)+1.503e-8
     FA(JJJ)=((((AA/CC)**2)*(cos(TEMPI(JJJ))**2))+(sin(TEMPI(JJJ))**2))**0.25
     G(JJJ)=1+((0.1+0.35*((AA/t)**2))*((1-sin(TEMPI(JJJ)))**2))
     F(JJJ)=(M1+(M2*((AA/t)**2))+(M3*((AA/t)**4)))*FA(JJJ)*G(JJJ)*FW
     KMAX(JJJ)=strsMax*sqrt(PI*(AA/QW))*F(JJJ)
     KOPEN(JJJ)=SPIK_%arg1%(JJJ,2)*strsMax*sqrt(pi*(AA/QW))*F(JJJ)
     SPIK_%arg1%(JJJ,1)=((KMAX(JJJ)-KOPEN(JJJ))**2.881)*CONS(JJJ)
```

```
    *ENDDO


!swap the delta k value to the current JUNK mat


    *DO,B,1,nodeNO
     *DO,BB,1,nodeNO
      *IF,SPIK_%arg1%(BB,5)+SPIK_%arg1%(BB,6),EQ,JUNK_%arg1%(B,3),THEN
       JUNK_%arg1%(B,1)=SPIK_%arg1%(BB,1)
      *ENDIF
     *ENDDO
    *ENDDO


!sort the array in ascENDing ORDEr
    *DIM,ORDE,,nodeNO
    *MOPER,ORDE(1),JUNK_%arg1%(1,1),sort,JUNK_%arg1%(1,1)

!Delta K effective

    *DO,JJJ,2,nodeNO
     JUNK_%arg1%(JJJ,1)=NINT(JUNK_%arg1%(JJJ,1)/JUNK_%arg1%(1,1))
    *ENDDO

!min. delta K effective FActor

    JUNK_%arg1%(1,1)=1
    PQP=JUNK_%arg1%(nodeNO,1)

!rearranging the array

    *MOPER,ORDE(1),JUNK_%arg1%(1,1),sort,ORDE(1,1)

    *DO,SP,1,nodeNo
     *DO,SPS,1,nodeNo
      *IF,JUNK_%arg1%(SP,3),EQ,NEXT_%arg1%(SPS,3),THEN
       NEXT_%arg1%(SPS,1)=JUNK_%arg1%(SP,1)
      *ENDIF
     *ENDDO
    *ENDDO


    *IF,PQP,GT,1,THEN
     *DO,PPQ,2,PQP
      QLQ=arg1+PPQ-1
      DD_%QLQ%=0
      *DO,QA,1,nodeNO
       *IF,JUNK_%arg1%(QA,1),GE,PPQ,THEN
        DD_%QLQ%=DD_%QLQ%+1
       *ENDIF
      *ENDDO
     *ENDDO
    *ENDIF

    *IF,PQP,GT,1,THEN
     *DO,PPQ,2,PQP
      QQQ=1
      QLQ=arg1+PPQ-1
      *DIM,JUNK_%QLQ%,array,DD_%QLQ%,4
```

```
    *DO,QA,1,nodeNO
     *IF,JUNK_%arg1%(QA,1),GE,PPQ,THEN
       JUNK_%QLQ%(QQQ,1)=JUNK_%arg1%(QA,1)
       JUNK_%QLQ%(QQQ,2)=JUNK_%arg1%(QA,2)
       JUNK_%QLQ%(QQQ,3)=JUNK_%arg1%(QA,3)
       JUNK_%QLQ%(QQQ,4)=JUNK_%arg1%(QA,4)
       QQQ=1+QQQ
     *ENDIF
    *ENDDO
   *ENDDO
  *ENDIF

!write array in to file

   *CFOPEN,%JN%_mat_%arg1%,dat
   *vwrite,JUNK_%arg1%(1,1),JUNK_%arg1%(1,2),JUNK_%arg1%(1,3),JUNK_%arg1%(1,4)
    (F8.6,2X,E12.6,2X,F6.0,2X,E12.6,2X)
   *CFCLOSE


  *ELSE

!for normal cycles, up to SPike overload

!Newman Raju Equation to find SIF


   *DO,JJJ,1,nodeNO
    AA=NZ(FNO)
    CC=NX(LNO)
    TEMPI(JJJ)=JUNK_%arg1%(JJJ,4)*(PI/180)
    CONS(JJJ)=(8.1932965e-9)*TEMPI(JJJ)+1.503e-8
    FA(JJJ)=(((AA/CC)**2)*(cos(TEMPI(JJJ))**2))+(sin(TEMPI(JJJ))**2))**0.25
    G(JJJ)=1+((0.1+0.35*((AA/t)**2))*((1-sin(TEMPI(JJJ)))**2))
    F(JJJ)=(M1+(M2*((AA/t)**2))+(M3*((AA/t)**4)))*FA(JJJ)*G(JJJ)*FW
    KMAX(JJJ)=strsMax*sqrt(PI*(AA/QW))*F(JJJ)
    KOPEN(JJJ)=JUNK_%arg1%(JJJ,2)*strsMax*sqrt(PI*(AA/QW))*F(JJJ)
    JUNK_%arg1%(JJJ,1)=((KMAX(JJJ)-KOPEN(JJJ))**2.881)*CONS(JJJ)
   *ENDDO

!sort the array in ascENDing ORDEr

   *DIM,ORDE,,nodeNO
   *MOPER,ORDE(1),JUNK_%arg1%(1,1),sort,JUNK_%arg1%(1,1)

!Delta K effective

   *DO,JJJ,2,nodeNO
    JUNK_%arg1%(JJJ,1)=NINT(JUNK_%arg1%(JJJ,1)/JUNK_%arg1%(1,1))
   *ENDDO

!min. delta K effective FActor

   JUNK_%arg1%(1,1)=1
   PQP=JUNK_%arg1%(nodeNO,1)

!rearranging the array

   *MOPER,ORDE(1),JUNK_%arg1%(1,1),sort,ORDE(1,1)
```

```
    *DO,SP,1,nodeNo
     *DO,SPS,1,nodeNo
      *IF,JUNK_%arg1%(SP,3),EQ,NEXT_%arg1%(SPS,3),THEN
       NEXT_%arg1%(SPS,1)=JUNK_%arg1%(SP,1)
      *ENDIF
     *ENDDO
    *ENDDO

    *IF,PQP,GT,1,THEN
     *DO,PPQ,2,PQP
      QLQ=arg1+PPQ-1
      DD_%QLQ%=0
      *DO,QA,1,nodeNO
       *IF,JUNK_%arg1%(QA,1),ge,PPQ,THEN
        DD_%QLQ%=DD_%QLQ%+1
       *ENDIF
      *ENDDO
     *ENDDO
    *ENDIF

    *IF,PQP,GT,1,THEN
     *DO,PPQ,2,PQP
      QQQ=1
      QLQ=arg1+PPQ-1
      *DIM,JUNK_%QLQ%,array,DD_%QLQ%,4
      *DO,QA,1,nodeNO
       *IF,JUNK_%arg1%(QA,1),GE,PPQ,THEN
        JUNK_%QLQ%(QQQ,1)=JUNK_%arg1%(QA,1)
        JUNK_%QLQ%(QQQ,2)=JUNK_%arg1%(QA,2)
        JUNK_%QLQ%(QQQ,3)=JUNK_%arg1%(QA,3)
        JUNK_%QLQ%(QQQ,4)=JUNK_%arg1%(QA,4)
        QQQ=1+QQQ
       *ENDIF
      *ENDDO
     *ENDDO
    *ENDIF

!write array in to file

    *CFOPEN,%JN%_mat_%arg1%,dat
    *vwrite,JUNK_%arg1%(1,1),JUNK_%arg1%(1,2),JUNK_%arg1%(1,3),JUNK_%arg1%(1,4)
       (F8.6,2X,E12.6,2X,F6.0,2X,E12.6,2X)
    *CFCLOSE
   *ENDIF
  *ENDIF
*ENDIF
```

APPENDIX C6

ANSYS INPUT FILE *UNLOADCRACK.MAC,* UNLOAD

MODEL, SPIKE OVERLOAD

```
AUTOTS,ON
NSUBST,1,100,1,OFF
*CFOPEN,%JN%_unload_%arg1%,dat



!*VWRITE
! ("NODE#   Node r      NodeAng  S/Smax    UY          OStat Remote Stress")
TimeVar=TimeVar+0.05
CurrLInc=UIBCC
StrsLvl=StrsMax/StrsMax
RStrs=StrsMax
*DO,JJ,1,arg1
  SelCTNodes,JJ
  NSEL,U,D,UY,0
  *GET,NSNODES,NODE,,COUNT
  *IF,NSNODES,GT,0,THEN
    NODNO=0
    *DO,JJJ,1,NSNODES
       NODNO=NDNEXT(NODNO)
       NODYSTRS=UY(NODNO)
       *IF,MTYPE,EQ,'SC',THEN
         CSYS,11
         NDANG=NY(NODNO)
         NXLOC=NX(NODNO)
         CSYS,0
       *ELSE
         NDANG=NZ(NODNO)
         NXLOC=NX(NODNO)
       *ENDIF
       NodeStat=0
       *VWRITE,NODNO,NXLOC,NDANG,StrsLvl,NODYSTRS,NODESTAT,RSTRS
          (F6.0,2X,E12.6,2X,E10.4,2X,F8.6,2X,E12.6,2X,F4.0,2X,E12.6)
    *ENDDO
  *ENDIF
*ENDDO

*DO,J,1,1/UIDCC
  TimeVar=TimeVar+CurrLInc*0.5
  RStrs=StrsMax-(StrsMax-StrsMin)*(TimeVar+0.5-arg1)/0.5
  *IF,TimeVar,GE,arg1,Then
    RStrs=StrsMin
    TimeVar=arg1
    Time,TimeVar
    AppLoad,height,RStrs
    SOLVE
    SAVE
!modified
    *DO,JJ,1,arg1
    SelCTNodes,JJ
    NSEL,U,D,UY,0
    *GET,NSNODES,NODE,,COUNT
    *IF,NSNODES,GT,0,THEN
      NODNO=0
      *DO,JJJ,1,NSNODES
        NodeStat=0
        NODNO=NDNEXT(NODNO)
        NODYSTRS=UY(NODNO)
        *IF,MTYPE,EQ,'SC',THEN
          CSYS,11
```

```
          NDANG=NY(NODNO)
          NXLOC=NX(NODNO)
          CSYS,0
        *ELSE
          NDANG=NZ(NODNO)
          NXLOC=NX(NODNO)
        *ENDIF
        *IF,NodYStrs*1e10,LT,0,THEN
          CurrLInc=UIDCC
          OPENSTAT=1
          NODESTAT=1
          D,NODNO,UY,0
        *ENDIF
        *VWRITE,NODNO,NXLOC,NDANG,StrsLvl,NODYSTRS,NodeStat,RStrs
            (F6.0,2X,E12.6,2X,E10.4,2X,F8.6,2X,E12.6,2X,F4.0,2X,E12.6)
      *ENDDO
      *endif
      *enddo
!end of modification
    *EXIT
  *ENDIF
  Time,TimeVar
  StrsLvl=RStrs/StrsMax
  AppLoad,height,RStrs
  SOLVE
  SAVE
  ClearRST,BDrive,BDir,''
  OPENSTAT=0
  OpnRwCnt=0
  *DO,JJ,1,arg1
    SelCTNodes,JJ
    NSEL,U,D,UY,0
    *GET,NSNODES,NODE,,COUNT
    *IF,NSNODES,GT,0,THEN
      NODNO=0
      *DO,JJJ,1,NSNODES
        NodeStat=0
        NODNO=NDNEXT(NODNO)
        NODYSTRS=UY(NODNO)
        *IF,MTYPE,EQ,'SC',THEN
          CSYS,11
          NDANG=NY(NODNO)
          NXLOC=NX(NODNO)
          CSYS,0
        *ELSE
          NDANG=NZ(NODNO)
          NXLOC=NX(NODNO)
        *ENDIF
        *IF,NodYStrs*1e10,LT,0,THEN
          CurrLInc=UIDCC
          OPENSTAT=1
          NODESTAT=1
          D,NODNO,UY,0
        *ENDIF
        *VWRITE,NODNO,NXLOC,NDANG,StrsLvl,NODYSTRS,NodeStat,RStrs
            (F6.0,2X,E12.6,2X,E10.4,2X,F8.6,2X,E12.6,2X,F4.0,2X,E12.6)
      *ENDDO
    *ELSEIF,NSNODES,EQ,0,THEN
      OpnRwCnt=OpnRwCnt+1
    *ENDIF
```

```
  *ENDDO
  NSEL,ALL
  *IF,OPENSTAT,EQ,1,THEN
    Time,Timevar+CurrLInc*0.01
    SOLVE
    SAVE
    ClearRST,BDrive,BDir,''
  *ENDIF
  *IF,OpnRwCnt,EQ,arg1,THEN
    CurrLInc=UIACC
  *ENDIF
*ENDDO
*CFCLOSE
```

APPENDIX C7

ANSYS INPUT FILE *STRTCYC.MAC,* CONTROL OF CYCLIC

LOADING, CRACK SHAPE EVOLUTION

```
TimeVar=0.45
FirstLoad
ClearRST,BDrive,BDir,MaxDir
PE=0


*DO,I,1,NLC
  *IF,PE,NE,0,THEN
    I=PE+1
  *ENDIF
  *IF,I,EQ,1,THEN
    UnloadCrack,I
    ClearRST,BDrive,BDir,MinDir
    *DO,O,1,I
      JK_%O%=1
    *ENDDO
    LoadCrack,I
    ClearRST,BDrive,BDir,MaxDir
    SU=I
    SU_%I%=I
    PE=I
  *else
    !sort the array in ascENDing order
    *MOPER,ORDE(1),JUNK_%SU%(1,1),sort,JUNK_%SU%(1,1)
    VES=JUNK_%SU%(NODENO,1)
    FUNI=SU+VES
    VES_%FUNI%=VES
    !rearranging the array
    *MOPER,ORDE(1),JUNK_%SU%(1,1),sort,ORDE(1,1)
    JUMP=1
    JUMP_%I%=1
    *DO,TEE,1,VES
      *IF,TEE,GT,1,THEN
        I=I+1
        JUMP_%I%=JUMP+1
        JUMP=JUMP+1
        *IF,TEE,EQ,VES,THEN
          JUMP_%I%=0
        *ENDIF
      *ENDIF
      *IF,TEE,EQ,VES,THEN
        JUMP_%I%=0
      *ENDIF
      UnloadCrack,I
      ClearRST,BDrive,BDir,MinDir
      *DO,O,1,I
        JK_%O%=1
      *ENDDO
      LoadCrack,I
      ClearRST,BDrive,BDir,MaxDir
    *ENDDO
    TEE=VES
    NLC=NLC+TEE-1
    SU=I
    JUMP=1
    SU_%I%=I
    PE=I
  *ENDIF
```

```
  SAVE
 *IF,PE,EQ,NLC,EXIT
*ENDDO
```

APPENDIX C8

ANSYS INPUT FILE *SELCTNODES.MAC*, SELECT CRACK

FRONT, CRACK SHAPE EVOLUTION

```
! SelCTNodes.mac
! Macro to Select the Crack tip nodes for load cycle "N" for surface crack
without spike overload
!
! Executed as follows:
!    SelCTNodes,N
!
! written by Kiran Solanki
! Set Coordinate System to Elliptical




*IF,arg1,eq,1,THEN
!for first cycle
  LOCAL,11,1,0,0,0,0,90,0,a/c
  NSEL,S,LOC,X,c-0.3*da,c+0.3*da
  NSEL,R,LOC,Z,0
  *GET,FNODNO,NODE,,NUM,MIN
  *GET,LNODNO,NODE,,NUM,MAX
  DELTANN=NDNEXT(FNODNO)-FNODNO
  *GET,NODCNT,NODE,,COUNT
  NODENO=((LNODNO-FNODNO)/DELTANN)+1
  NSEL,S,NODE,,FNODNO+(arg1-1),LNODNO+(arg1-1),DELTANN
  CSYS,0
*ENDIF




*IF,JUMP_%arg1%,GE,1,THEN
 *IF,arg1,NE,1,THEN
  !selction of node
  LOCAL,11,1,0,0,0,0,90,0,a/c
  NSEL,S,LOC,X,c-0.3*da,c+0.3*da
  NSEL,R,LOC,Z,0
  NSEL,S,NODE,,JUNK_%arg1%(1,3)+JUMP_%arg1%,JUNK_%arg1%(1,3)+JUMP_%arg1%,1
  *DO,QP,2,DD_%arg1%
   nsel,a,NODE,,JUNK_%arg1%(QP,3)+JUMP_%arg1%,JUNK_%arg1%(QP,3)+JUMP_%arg1%,1
  *ENDDO
  CSYS,0
 *ENDIF
*ENDIF




*IF,JUMP_%arg1%,EQ,0,THEN
 *IF,arg1,NE,1,THEN
 !selction of node
 LOCAL,11,1,0,0,0,0,90,0,a/c
 NSEL,S,LOC,X,c-0.3*da,c+0.3*da
 NSEL,R,LOC,Z,0
 KII=VES_%arg1%
 nsel,s,,,JUNK_%arg1-KII%(1,3)+JUNK_%arg1-KII%(1,1),JUNK_%arg1-
KII%(1,3)+JUNK_%arg1-KII%(1,1),1
 *DO,k,2,NODENO
  nsel,a,,,JUNK_%arg1-KII%(K,3)+JUNK_%arg1-KII%(K,1),JUNK_%arg1-
KII%(K,1)+JUNK_%arg1-KII%(K,3),1
```

```
 CSYS,0
*ENDDO
KIR_%arg1%=arg1
KIR=arg1
*ENDIF
*ENDIF
```

APPENDIX C9

ANSYS INPUT FILE *LOADCRACK.MAC,* LOAD MODEL,

CRACK SHAPE EVOLUTION

```
AUTOTS,ON
NSUBST,1,100,1,OFF
*CFOPEN,%JN%_load_%arg1%,dat
!*VWRITE
! ("NODE#   Node r       NodeAng S/Smax   SY           OStat Remote Stress")

  SelCTNodes,arg1
  NSEL,R,D,UY,0
  *GET,NSNODES,NODE,,COUNT
  *DIM,NEXT_%arg1%,ARRAY,NSNODES,4
  NSEL,ALL
  CurrLInc=LIBCO
  StrsLvl=StrsMin/StrsMax
  RStrs=StrsMin

  *DO,JJ,1,arg1
   SelCTNodes,JJ
   NSEL,R,D,UY,0
   *GET,NSNODES,NODE,,COUNT
   *DIM,PRE_%JJ%,ARRAY,NSNODES,3
   ! storing the no. of node for next cycle
   *IF,JJ,EQ,arg1,THEN
    *GET,FNO,NODE,,NUM,MIN
    *GET,LNO,NODE,,NUM,MAX
    K_%JJ%=NSNODES
   *ENDIF
   *IF,NSNODES,GT,0,THEN
    NODNO=0
    *DO,JJJ,1,NSNODES
       NODNO=NDNEXT(NODNO)
       *GET,NODYSTRS,NODE,NODNO,S,Y
       *IF,MTYPE,EQ,'SC',THEN
         CSYS,11
         NDANG=NY(NODNO)
         NXLOC=NX(NODNO)
         CSYS,0
       *ELSE
         NDANG=NZ(NODNO)
         NXLOC=NX(NODNO)
       *ENDIF
       NodeStat=0
       *IF,NodYStrs*1e10,GT,0,THEN
         CurrLInc=LIDCO
         OPENSTAT=1
         NODESTAT=1
         DDELE,NODNO,UY
       *ENDIF
       *VWRITE,NODNO,NXLOC,NDANG,StrsLvl,NODYSTRS,NODESTAT,RSTRS
         (F6.0,2X,E12.6,2X,E10.4,2X,F8.6,2X,E12.6,2X,F4.0,2X,E12.6)

       *IF,NodeStat,EQ,1,THEN
         *IF,JJ,EQ,arg1,THEN
          NEXT_%JJ%(JK_%JJ%,4)=NDANG
          NEXT_%JJ%(JK_%JJ%,3)=NODNO
          NEXT_%JJ%(JK_%JJ%,2)=StrsMin/StrsMax
          JK_%JJ%=JK_%JJ%+1
         *ENDIF
       *ELSE
         *IF,JJ,EQ,arg1,THEN
          PRE_%JJ%(JJJ,3)=NODNO
```

```
            PRE_%JJ%(JJJ,2)=StrsLvl
            PRE_%JJ%(JJJ,1)=NODYSTRS
          *ENDIF
        *ENDIF
     *ENDDO
    *ENDIF
  *ENDDO

*DO,J,1,1/LIDCO
   TimeVar=TimeVar+CurrLInc*0.45
   RStrs=(StrsMax-StrsMin)*(TimeVar-arg1)/0.45+StrsMin
   *IF,TimeVar,GE,arg1+0.45,Then
    RStrs=StrsMax
    TimeVar=arg1+0.45
    Time,TimeVar
    AppLoad,height,RStrs
    SOLVE
    SAVE
    *EXIT
   *ENDIF
   Time,TimeVar
   StrsLvl=RStrs/StrsMax
   AppLoad,height,RStrs
   SOLVE
   SAVE
   ClearRST,BDrive,BDir,''
   OPENSTAT=0
   OpnRwCnt=0
   *DO,JJ,1,arg1
    SelCTNodes,JJ
    NSEL,R,D,UY,0
    *GET,NSNODES,NODE,,COUNT
    *IF,NSNODES,GT,0,THEN
       NODNO=0
       *DO,JJJ,1,NSNODES
         NodeStat=0
         NODNO=NDNEXT(NODNO)
         *GET,NodYStrs,NODE,NODNO,S,Y
         *IF,MTYPE,EQ,'SC',THEN
           CSYS,11
           NDANG=NY(NODNO)
           NXLOC=NX(NODNO)
           CSYS,0
         *ELSE
           NDANG=NZ(NODNO)
           NXLOC=NX(NODNO)
         *ENDIF
         *IF,NodYStrs*1e10,GT,0,THEN
           CurrLInc=LIDCO
           OPENSTAT=1
           NODESTAT=1
           DDELE,NODNO,UY
         *ENDIF
         *VWRITE,NODNO,NXLOC,NDANG,StrsLvl,NODYSTRS,NodeStat,RStrs
            (F6.0,2X,E12.6,2X,E10.4,2X,F8.6,2X,E12.6,2X,F4.0,2X,E12.6)
         *IF,NodeStat,EQ,1,THEN
          *IF,JJ,EQ,arg1,THEN
          NEXT_%JJ%(JK_%JJ%,4)=NDANG
          NEXT_%JJ%(JK_%JJ%,3)=NODNO
           *DO,L,1,K_%JJ%
```

```
          *IF,NODNO,EQ,PRE_%JJ%(L,3),THEN
           JUNK=(NODYSTRS-PRE_%JJ%(L,1))
           Q1=PRE_%JJ%(L,2)
           NEXT_%JJ%(JK_%JJ%,2)=((NODYSTRS*Q1)-(PRE_%JJ%(L,1)*StrsLvl))/JUNK
          *ENDIF
         *ENDDO
        JK_%JJ%=JK_%JJ%+1
        *ENDIF
       *ELSE
        *IF,JJ,EQ,arg1,THEN
         *DO,L,1,K_%JJ%
          *IF,PRE_%JJ%(L,3),EQ,NODNO,THEN
           PRE_%JJ%(L,3)=NODNO
           PRE_%JJ%(L,2)=StrsLvl
           PRE_%JJ%(L,1)=NODYSTRS
          *ENDIF
         *ENDDO
        *ENDIF
       *ENDIF
      *ENDDO
    *ELSEIF,NSNODES,EQ,0,THEN
      OpnRwCnt=OpnRwCnt+1
    *ENDIF
  *ENDDO
  NSEL,ALL
  *IF,OPENSTAT,EQ,1,THEN
    Time,Timevar+CurrLInc*0.01
    SOLVE
    SAVE
    ClearRST,BDrive,BDir,''
  *ENDIF
  *IF,OpnRwCnt,EQ,arg1,THEN
    CurrLInc=LIACO
  *ENDIF
*ENDDO
*CFCLOSE



*IF,arg1,EQ,1,THEN
  !Newman Raju Equation to find SIF
  *DIM,TEMPI,array,NODENO
  *DIM,FA,array,NODENO
  *DIM,G,array,NODENO
  *DIM,F,array,NODENO
  *DIM,KMAX,array,NODENO
  *DIM,KOPEN,array,NODENO
  *DIM,CONS,array,NODENO
  *DO,JJJ,1,NODENO
    TEMPI(JJJ)=NEXT_%arg1%(JJJ,4)*(PI/180)
    AA=NZ(FNO)
    CC=NX(LNO)
    CONS(JJJ)=(8.1932965e-9)*TEMPI(JJJ)+1.503e-8
    FA(JJJ)=(((((AA/CC)**2)*(cos(TEMPI(JJJ))**2))+(sin(TEMPI(JJJ))**2))**0.25
    G(JJJ)=1+((0.1+0.35*((AA/T)**2))*((1-sin(TEMPI(JJJ)))**2))
    F(JJJ)=(M1+(M2*((AA/T)**2))+(M3*((AA/T)**4)))*FA(JJJ)*G(JJJ)*FW
    KMAXx(JJJ)=strsMax*sqrt(PI*(AA/QW))*F(JJJ)
    KOPEN(JJJ)=NEXT_%arg1%(JJJ,2)*strsMax*sqrt(PI*(AA/QW))*F(JJJ)
    NEXT_%arg1%(JJJ,1)=((KMAX(JJJ)-KOPEN(JJJ))**2.881)*CONS(JJJ)
  *ENDDO
```

```
!sort the array in ascending order
*DIM,ORDE,,NODENO
*MOPER,ORDE(1),NEXT_%arg1%(1,1),sort,NEXT_%arg1%(1,1)
!Delta k effective
*DO,JJJ,2,NODENO
  NEXT_%arg1%(JJJ,1)=NEXT_%arg1%(JJJ,1)/NEXT_%arg1%(1,1)
*ENDDO
!min. delta K effective
NEXT_%arg1%(1,1)=1
PQP=NINT(NEXT_%arg1%(NODENO,1))
!rearranging the array
*MOPER,ORDE(1),NEXT_%arg1%(1,1),sort,ORDE(1,1)
!Exchange of the matrix values to store permanently
*DIM,JUNK_%arg1%,array,NODENO,4
*DO,JJJ,1,NODENO
  JUNK_%arg1%(JJJ,1)=NINT(NEXT_%arg1%(JJJ,1))
  JUNK_%arg1%(JJJ,2)=NEXT_%arg1%(JJJ,2)
  JUNK_%arg1%(JJJ,3)=NEXT_%arg1%(JJJ,3)
  JUNK_%arg1%(JJJ,4)=NEXT_%arg1%(JJJ,4)
*ENDDO
!JUNK stuff
*IF,PQP,GT,1,THEN
  *DO,PPQ,2,PQP
    DD_%PPQ%=0
    *DO,QA,1,NODENO
      *IF,JUNK_%arg1%(QA,1),GE,PPQ,THEN
        DD_%PPQ%=DD_%PPQ%+1
      *ENDIF
    *ENDDO
  *ENDDO
*ENDIF
!JUNK stuff
*IF,PQP,GT,1,THEN
  *DO,PPQ,2,PQP
    QQQ=1
    *DIM,JUNK_%PPQ%,array,DD_%PPQ%,4
    *DO,QA,1,NODENO
      *IF,JUNK_%arg1%(QA,1),GE,PPQ,THEN
        JUNK_%ppq%(QQQ,1)=JUNK_%arg1%(QA,1)
        JUNK_%ppq%(QQQ,2)=JUNK_%arg1%(QA,2)
        JUNK_%ppq%(QQQ,3)=JUNK_%arg1%(QA,3)
        JUNK_%ppq%(QQQ,4)=JUNK_%arg1%(QA,4)
        QQQ=1+QQQ
      *ENDIF
    *ENDDO
  *ENDDO
*ENDIF
!write array in to file
*CFOPEN,%JN%_mat_%arg1%,dat
*vwrite,JUNK_%arg1%(1,1),JUNK_%arg1%(1,2),JUNK_%arg1%(1,3),JUNK_%arg1%(1,4)
  (F8.6,2X,E12.6,2X,F6.0,2X,E12.6,2X)
*CFCLOSE
*ELSE
!swap the required matrix
*IF,JUMP,EQ,VES,THEN
  *DIM,JUNK_%arg1%,array,NODENO,4
  *DO,KO,1,NODENO
    JUNK_%arg1%(KO,1)=NEXT_%arg1%(KO,1)
    JUNK_%arg1%(KO,2)=NEXT_%arg1%(KO,2)
    JUNK_%arg1%(KO,3)=NEXT_%arg1%(KO,3)
```

```
      JUNK_%arg1%(KO,4)=NEXT_%arg1%(KO,4)
*ENDDO
*DO,J,1,NODENO
  *IF,JUNK_%arg1%(J,3),EQ,0,THEN
    JUNK_%arg1%(J,3)=JUNK_%arg1-1%(J,3)+JUNK_%arg1-1%(J,1)
    JUNK_%arg1%(J,2)=StrsMin/StrsMax
    DUM=JUNK_%arg1-1%(J,4)
    JUNK_%arg1%(J,4)=JUNK_%arg1-1%(J,4)
  *ENDIF
*ENDDO
!Newman Raju Equation to find SIF
*DO,JJJ,1,NODENO
  AA=NZ(FNO)
  CC=NX(LNO)
  TEMPI(JJJ)=JUNK_%arg1%(JJJ,4)*(PI/180)
  CONS(JJJ)=(8.1932965e-9)*TEMPI(JJJ)+1.503e-8
  FA(JJJ)=((((AA/CC)**2)*(cos(TEMPI(JJJ))**2))+(sin(TEMPI(JJJ))**2))**0.25
  G(JJJ)=1+((0.1+0.35*((AA/T)**2))*((1-sin(TEMPI(JJJ)))**2))
  F(JJJ)=(M1+(M2*((AA/T)**2))+(M3*((AA/T)**4)))*FA(JJJ)*G(JJJ)*FW
  KMAX(JJJ)=strsMax*sqrt(PI*(AA/QW))*F(JJJ)
  KOPEN(JJJ)=JUNK_%arg1%(JJJ,2)*strsMax*sqrt(PI*(AA/QW))*F(JJJ)
  JUNK_%arg1%(JJJ,1)=((KMAX(JJJ)-KOPEN(JJJ))**2.881)*CONS(JJJ)
*ENDDO
!sort the array in ascending order
*DIM,ORDE,,NODENO
*MOPER,ORDE(1),JUNK_%arg1%(1,1),sort,JUNK_%arg1%(1,1)
!Delta K effective
*DO,JJJ,2,NODENO
  JUNK_%arg1%(JJJ,1)=NINT(JUNK_%arg1%(JJJ,1)/JUNK_%arg1%(1,1))
*ENDDO
!min. delta K effective factor
JUNK_%arg1%(1,1)=1
PQP=JUNK_%arg1%(NODENO,1)
!rearranging the array
*MOPER,ORDE(1),JUNK_%arg1%(1,1),sort,ORDE(1,1)
!JUNK stuff
*IF,PQP,GT,1,THEN
  *DO,PPQ,2,PQP
    QLQ=arg1+PPQ-1
    DD_%QLQ%=0
    *DO,QA,1,NODENO
      *IF,JUNK_%arg1%(QA,1),QE,PPQ,THEN
        DD_%QLQ%=DD_%QLQ%+1
      *ENDIF
    *ENDDO
  *ENDDO
*ENDIF
!JUNK stuff
*IF,PQP,GT,1,THEN
  *DO,PPQ,2,PQP
    QQQ=1
    QLQ=arg1+PPQ-1
    *DIM,JUNK_%QLQ%,array,DD_%QLQ%,4
    *DO,QA,1,NODENO
      *IF,JUNK_%arg1%(QA,1),GE,PPQ,THEN
        JUNK_%QLQ%(QQQ,1)=JUNK_%arg1%(QA,1)
        JUNK_%QLQ%(QQQ,2)=JUNK_%arg1%(QA,2)
        JUNK_%QLQ%(QQQ,3)=JUNK_%arg1%(QA,3)
        JUNK_%QLQ%(QQQ,4)=JUNK_%arg1%(QA,4)
        QQQ=1+QQQ
```

```
      *ENDIF
     *ENDDO
    *ENDDO
   *ENDIF
   !write array in to file
   *CFOPEN,%JN%_mat_%arg1%,dat
   *vwrite,JUNK_%arg1%(1,1),JUNK_%arg1%(1,2),JUNK_%arg1%(1,3),JUNK_%arg1%(1,4)
     (F8.6,2X,E12.6,2X,F6.0,2X,E12.6,2X)
   *CFCLOSE
  *ENDIF
*ENDIF
```

APPENDIX C10

ANSYS INPUT FILE *UNLOADCRACK.MAC,* UNLOAD MODEL,

CRACK SHAPE EVOLUTION

```
AUTOTS,ON
NSUBST,1,100,1,OFF
*CFOPEN,%JN%_unload_%arg1%,dat
!*VWRITE
! ("NODE#   Node r      NodeAng  S/Smax   UY          OStat Remote Stress")
TimeVar=TimeVar+0.05
CurrLInc=UIBCC
StrsLvl=StrsMax/StrsMax
RStrs=StrsMax
*DO,JJ,1,arg1
  SelCTNodes,JJ
  NSEL,U,D,UY,0
  *GET,NSNODES,NODE,,COUNT
  *IF,NSNODES,GT,0,THEN
    NODNO=0
    *DO,JJJ,1,NSNODES
       NODNO=NDNEXT(NODNO)
       NODYSTRS=UY(NODNO)
       *IF,MTYPE,EQ,'SC',THEN
         CSYS,11
         NDANG=NY(NODNO)
         NXLOC=NX(NODNO)
         CSYS,0
       *ELSE
         NDANG=NZ(NODNO)
         NXLOC=NX(NODNO)
       *ENDIF
       NodeStat=0
       *VWRITE,NODNO,NXLOC,NDANG,StrsLvl,NODYSTRS,NODESTAT,RSTRS
          (F6.0,2X,E12.6,2X,E10.4,2X,F8.6,2X,E12.6,2X,F4.0,2X,E12.6)
    *ENDDO
  *ENDIF
*ENDDO

*DO,J,1,1/UIDCC
  TimeVar=TimeVar+CurrLInc*0.5
  RStrs=StrsMax-(StrsMax-StrsMin)*(TimeVar+0.5-arg1)/0.5
  *IF,TimeVar,GE,arg1,Then
    RStrs=StrsMin
    TimeVar=arg1
    Time,TimeVar
    AppLoad,height,RStrs
    SOLVE
    SAVE
!modified
    *DO,JJ,1,arg1
    SelCTNodes,JJ
    NSEL,U,D,UY,0
    *GET,NSNODES,NODE,,COUNT
    *IF,NSNODES,GT,0,THEN
      NODNO=0
      *DO,JJJ,1,NSNODES
        NodeStat=0
        NODNO=NDNEXT(NODNO)
        NODYSTRS=UY(NODNO)
        *IF,MTYPE,EQ,'SC',THEN
          CSYS,11
          NDANG=NY(NODNO)
          NXLOC=NX(NODNO)
          CSYS,0
```

```
             *ELSE
               NDANG=NZ(NODNO)
               NXLOC=NX(NODNO)
             *ENDIF
             *IF,NodYStrs*1e10,LT,0,THEN
               CurrLInc=UIDCC
               OPENSTAT=1
               NODESTAT=1
               D,NODNO,UY,0
             *ENDIF
             *VWRITE,NODNO,NXLOC,NDANG,StrsLvl,NODYSTRS,NodeStat,RStrs
                 (F6.0,2X,E12.6,2X,E10.4,2X,F8.6,2X,E12.6,2X,F4.0,2X,E12.6)
          *ENDDO
          *endif
          *enddo
!end of modification
       *EXIT
     *ENDIF
     Time,TimeVar
     StrsLvl=RStrs/StrsMax
     AppLoad,height,RStrs
     SOLVE
     SAVE
     ClearRST,BDrive,BDir,''
     OPENSTAT=0
     OpnRwCnt=0
     *DO,JJ,1,arg1
       SelCTNodes,JJ
       NSEL,U,D,UY,0
       *GET,NSNODES,NODE,,COUNT
       *IF,NSNODES,GT,0,THEN
         NODNO=0
         *DO,JJJ,1,NSNODES
           NodeStat=0
           NODNO=NDNEXT(NODNO)
           NODYSTRS=UY(NODNO)
           *IF,MTYPE,EQ,'SC',THEN
             CSYS,11
             NDANG=NY(NODNO)
             NXLOC=NX(NODNO)
             CSYS,0
           *ELSE
             NDANG=NZ(NODNO)
             NXLOC=NX(NODNO)
           *ENDIF
           *IF,NodYStrs*1e10,LT,0,THEN
             CurrLInc=UIDCC
             OPENSTAT=1
             NODESTAT=1
             D,NODNO,UY,0
           *ENDIF
           *VWRITE,NODNO,NXLOC,NDANG,StrsLvl,NODYSTRS,NodeStat,RStrs
               (F6.0,2X,E12.6,2X,E10.4,2X,F8.6,2X,E12.6,2X,F4.0,2X,E12.6)
         *ENDDO
       *ELSEIF,NSNODES,EQ,0,THEN
         OpnRwCnt=OpnRwCnt+1
       *ENDIF
     *ENDDO
     NSEL,ALL
     *IF,OPENSTAT,EQ,1,THEN
```

```
      Time,Timevar+CurrLInc*0.01
      SOLVE
      SAVE
      ClearRST,BDrive,BDir,''
   *ENDIF
   *IF,OpnRwCnt,EQ,arg1,THEN
      CurrLInc=UIACC
   *ENDIF
*ENDDO
*CFCLOSE
```

APPENDIX C11

ANSYS INPUT FILE *SURFACECRACK.MAC,* SAMPLE INPUT

FILE, CRACK SHAPE EVOLUTION

```
/BATCH
! This is the input file for pca1548
! This runs the script "appbcs.mac"  to import the Solid
! Elements and Nodes from the files "jobname.crd" & "jobname.elm",
! and applies necessary boundary conditions for Crack Growth
! It then calls "strtcyc.mac"  to run growth analysis.
!
! This script has been modified to work w/ ANSYS 5.6 and ANSYS 5.7
! with the addition of the RESCONTROL Command (not valid for ANSYS 5.5 and
below)
!


!Note all lengths are in mm, and pressures in MPa

/CONFIG,NPROC,1

!Loading information:

StrsMax=22e3            ! Maximum Applied Stress
StrsMin=2.2e3            ! Minimum Applied Stress
NLC=6                   ! Total Number of Loading Cycles to execute

!Geometry Information:

MTYPE='SC'

t=0.5                   ! Thickness of plate
w=0.5               ! Plate Half-Width
height=1.1875           ! Model Height
c=0.0501                ! Initial Crack half-length
a=0.05              ! Initial Depth of Surface Crack
da=0.00012500/2            ! Crack Growth Increment

!  Material Properties:

E=10.6E6                ! Young's Modulus
YS=75e3                 ! Yield Stress

!  Crack Growth Options:

NCGECut=5               ! Number of bisections to matrix stiffness before death
CGERF=2                 ! Crack Growth Element Stiffness Reduction Factor

*get,JN,ACTIVE,,JOBNAM
/TITLE, Plasticity Induced Closure of model %JN%

AppBCs                  ! Import Solid model and apply BC's

BDrive='e:'             ! Drive for file backups
BDir='\backup'          ! Directory for file backups
MaxDir='\maxload'       ! Directory for backup at Max Load
MinDir='\minload'       ! Directory for Backup at Min Load

!Solution Information:

/SOLU                   ! Enter Solution Processor

LIBCO=0.05              ! Loading Increment before crack opening
LIDCO=0.025             ! Loading Increment during crack opening
```

```
LIACO=0.10                 ! Loading Increment after crack opening
UIBCC=0.05                 ! Un-load Increment before crack closing
UIDCC=0.025                ! Un-load Increment during crack closing
UIACC=0.10                 ! Un-load Increment after crack closing
SOLCONTROL,ON
NSUB,1
NEQIT,8                    ! Number of Equilibrium Iterations before bisection
NROPT,FULL,,ON             ! Full Newton Rapson Option, Adaptive Descent ON
EQSLV,PCG,1.0e-8           ! Use the Pre-Conditioned Conjugate Solver (In Core,
default tolerance)

RESCONTROL,DEFINE,NONE,NONE,0   ! Set Resume Controls to act like ANSYS 5.5.3
and below
                                ! (Single Frame Restart)

raju
```

APPENDIX C12

ANSYS INPUT FILE *SURFACECRACKSPIKE.MAC*

SAMPLE INPUT FILE, SPIKE OVERLOAD

```
/BATCH
! This is the input file for pca1548
! This runs the script "appbcs.mac"  to import the Solid
! Elements and Nodes from the files "jobname.crd" & "jobname.elm",
! and applies necessary boundary conditions for Crack Growth
! It then calls "strtcyc.mac"  to run growth analysis.
!
! This script has been modified to work w/ ANSYS 5.6 and ANSYS 5.7
! with the addition of the RESCONTROL Command (not valid for ANSYS 5.5 and
below)



/CONFIG,NPROC,1

!Loading information:

StrsMax=22e3            ! Maximum Applied Stress
StrsMin=2.2e3           ! Minimum Applied Stress
spmax=44e3              ! spike overload
smax=22e3             ! Maximum applied stress
NLC=1                    ! Total Number of Loading Cycles to execute

!Geometry Information:

MTYPE='SC'

t=0.5                   ! Thickness of plate
w=0.5                 ! Plate Half-Width
height=1.1875            ! Model Height
c=0.0501              ! Initial Crack half-length
a=0.05              ! Initial Depth of Surface Crack
da=0.0002500/2           ! Crack Growth Increment

!  Material Properties:

E=10.6E6                ! Young's Modulus
YS=75e3                 ! Yield Stress

!  Crack Growth Options:

NCGECut=5               ! Number of bisections to matrix stiffness before death
CGERF=2                 ! Crack Growth Element Stiffness Reduction Factor

*get,JN,ACTIVE,,JOBNAM
/TITLE, Plasticity Induced Closure of model %JN%

AppBCs                ! Import Solid model and apply BC's

BDrive='e:'            ! Drive for file backups
BDir='\backup'        ! Directory for file backups
MaxDir='\maxload'     ! Directory for backup at Max Load
MinDir='\minload'     ! Directory for Backup at Min Load

!Solution Information:

/SOLU                 ! Enter Solution Processor

LIBCO=0.05            ! Loading Increment before crack opening
LIDCO=0.025           ! Loading Increment during crack opening
```

```
LIACO=0.10                ! Loading Increment after crack opening
UIBCC=0.05                ! Un-load Increment before crack closing
UIDCC=0.025               ! Un-load Increment during crack closing
UIACC=0.10                ! Un-load Increment after crack closing
SOLCONTROL,ON
NSUB,1
NEQIT,8                   ! Number of Equilibrium Iterations before bisection
NROPT,FULL,,ON            ! Full Newton Rapson Option, Adaptive Descent ON
EQSLV,PCG,1.0e-8          ! Use the Pre-Conditioned Conjugate Solver (In Core,
default tolerance)

RESCONTROL,DEFINE,NONE,NONE,0   ! Set Resume Controls to act like ANSYS 5.5.3
and below
                                !  (Single Frame Restart)

raju
```